Gravity and magnetic surveys over the Santa Rita fault system, southeastern Arizona

By Mary Hegmann[1]

Open-File Report 01-503

2001

U. S. DEPARTMENT OF THE INTERIOR
U.S. GEOLOGICAL SURVEY

[1]U.S. Geological Survey, Tucson, Arizona. This Master's Thesis was funded by the Southwest Mineral and Environmental Investigations Project, Mineral Resources Program, Geologic Division, U.S. Geological Survey.

GRAVITY AND MAGNETIC SURVEYS OVER THE SANTA RITA FAULT SYSTEM, SOUTHEASTERN ARIZONA

By

Mary Hegmann

A Thesis Submitted to the Faculty of the

DEPARTMENT OF GEOSCIENCES

In Partial Fulfillment of the Requirements
For the Degree of

MASTER OF GEOSCIENCES

With a Major in

GEOPHYSICS

In the Graduate College

THE UNIVERSITY OF ARIZONA

1 9 9 8

STATEMENT BY AUTHOR

This thesis has been submitted in partial fulfillment of requirements for an advanced degree at the University of Arizona and is deposited in the University Library to be made available to borrowers under rules of the Library.

Brief quotations from this thesis are allowable without special permission, provided that accurate acknowledgment of source is made. Requests for permission for extended quotation from or reproduction of this manuscript in whole or in part may be granted by the head of the major department or the Dean of the Graduate College when in his or her judgment the proposed use of the material is in the interests of scholarship. In all other instances, however, permission must be obtained by the author.

SIGNED:_____

APPROVAL BY THESIS DIRECTOR

This thesis has been approved on the date shown below:

_____ _____

Roy A. Johnson Date

Associate Professor of Geosciences

ACKNOWLEDGEMENTS

The author gratefully acknowledges the USGS Southwest Field Office in Tucson, Arizona, and Mark Gettings in particular for offering me the use of magnetic surveying equipment, GPS equipment, computers, and software. The author also would like to thank Scott Thomas of Placer Dome Inc. for providing modeling software, and Jim Fink of Hydrogeophysics, Inc., for providing electromagnetic surveying equipment.

TABLE OF CONTENTS

TABLE OF CONTENTS — *continued*

LIST OF FIGURES

LIST OF FIGURES — *continued*

LIST OF TABLES

ABSTRACT

Gravity and magnetic surveys were performed in the northeast portion of the Santa Rita Experimental Range, in southeastern Arizona, to identify faults and gain a better understanding of the subsurface geology. A total of 234 gravity stations were established, and numerous magnetic data were collected with portable and truck-mounted proton precession magnetometers. In addition, one line of very low frequency electromagnetic data was collected together with magnetic data.

Gravity anomalies are used to identify two normal faults that project northward toward a previously identified fault. The gravity data also confirm the location of a second previously interpreted normal fault. Interpretation of magnetic anomaly data indicates the presence of a higher-susceptibility sedimentary unit located beneath lower-susceptibility surficial sediments. Magnetic anomaly data identify a 1-km-wide negative anomaly east of these faults caused by an unknown source and reveal the high variability of susceptibility in the Tertiary intrusive rocks in the area.

INTRODUCTION

The area of study is in the northeast corner of the Santa Rita Experimental Range and Wildlife Area, and is located some 55 km south of Tucson and about 15 km southeast of Sahuarita, Arizona. The area is situated on the western pediment of the northern Santa Rita Mountains. Figure 1 shows the location of the field area and the jeep trails north of Santa Rita Road along several of which much of the magnetic and gravity anomaly data were taken.

The purpose of this study was to better define the Santa Rita fault system and the subsurface geology by performing magnetic and gravity surveys across the fault system and modeling the results. While other workers such as Tanbal (1987) have been successful in locating faults near the study area by applying gravity methods, it was thought in this case that collecting magnetic data along with the gravity data might also prove useful. In addition to gravity and magnetic data, one line of very low-frequency electromagnetic (VLF) data was collected along one of the magnetic survey lines to determine what kind of response could be obtained over the faults. It was also hoped that dip of the faults might be resolved.

Prior to this study, there were sparsely spaced regional gravity data collected in the surrounding area by various workers and compiled into a database by the U.S. Geological Survey (M.E. Gettings, unpublished data). Other geophysical work in the area includes that of Tanbal (1987), who collected several lines of gravity data across fault scarps a few kilometers south of the present study area in order to pinpoint fault locations. Rutledge (1984) performed a shallow seismic refraction survey over a fault

11

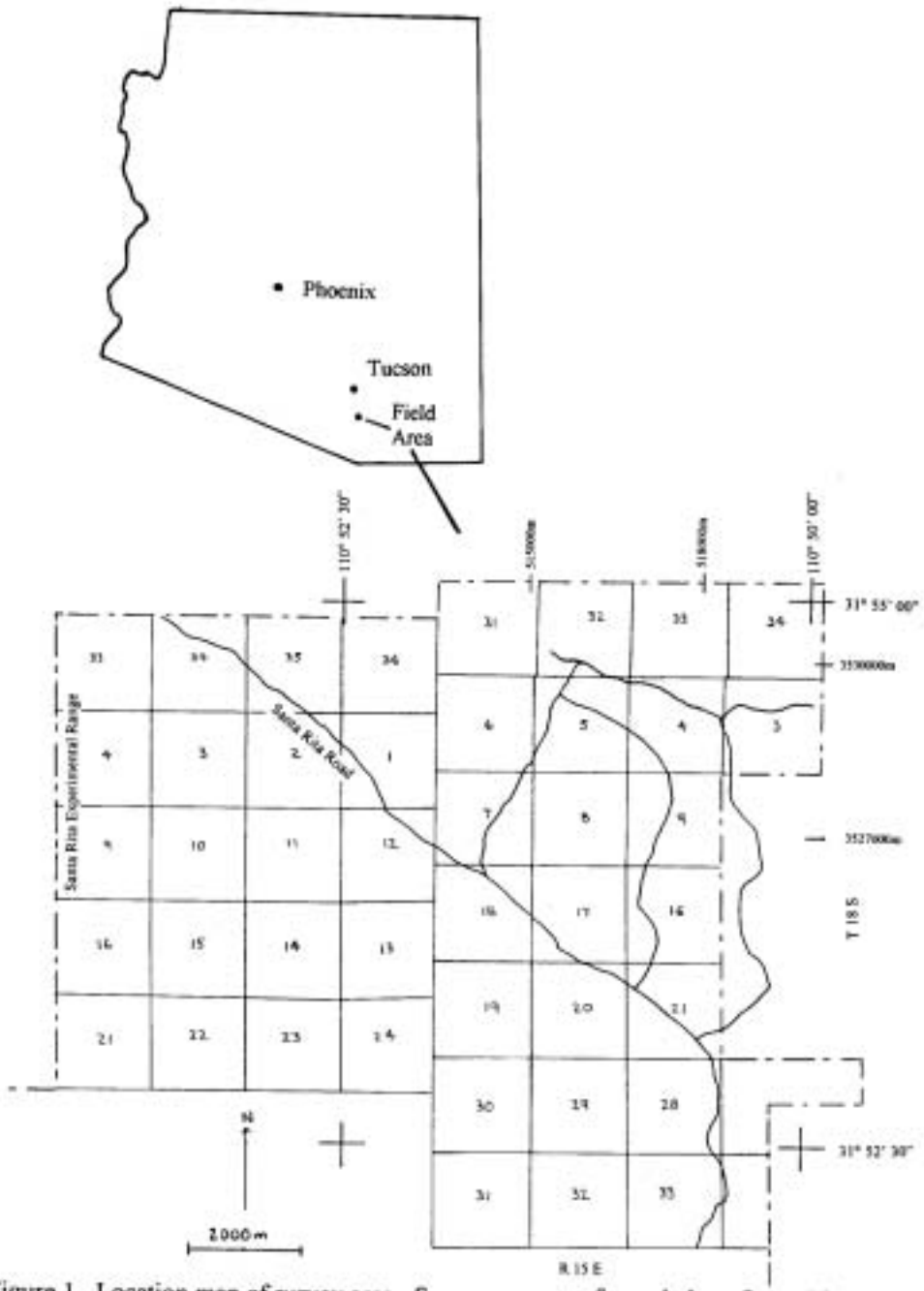

Figure 1. Location map of survey area. Surveys were performed along Santa Rita Road and jeep trails north of the road.

scarp several kilometers north of the area. Currently, studies are in progress to determine whether the major fault is a seismogenic low-angle normal fault (see Johnson and Loy, 1992). Rieth (in preparation) is trying to resolve this by analyzing reflection data that was obtained along a line which was also a part of the present magnetics and gravity survey. Pearthree and Calvo (1987) analyzed fault scarps and soils in the area in an effort to date and better define faulting in the Santa Rita fault zone. Pearthree et al. (1983) analyzed fault scarps to determine ages and recurrence of faulting. Aeromagnetic data has been collected by the USGS in the area, but the data has not yet been released (M.E. Gettings, pers. comm., 1998). Magnetic data along many of the roads in the surrounding area (see Gettings et al., 1995) have been collected with the USGS truck-mounted system and can be obtained through that agency.

The study area lies within the southern Basin and Range province of the western U.S., on the west bajada of the Santa Rita Mountains. Figure 2 shows the geology of the study area, most of it mapped by Drewes (e.g., 1971a, 1971b, 1972, 1976). The study area is believed to be underlain mostly by Precambrian Continental Granodiorite, with local stocks and plugs of Paleocene granodiorite and quartz monzonite. Various Quaternary alluvial deposits conceal these basement rocks throughout most of the area, with the exception of several buttes in the eastern section. These buttes are composed of faulted blocks of mostly Paleozoic sedimentary rocks, along with a small outcrop of Continental Granodiorite. The Paleozoic rocks exposed are predominantly the Pennsylvanian Horquilla Limestone, and to a much lesser extent, the Mississippian Escabrosa Limestone, Devonian Martin Formation, and the Cambrian Abrigo and Bolsa

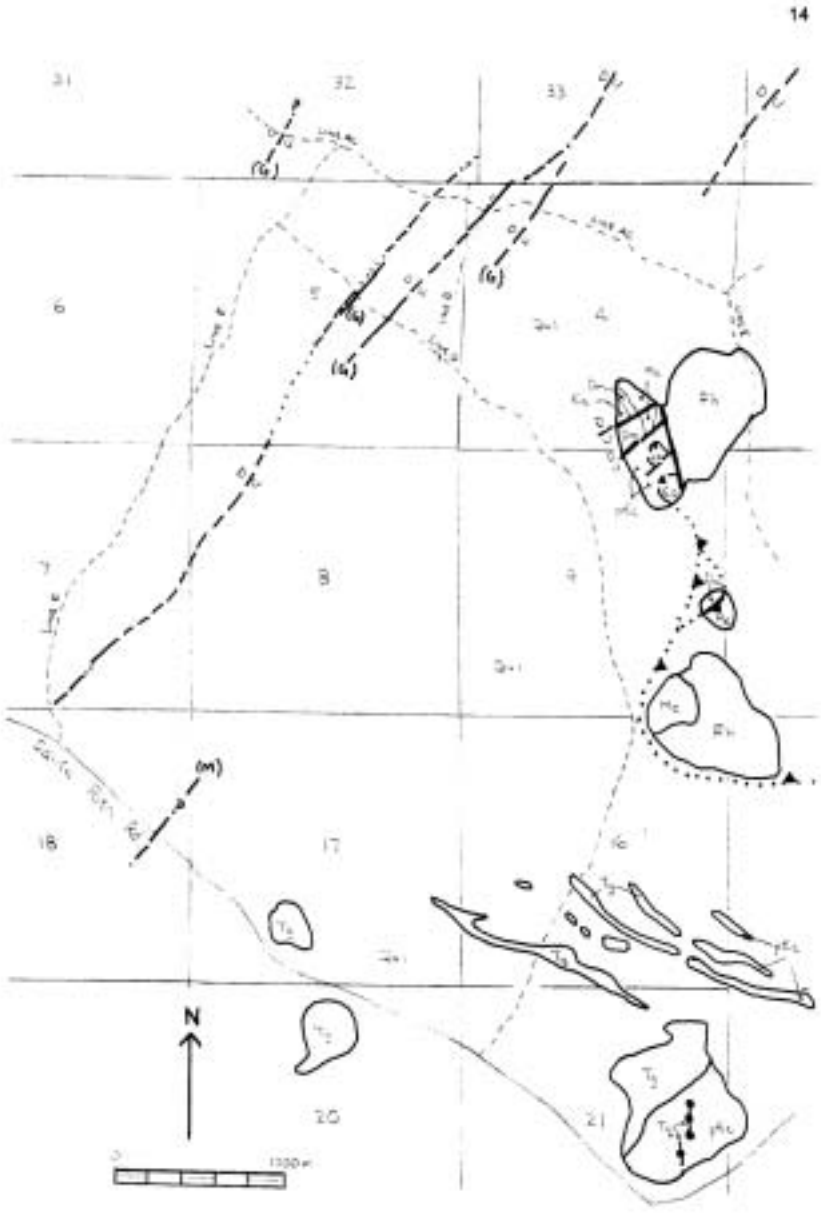

Figure 2. Geologic map of the area. Geology is annotated from Drewes (1971a). Fault projections have been added using gravity and magnetic data. See Table 1 for a description of rock units.

Table 1. Rock units and symbols for geologic map of survey area (after Drewes, 1971a)

Qal	Alluvial sands and gravels, undifferentiated
Tq	Quartz veins
Tg	Granitic rocks, undifferentiated. Includes granodiorite and quartz monzonite stocks, quartz diorite stocks, and aplite masses.
Ph	Horquilla Limestone; fine-grained, moderately thin-bedded limestone and siltstone
Me	Escabrosa Limestone; coarse-grained, thick-bedded crinoidal limestone
Dm	Martin Formation; dolomite, limestone, and siltstone
Ca	Abrigo Formation; shale, quartzitic sandstone, limestone
Cb	Bolsa Quartzite
pCc	Continental Granodiorite, undifferentiated. Includes granodiorite porphyry, aplite, and fine-grained quartz monzonite
	Thrust fault, teeth on upper plate
	Normal fault, with relative movement
	Fault projection based on gravity data
	Fault projection based on magnetic data

Quartzite Formations. These shallow marine deposits, in combination with several Unconformities, reflect a history of alternating marine transgressions and regressions (Drewes, 1972). The Paleozoic sequence unconformably overlies the Precambrian rocks and is thought to have been thrust-faulted over them during the Piman phase of the Laramide orogeny (the Cordilleran orogeny of Drewes, 1981). Buttes composed of both the Precambrian and Paleocene granitic intrusives occur in the southeast portion of the field area.

The several buttes on the eastern end of the survey area have apparently been explored for mineralization as evidenced by several adits and small rectangular pits. The Helvetia mining district is located just to the southeast of the study area along the western flank of the Santa Rita Mountains. The district is composed of four skarn-type copper porphyry systems occuring within Paleozoic and Mesozoic sedimentary rocks (Anzalone, 1995). These rocks have been intruded by two Paleocene intrusives, one of which, a quartz latite porphyry, is closely associated with copper mineralization. Limestones surrounding the quartz latite porphyry are locally altered to skarns, and sulfide mineralization, predominantly chalcopyrite and pyrite, occurs throughout the altered sediments (Anzalone, 1995).

GRAVITY SURVEYS

METHOD

Density variations of crustal rocks cause local variations in the earth s gravitational field. These gravity anomalies can be detected by performing a gravity survey and geologically interpreted by modeling with a 2-D software package such as SAKI (see Webring, 1985).

The gravity meter used in this survey, a LaCoste and Romberg Model G Gravity Meter (Serial No. 575), utilizes a zero-length spring (Telford et al., 1976) supporting a beam with a mass at one end. The earth s gravitational force acts upon this mass producing a change in spring length proportional to the change in the vertical gravity component of the field (Telford et al., 1976). The meter dial reading is converted to milligals by using calibration factors specific to that instrument. Corrections are made for instrument drift by comparing repeated readings at base stations, and theoretical earth tide corrections are made to account for the distortion of the earth caused by the gravitational pull of the sun and moon.

The meter does not measure absolute gravity but measures changes in gravitational attraction from station to station. During a gravity survey, one uses a base station network for which the values of absolute gravity are known, and then values for absolute gravity for field stations can be determined. The primary base station used in this survey, located in the basement of the Gould-Simpson building at the University of Arizona, is tied to the International Gravity Standardization Network 1971 (IGSN 71).

After observed gravity is determined for each station, several corrections are made to remove variations in the gravitational field which are due to a standard earth model. These include the free-air, Bouguer, terrain, and curvature corrections. Application of these corrections results in the complete Bouguer gravity anomaly (CBGA), which is the parameter used in modeling all gravity lines in this study.

DATA ACQUISITION

Survey Lines

Figure 3 shows the locations of the gravity survey lines as well as the field base station. Gravity data were collected along 6 lines, 3 trending perpendicular to the basin-bounding normal fault system and 3 trending parallel to the faults. Line AC is 3.1 km in length and trends roughly ESE. Most stations on this profile are located just off the north side of a jeep trail, veering to the north near the center of the profile to traverse an apparent fault scarp. Spacing varies from about 50 m on either end to as little as 6 m along the fault scarp which is located 2 km from the west end of the line, near station sra-5.5. Most stations are spaced between approximately 10 and 25 m apart. Because Line AC is a concatenation of 2 individual lines, stations are labeled as sra-xx on the west end and src-xx on the east end. The westernmost station is sra-90, the two sub-lines join between sra-02 and src-01, and the easternmost station is src-56. Note that the local base station, sra-01, is located a few meters south of sra-20, near the intersection with Line B; it is not located near sra-02.

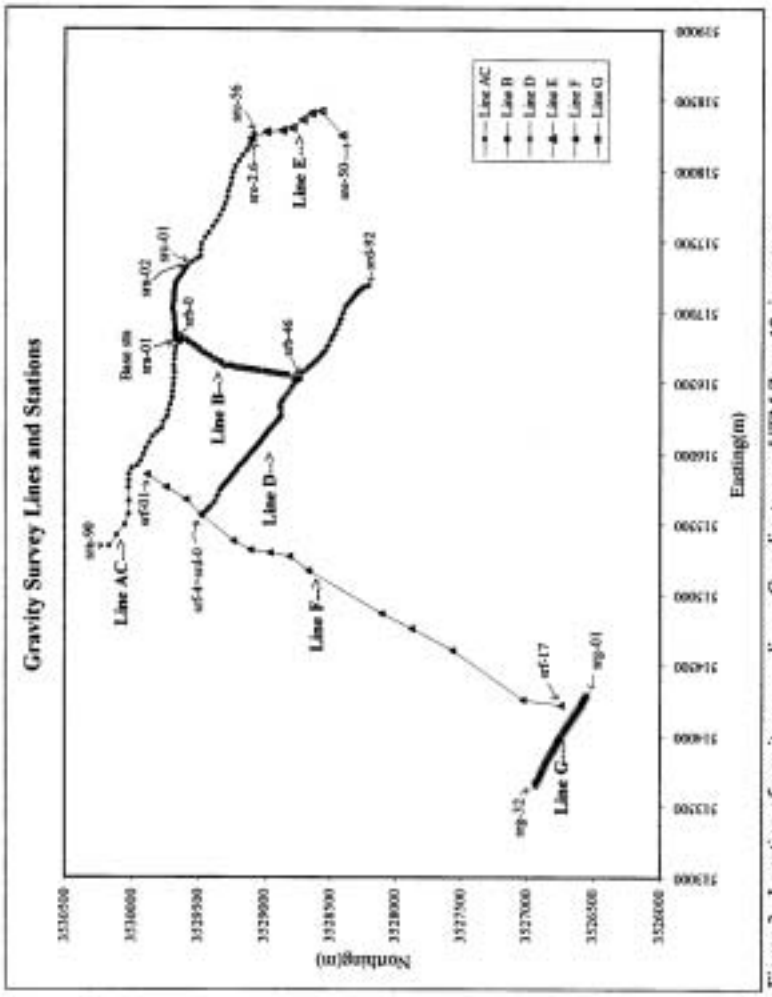

Figure 3. Location of gravity survey lines. Coordinates are UTM Zone 12, in meters.

Line D is approximately parallel to Line AC, trends SE, and is located about 1 km south of Line AC along the north side of a jeep trail. It is about 2 km in length and stations are spaced at about 25 and 50 m apart depending on their proximity to expected fault locations. No fault scarps were evident along this line. Gravity station srd-0 is located at the west end of the line. Line B is about 1 km in length, trends roughly SSW and intersects Lines AC and D at its endpoints. Stations are about 50 m apart, with the northernmost station labeled srb-00 (same station as sra-17) and the southernmost labeled srb-46 (same as srd-54). Line E begins at src-54, which is adjacent to the easternmost station of Line AC. The southernmost station of Line E is sre-46. The line trends roughly SSE along a jeep trail, and the 6 gravity stations are located just off the west side at spacings of about 70 to 100 m. The line is only 0.56 km in length, but a gravity survey was performed because the line partially traverses limestone bedrock at its southern end. Note that station sre-50 is located on a National Geodetic Survey triangulation survey marker at the top of a limestone butte located southwest of Line E, and the gravity data collected at that station were not modeled as part of Line E.

Line F consists of 14 stations along the east side of a northeast-trending jeep trail which intersects Santa Rita Road at its south end and Line AC at its north end. The stations are spaced between 1.5 and 3 km apart, with srf-01 located near the north end of the road and srf-17 near the south end. Several stations are located near deep washes and may need inner-zone (to a radius of 68 m) terrain corrections; however, judging from the topography, the inner-zone corrections are not expected to exceed 0.01 to 0.03 milliGals

(mGal). Elevation control is poor, with elevations for stations srf-6, 8, 9, 12, and 14 estimated from 1:24000 topographic maps.

Line G consists of 32 stations and is located north of and parallel to Santa Rita Road. Station srg-32 is located at the west end, and srg-01 is at the east end. The data collected along Lines F and G are included in Appendix A, but the lines were not modeled.

Station Location Control

All gravity stations, except for several along Line F, were surveyed for relative easting, northing, and elevation using a Trimble differential Global Positioning System (GPS) unit. The survey was tied to a National Geodetic Survey (NGS) triangulation station (NGS Id. No. CG1063) located at the summit of a limestone bluff at the east end of the field area (which coincides with gravity station sre-50). National Geodetic Survey data sheets describe this station in North American Datum 1983 (NAD 83) and North American Vertical Datum 1988 (NAVD 88) coordinates. CORPSCON, an MS-DOS-based coordinate transformation program developed by the Surveying Division of the U.S. Army Topographic Engineering Center, was used to perform the coordinate transformations from NAD 83 datum to NAD 27 datum. Software and documentation are available at the following internet site:

http://www.tec.army.mil/TD/pub/software/corpscon.410.

For input to gravity reduction programs, all gravity station locations were converted to NAD 27 geographical coordinates. For plotting purposes, station locations were converted to NAD 27 UTM (Zone 12) coordinates.

Base Stations

The primary base station used is located in the basement of the Gould-Simpson Building on the University of Arizona campus. This base is tied to an absolute gravity station in northeast Tucson established by the National Geodetic Survey and has a provisional value of 979241.136 mGal (M.E. Gettings, pers. comm., 1997). One mGal is equivalent to $1x10^{-3}$Gal, and the Gal is equivalent to 1 cm/sec^2, which is the unit of acceleration of gravity (Telford et al., 1976). Readings at this base were taken every morning and evening of the survey. One secondary station was utilized in the field area (station sra-01 on Line AC), and readings were repeated there several times during the course of each day of field measurements. During data reduction, the value of absolute gravity at this field station was determined to be 979,130.613 mGal.

Procedure

At each station the LaCoste and Romberg G-575 gravity meter was placed upon a base plate, leveled, and the null dial rotated until the electronic readout scale was centered (always from the left). The counter wheel was read to hundredths of units (corresponding to hundredths of mGals) while the thousandths was estimated. The sensitivity of the instrument is 0.005 units, which approximately corresponds to 0.005 mGal. The instrument was shielded from wind gusts, and the face plate was shaded during leveling and reading. It was noticed that only a few seconds of exposure of the black face plate to the sun s direct rays caused variations in the two bubble levels, as well as in the meter reading. For this reason it was necessary to keep the face plate continuously shaded during leveling and reading.

Terrain Corrections

All stations were examined for the necessity of inner-zone terrain corrections. Inner-zone, in this case, means to a radius of 68 m from the station, which corresponds to the outer radius of the Hayford-Bowie B zone. Slope angles, distances, heights and other data pertaining to terrain corrections were noted and topography sketched for later calculation in the office. Of approximately 40 stations for which inner-zone corrections were calculated, only 23 proved to be significant, that is, exceeded 0.005 mGal.

DATA REDUCTION

Corrections to Data

Along with the meter dial reading, several other data were collected at each gravity station including location (latitude, longitude, elevation), date, and time. Meter readings are converted to observed gravity (g_{obs}) by applying meter calibration constants, tidal corrections, and drift corrections and by applying the difference to the base station value. The meter calibration constants are supplied by the manufacturer and vary with the meter reading. Earth tide corrections are calculated theoretically and account for the gravitational pull of the sun and moon, and drift corrections remove the effects of instrument drift, which is assumed to be piecewise linear in time.

The theoretical value of gravity on the ellipsoid is then calculated using the 1967 Geodetic Reference System Equation (GRS 67), given by (Cordell et al., 1982):

$$g_{\phi} = \frac{978031.84558(1 + 1.93166338321\text{x}10^{-3}\ \sin^2\phi)}{(1 - 6.69460532856\text{x}10^{-3}\ \sin^2\phi)^{0.5}} \quad \text{(mGals)}$$

where ϕ is the latitude of the station.

The theoretical value of gravity accounts for gravity on the ellipsoid of a rotating earth. One must also apply the free-air and Bouguer corrections. The free-air correction accounts for a station s elevation above the ellipsoid and assumes a vacuum between station and the ellipsoid. This correction is added to observed gravity because the increased radial distance of the station from the center of the earth results in a lower observed gravity measurement than would be observed if the station were at datum. The free-air correction is given by (Cordell et al., 1982):

$$FAC = \frac{(0.09411549-0.137789\sin^2\phi)h}{0.3048} - \frac{0.67x10^{-8}h^2}{(0.3048)^2} \quad \text{(mGals)}$$

where h is station elevation in meters.

The Bouguer correction accounts for the rock mass that is actually present between station and datum, and assumes an infinite horizontal slab of rock between the station and datum. The downward pull of this slab must be subtracted from observed gravity because the rock mass between the datum and the station exerts a downward pull on the station. The Bouguer correction is given by (Cordell et al., 1982):

$$BC = \frac{0.012774\ \rho\ h}{0.3048} \quad \text{(mGals)}$$

where ρ is density of the slab in gm/cm^3 (commonly a value of 2.67g/cc is assumed), and h is station elevation in meters.

The Bouguer correction assumes a flat slab of rock between station and datum, so if the actual topography surrounding the station is not relatively flat, an additional correction called the terrain correction (TC) must be applied. Features such as hills or nearby cliffs, which have mass located above the station, exert a component of upward pull on the station. This causes the value of observed gravity to be lower than if the topography were flat, so a correction must be added to observed gravity at the station. Depressional features such as valleys and downhill slopes lack rock mass at the station elevation, causing measured gravity to be less than if the feature were flat. Therefore terrain corrections for depressional features are also added to observed gravity. For the

surveys described in this paper, terrain corrections were calculated using methods described in Robbins and Oliver (1970), and Plouff (1977).

A final correction, the curvature correction, is applied to correct for the infinite horizontal slab used in the Bouguer correction. The curvature correction is (Cordell et al., 1982) :

$$CC = \frac{4.462\text{x}10^{-4}\ h}{0.3048} - \frac{3.282\text{x}10^{-8}\ h^2}{(0.3048)^2} + \frac{1.27\text{x}10^{-15}\ h^3}{(0.3048)^3} \qquad \text{(mGals)}$$

where h is station elevation in meters.

The application of all the preceding corrections results in the complete Bouguer gravity anomaly, as follows:

$$CBGA = g_{obs} - g_{\phi} + FAC — BC + TC — CC \qquad \text{(mGals)}$$

Reduction Programs

Several USGS computer programs were utilized to reduce meter readings to complete Bouguer gravity anomaly (CBGA). Program **grvrdn**, written by M.E. Gettings (pers. comm., 1997) converts the meter reading to mGals, corrects for earth tides and instrument drift and calculates observed gravity for a particular meter. Initially, the data were reduced using the Gould-Simpson base station known as tucgs85 as the only base station, in order to estimate the value of observed gravity at the field base station sra-01. Figure 4 shows how observed gravity at base sra-01 varied over time. The data appear to be affected by tares of up to about 0.45 mGal, as well as instrument drift. Therefore, five

of the lowest values of observed gravity were averaged to determine a value for observed gravity of 979130.613 mGal at the field base sra-01. The data were then re-run through **grvrdn** using both the Gould-Simpson base and the local field base to reduce the data to observed gravity.

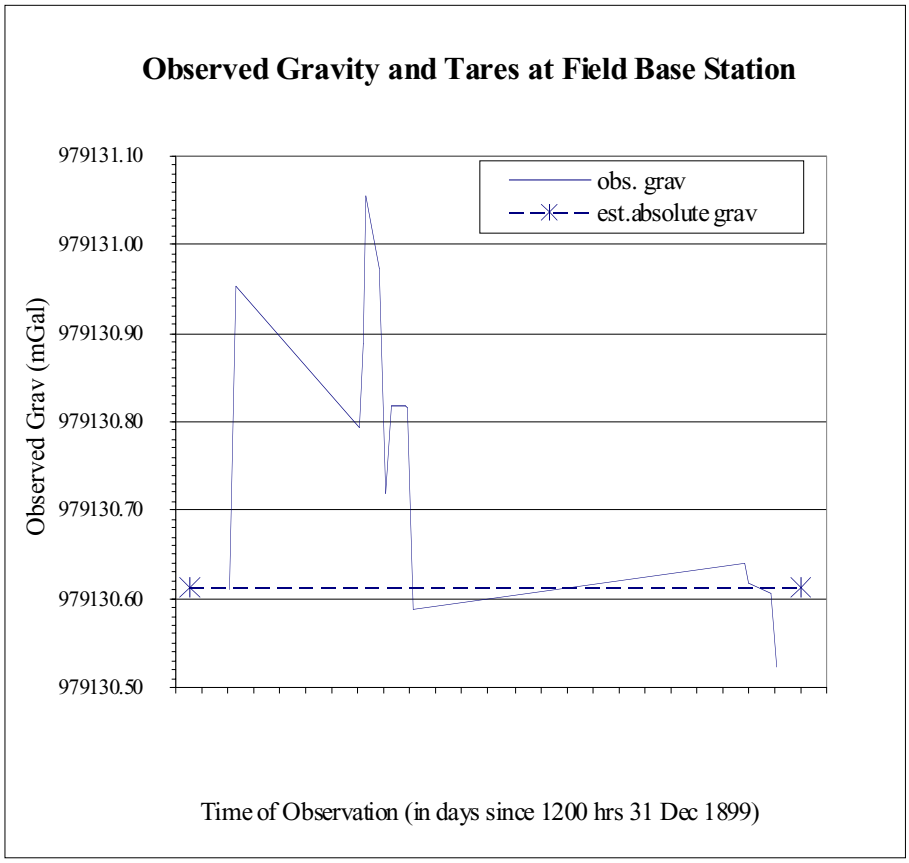

Figure 4. Observed gravity at the local base station. The lower dashed line indicates the average value obtained for observed gravity.

Inner-zone terrain corrections to a radius of 68 m (corresponding to the Hayford-Bowie AB correction) were calculated using several computer programs (**hhslope**, **bhslope**, **hcone**, and **sect**) written by P.E.Gettings (M.E.Gettings, pers. comm., 1997) and based on methods described in Robbins and Oliver (1970). These inner-zone terrain

corrections were edited back into the observed gravity file, and program **terrain_correct** was run to compute the total terrain correction for each station to a radius of 167 km. This program utilizes a digital elevation database to compute a correction out to radius 167 km, then adds this correction to the inner zone correction supplied by the user. Finally program **pfact** was used to calculate the free-air Anomaly (FAA), and the simple Bouguer and complete Bouguer gravity anomalies (SBGA and CBGA, respectively) using a crustal density of 2.67 g/cc. The CBGA values plotted versus true distance (station-to-station) for each line are shown in Figures 5 through 10.

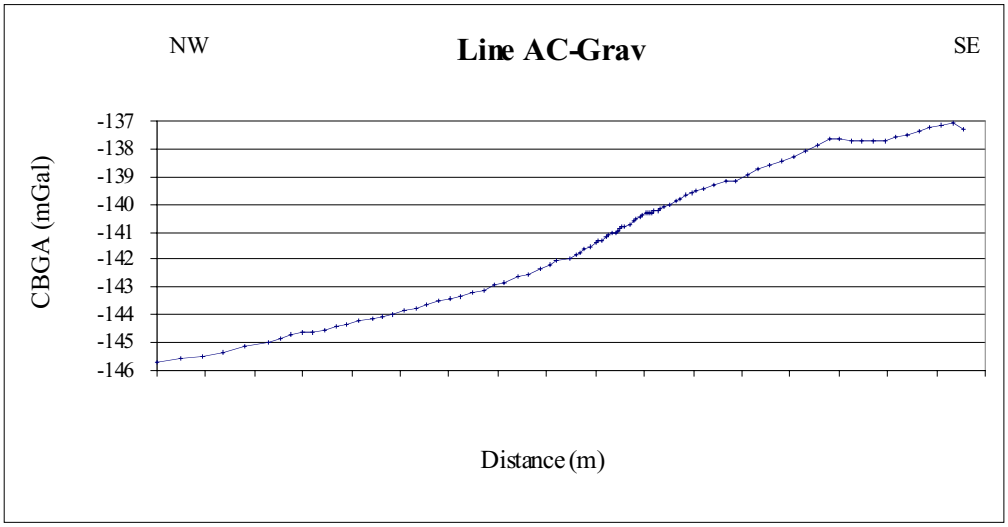

Figure 5. Complete Bouguer gravity anomaly data for Line AC. Fault scarp is located at 2000 m.

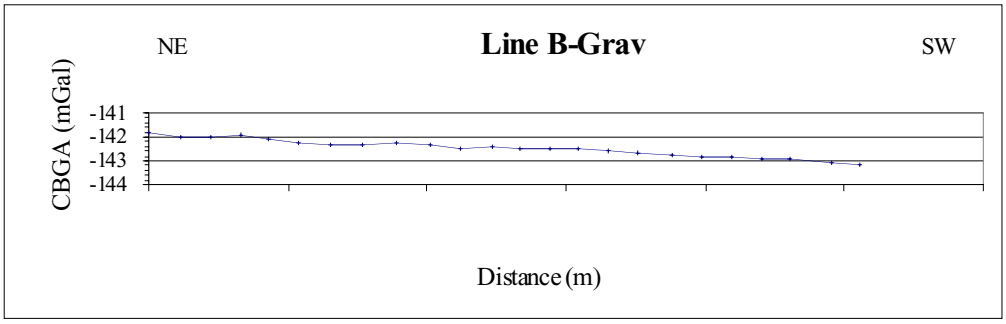

Figure 6. Complete Bouguer gravity anomaly data for Line B.

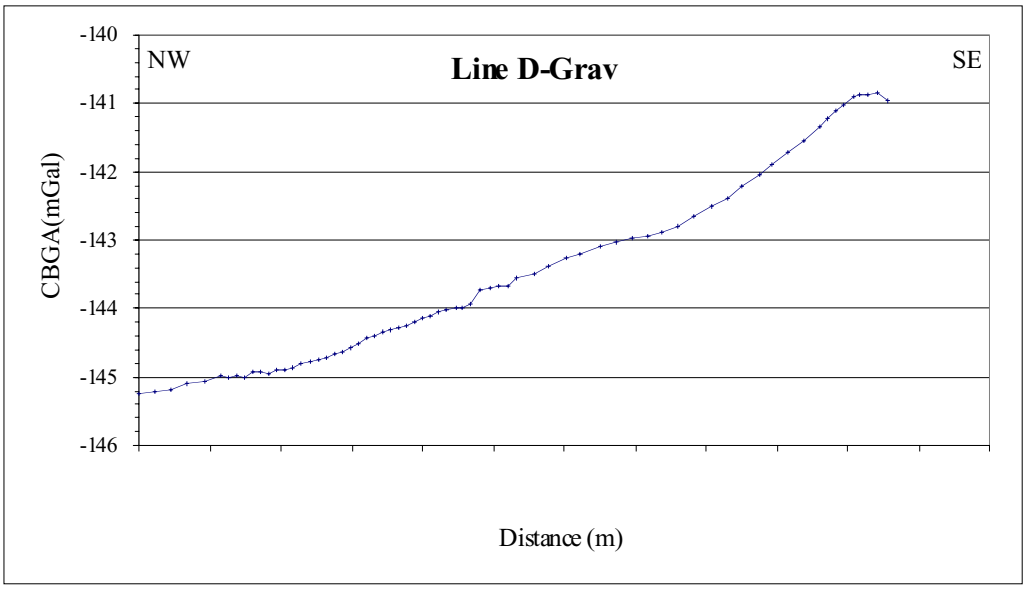

Figure 7. Complete Bouguer gravity anomaly data for Line D.

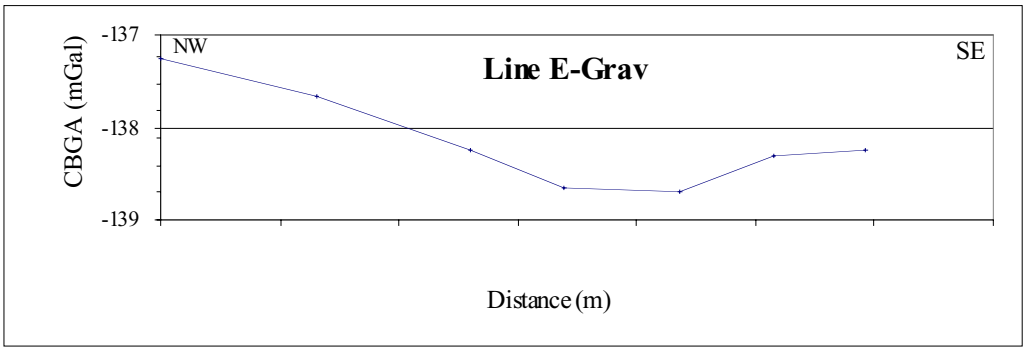

Figure 8. Complete Bouguer gravity anomaly data for Line E. The last station on the southeast end is situated on limestone bedrock.

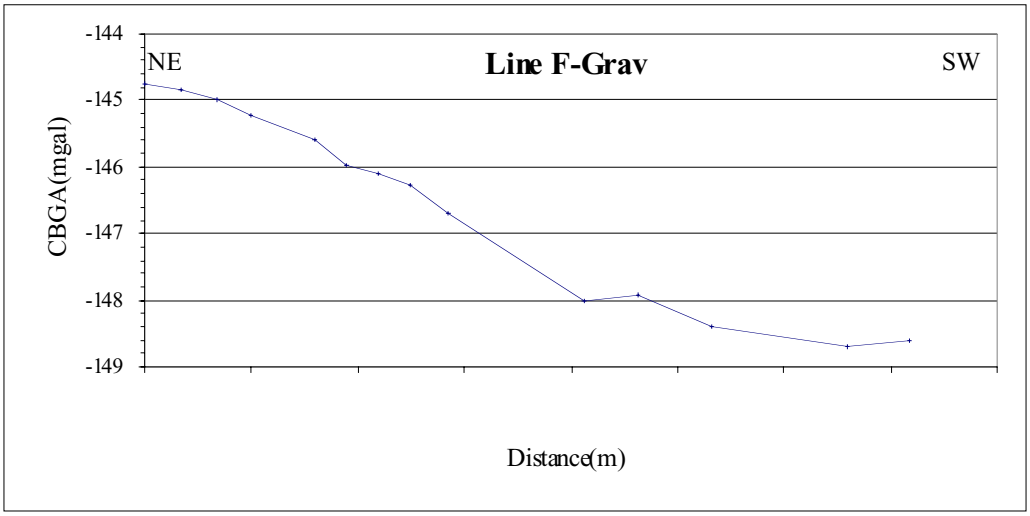

Figure 9. Complete Bouguer gravity anomaly data for Line F. Several of the data points probably require inner-zone (to 68 m) terrain corrections that are not expected to exceed 0.03 mGals.

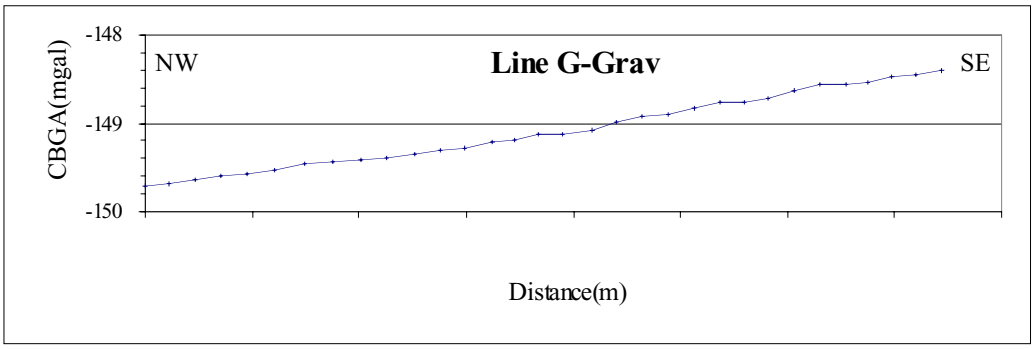

Figure 10. Complete Bouguer gravity anomaly data for Line G.

MAGNETIC SURVEYS

METHOD

Local variations in magnetic properties of crustal rocks cause anomalies in the earth s magnetic field. These local variations are usually caused by the presence of magnetite or its related minerals in the iron-titanium-oxygen geochemical group, or much less commonly, by pyrrhotite, an iron sulfide, or ilmenite (Breiner, 1992). Hematite is weakly magnetic, much less so than magnetite. Man-made objects which contain iron or nickel, such as fences and underground pipes also can produce disturbances in the local magnetic field and should be noted during surveys.

There are two types of magnetism which cause disturbances in the local magnetic field. Induced magnetism is the ability of a material to enhance the earth s field, and it is induced by and superimposed upon the earth s present field. The magnitude is a function of both the earth s ambient field strength and the material s magnetic susceptibility, which usually is dependent upon its volume percent of magnetite (or less commonly, other magnetic minerals). Magnetite itself has a susceptibility of between 0.3 and 0.8 cgs (Dobrin, 1976), so a rock body containing 1% by volume magnetite would have a susceptibility of between 0.003 and 0.008 cgs. Iron alloys can have much higher susceptibilities, between 1 and 1,000,000 (Breiner, 1992), and so can cause very strong anomalies.

Remanent magnetization is a permanent magnetization which depends upon the magnetic field that existed when the rock formed, and to a lesser extent on exposure to

subsequent magnetic fields. In the case of igneous rocks, remanent magnetization depends on the volume percent and grain-size distribution of magnetite, the direction of the earth s magnetic field at the time the rock cooled, and later chemical or thermal disturbances.

DATA ACQUISITION

Instrument

All magnetic data were collected with proton precession magnetometers, either truck-mounted, or of a portable hand-held type. These instruments contain a coil immersed in a hydrocarbon-rich fluid. A current is applied to the coil, causing the hydrogen nuclei (protons) in the fluid to align along the applied field. When the current is removed the protons precess about the direction of the earth s magnetic field. The instrument measures the frequency of the signal generated by the precessions, which is proportional to the total magnetic field intensity (Breiner, 1992), and the instrument records total magnetic field vector intensity but not its direction.

The portable instrument used in this survey was the Geometrics G-856 magnetometer. The sensor was located at the top of a 2.4 m staff. The instrument has an electronic readout and stores data so that the data can later be dumped to a computer. In the case of the particular instrument used, the magnetometer reading itself could not be successfully downloaded to 3 of the 4 computers with which it was attempted. It is possible that data transfer parameters were not compatible. The magnetic readings appeared to become corrupt during downloading. Other pertinent data such as line number, day, and time were not affected, so for most stations, these data were dumped and the magnetic field reading was entered into the computer by hand.

The truck-mounted instrument used along both Line D and Santa Rita Road was a Geometrics G-811 airborne proton precession magnetometer. However the data collected along Santa Rita road in 1989 were acquired without concurrent GPS data, while the data

along Line D were collected concurrently with GPS data. In both surveys the instrument was towed 4.6 m behind the truck at a height of 3.8 m.

Survey Lines

Magnetic data were collected on all gravity lines, as well as along Line V which is located between Lines AC and D, and along Santa Rita Road. The portable G-856 magnetometer was used on Lines AC, B, E, and V. Readings were taken at all former gravity stations as well as between these stations, at spacings varying from about 6 m to about 12m. For Line V, which had no gravity stations, readings were collected approximately every 8m. Figure 11 shows the location of all magnetic survey lines in the field area.

The USGS truck-mounted system was used to collect data along Line D. Data along Santa Rita Road were previously collected in 1989 with the USGS truck magnetometer system; see Gettings et al. (1995) for a detailed description of data collection and reduction procedures and programs for the truck magnetometer system.

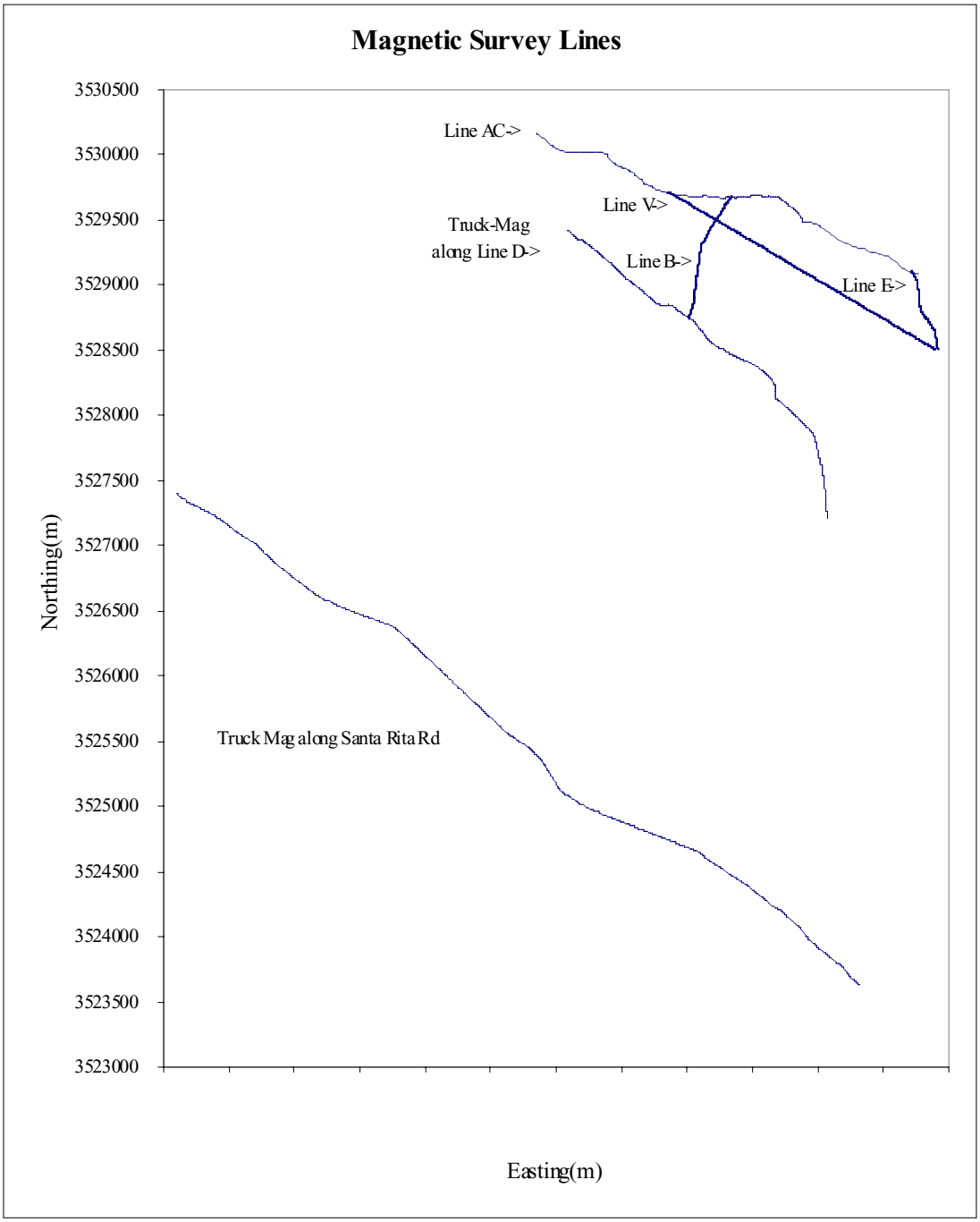

Figure 11. Location of magnetic survey lines. Map coordinates are UTM, zone 12, in meters.

Station Location Control

Most magnetic stations were located between the previously surveyed gravity stations, and so their locations had to be interpolated. This was the case for Lines AC, B, and E. On Line V, a USGS military-issue GPS unit, accurate to ±10 m horizontally (M.E. Gettings, pers. comm, 1998) was used to survey some of the stations. On average, every 15th station was surveyed, and rarely every 18th. Locations of stations between these points were linearly interpolated. Elevations were estimated from 7.5 minute topographic maps.

For the truck magnetometer data collected along Line D, latitude and longitude coordinates of the station collected by the on-board GPS unit were used for station locations. The archived truck magnetometer data collected along Santa Rita Road were previously corrected for location by digitizing the truck s route, and comparing known positions in the data with known positions on the map (Gettings et al., 1995).

Base Stations

Several field base stations were used in the portable G-856 survey. The primary base station was sra-01 on Line AC, the same station used as the field gravity base. The average of the first 3 readings at this station, 48680.70 nT, was used as the value of total field at this base, and all subsequent readings were tied to this base reading. Readings at the base were normally performed every 1 to 3 hours, while secondary bases on each individual line were used between primary base readings.

For the truck magnetometer surveys, magnetic data collected by an automated system at the Tucson Magnetic Observatory were used as base station data. These data as

well as data collected worldwide can be downloaded from the Space Physics Interactive Data Resource (SPIDR) website maintained by the National Geophysical Data Center at:

http://www.ngdc.noaa.gov:8080/production/html/GEOMAG/geo_search_frames.html

Both one-minute and hourly data values are available for downloading. In this study, the one-minute data was used as base station data for the truck magnetometer surveys.

Procedure

For surveys using the portable G-856 unit, extreme care was taken to carry no metal objects, except for hiking boots with metal eyelets. Cultural sources of noise such as cattle guards and barbed-wire fences were noted, and these data later were removed from the model datasets. Three successive readings were taken each time a station was occupied to help detect high gradients and geomagnetic transients. The instrument was tuned to 48700 nT at the beginning of each day, and at least 3 successive readings were taken at the primary base station located on Line 1. Generally another station or two on each line was used as a secondary base, depending on the length of the line and distance to the primary base. These local bases were occupied two or more times during the course of surveying the line. Data collection procedures for the truck magnetometer data collected along Santa Rita Road and Line D are outlined in Gettings et al. (1995).

DATA REDUCTION

The data collected with the portable G-856 magnetometer were reduced using Excel spreadsheets in a manner consistent with standard USGS practice. The data were corrected for diurnal variations by comparison with base station data, and the International Geomagnetic Reference Field (IGRF) was removed.

The 3 readings taken at each station were averaged to produce one value per station. Magnetic readings were assumed to vary linearly in time between successive base station readings. Each set of data was then adjusted by a static amount to reduce the set of readings to the primary local base sra-01, which was assigned a value 48680.70 nT. The final step was to remove the IGRF, which was calculated at numerous stations along each survey line and linearly interpolated between calculated points.

The truck magnetic data collected along Line D were reduced in a similar manner, with the addition of a heading correction (see Gettings et al., 1995). The heading correction removes the magnetic effect of the truck, which varies depending on the direction of travel. The heading was calculated for each station based on its location and the location of the previous station. The Tucson Magnetic Observatory one-minute interval data were used as base station data. Corrected and reduced magnetic data are shown in Figures 12 through 17. Also see Appendix B for a listing of magnetic data collected with the portable magnetometer along Lines AC, B, E, and V. The data collected with the truck-mounted system are available from the USGS through anonymous FTP at strider.tfo.arizona.edu:/pub/open_file/truckmag.

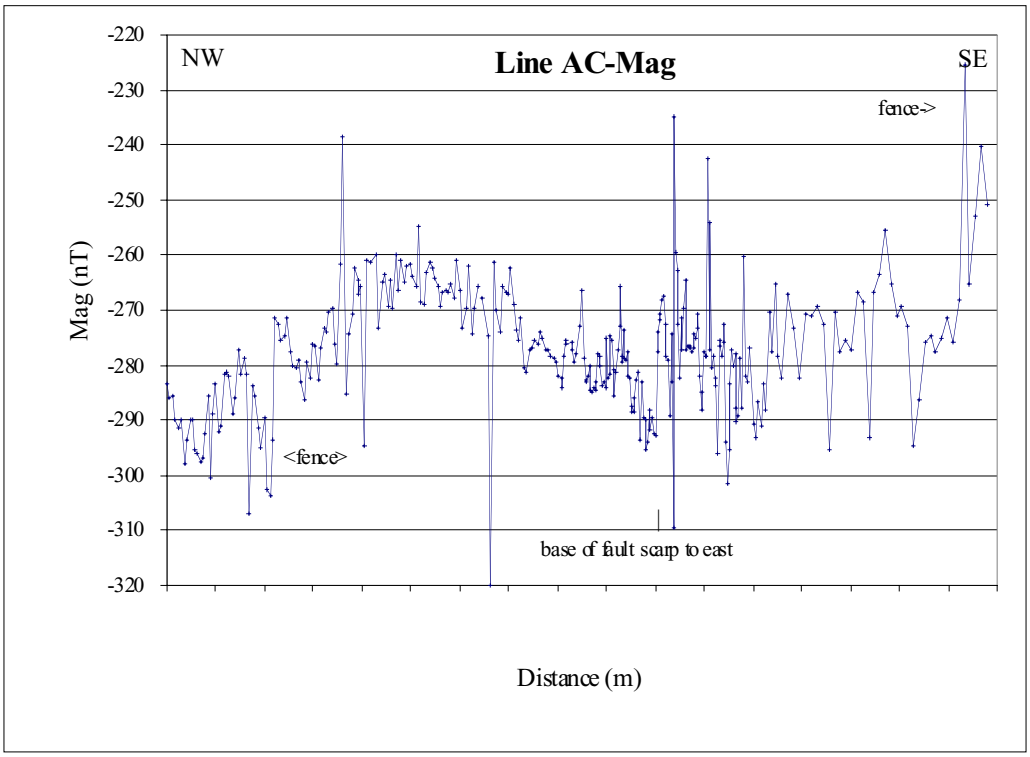

Figure 12. Line AC magnetic anomaly profile

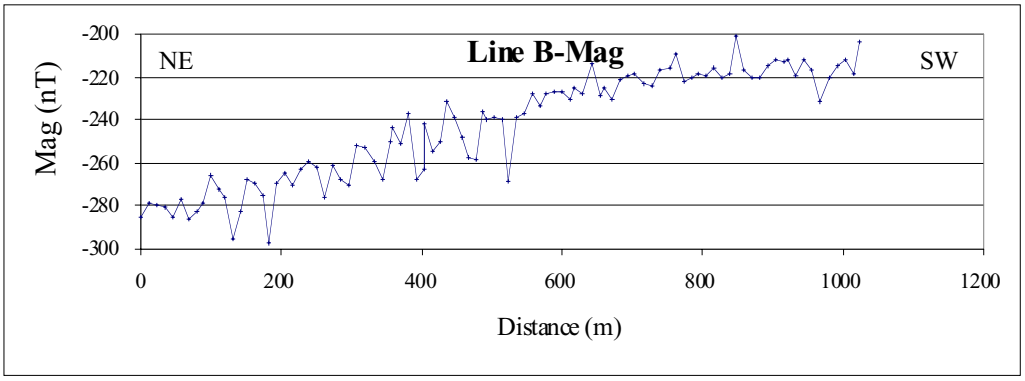

Figure 13. Line B magnetic anomaly profile.

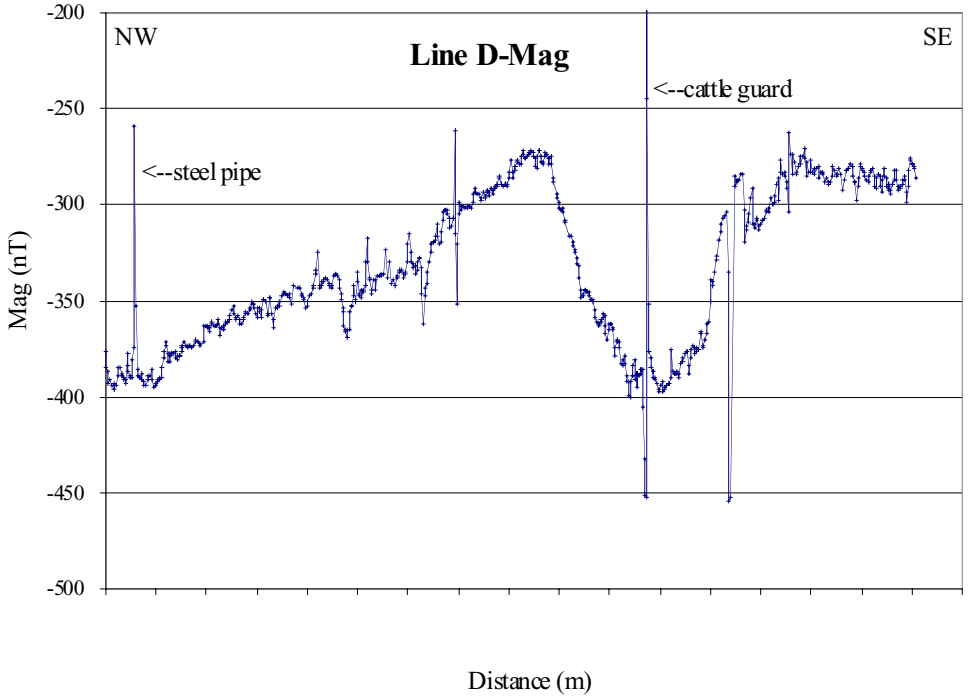

Figure 14. Line D magnetic anomaly profile. The data were collected with the USGS truck-mounted system. Gravity data for this line were acquired only from 0 to 2100 m.

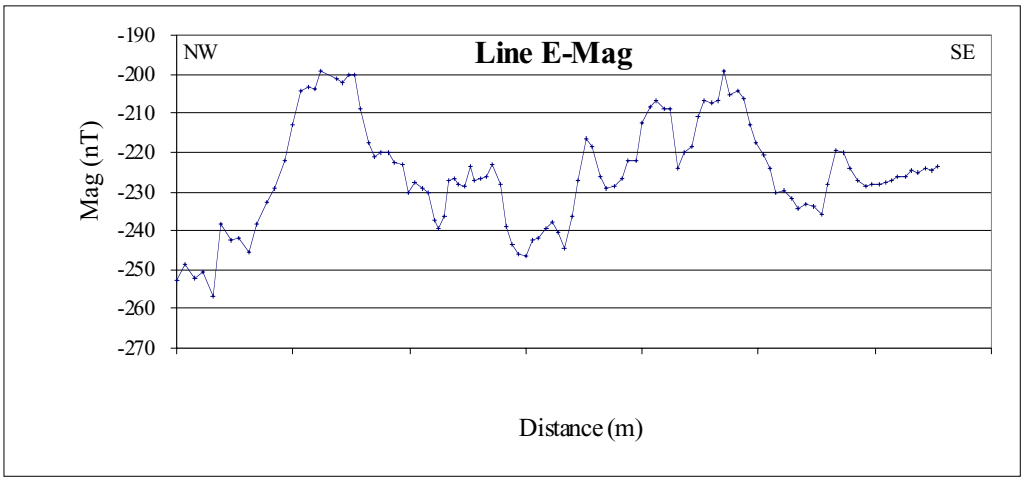

Figure 15. Line E magnetic anomaly profile.

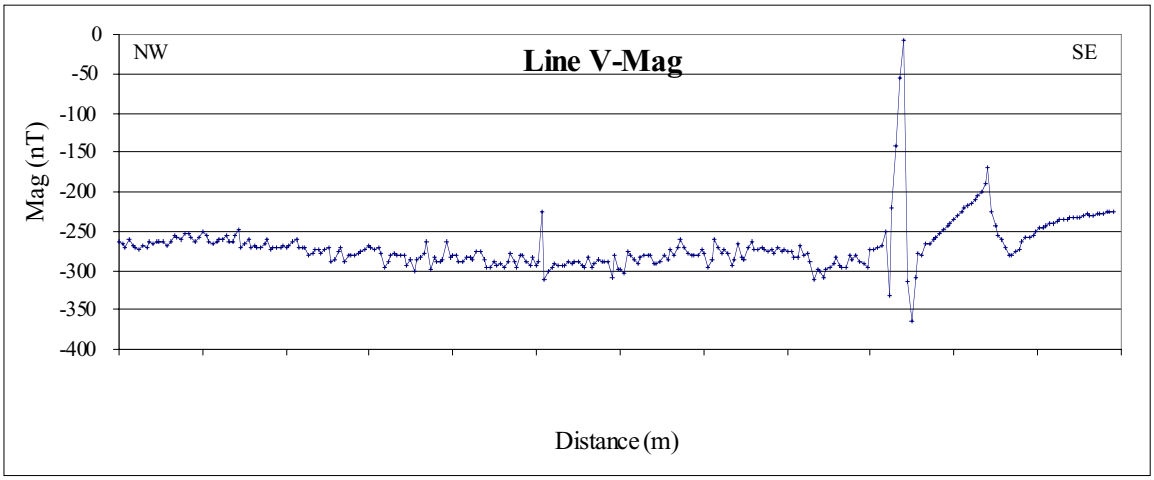

Figure 16. Line V magnetic anomaly profile.

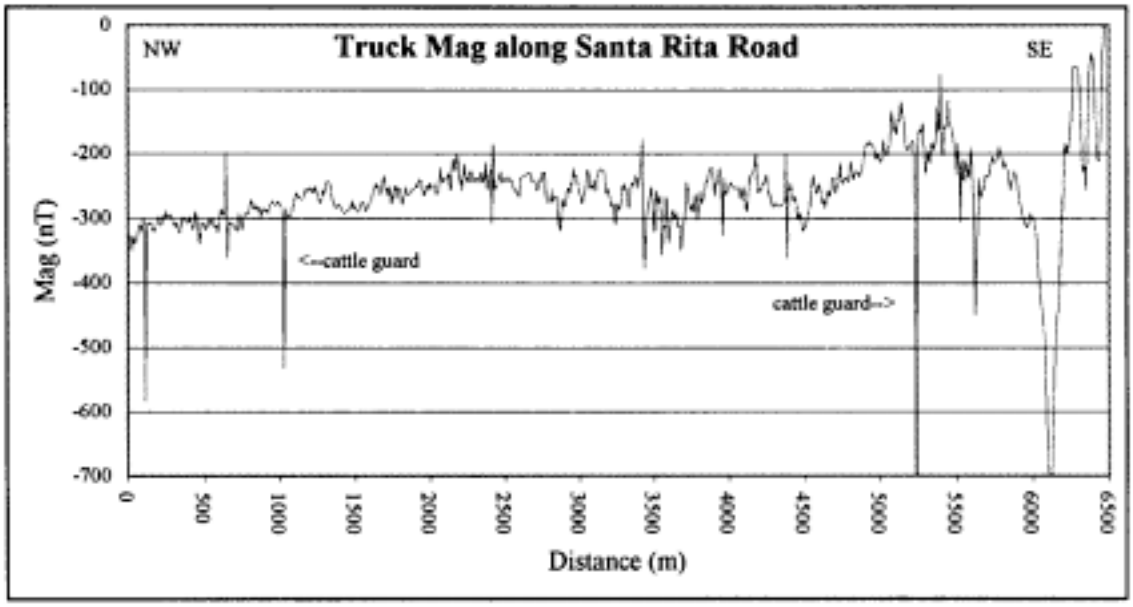

Figure 17. Santa Rita Road magnetic anomaly profile. The data were collected with the USGS truck-mounted system.

MODELING AND INTERPRETATION

Software

The bulk of the two-dimensional forward modeling was performed with the program SAKI, written by Webring (1985) for the USGS and based on the methods of Talwani et al. (1959) and Marquardt (1963). Other modeling software based on the same methods was also used. The program calculates and displays the gravity and magnetic response from a user-defined geologic cross section, and also allows inversion based on least-squares best fit. The cross section is defined by closed polygons, each of which is assigned a constant value of density, magnetic susceptibility, and possibly magnetic remanence. Initial estimates of these values were based on geologic mapping by Drewes (1971), geophysical modeling by Gettings and Gettings (1996), average values given in textbooks (see Dobrin, 1976; Carmichael, 1982; Heiland 1968), and field observations.

Projection to straight line

Because the modeling software requires straight line profiles, a least-squares best-fit line was calculated for each survey line using all magnetic and gravity station locations. All stations were projected perpendicularly onto this line, and station distances were calculated from the first station on each line (always the northernmost or westernmost station). Azimuth of each best-fit line was also calculated for input to the modeling software. Figure 18 shows the map locations of both surveyed and projected lines.

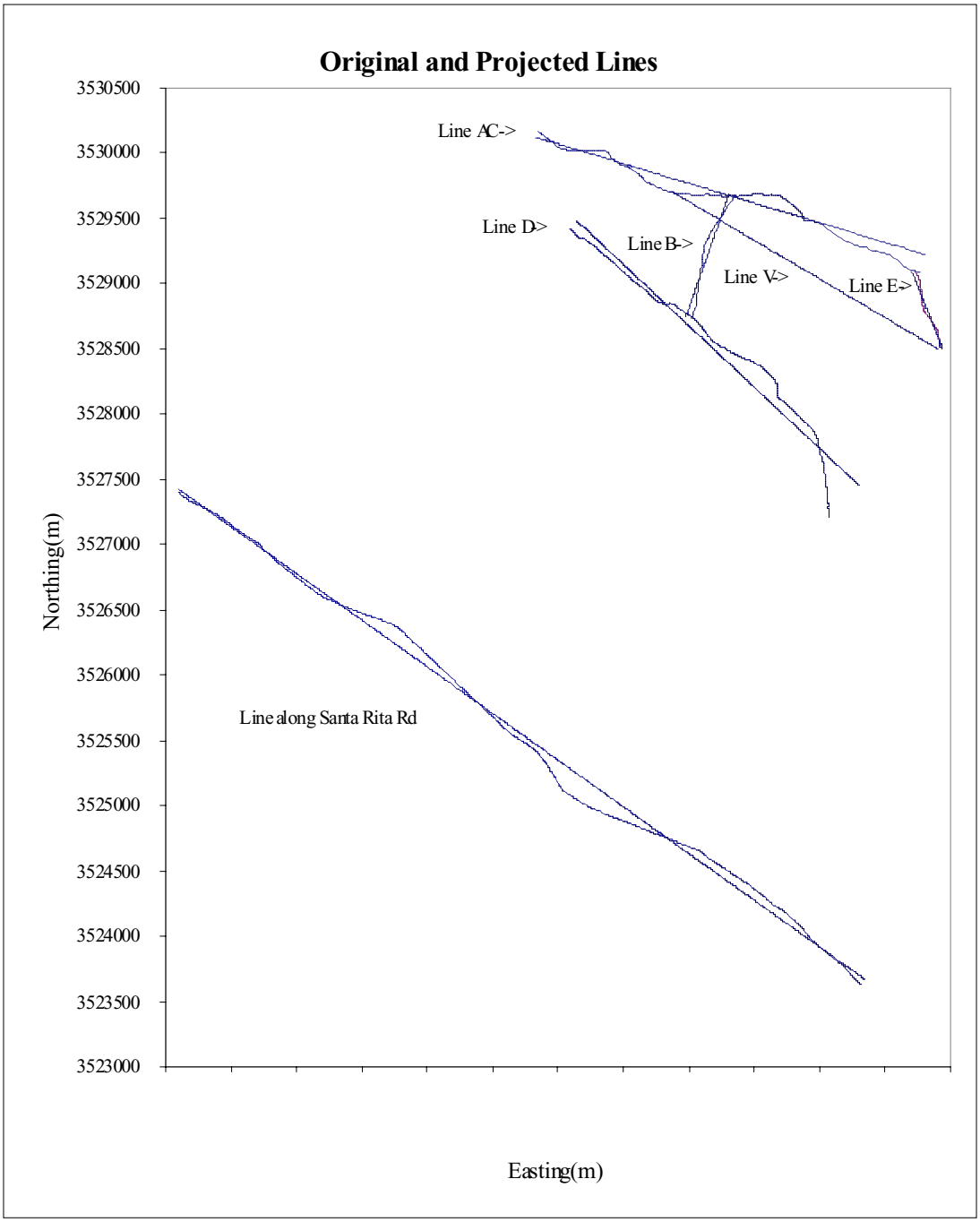

Figure 18. Location of original lines and projected lines. Original and projected lines for Line V are nearly identical.

The modeling software is limited to a maximum of 500 observation points, and the two truck magnetometer lines along Santa Rita Road and Line D originally contained between 700 and 900 observations each. Both lines were decimated in the same manner, by removing every other reading, then every 10^{th} reading. Also at this point, magnetic anomalies which could be attributed to cattle guards, drainage pipes, and fences were removed from the modeled lines. These cultural features had previously been noted in the field, and if an anomaly was observed in the same location, it was removed from the data. Also if the magnetic anomaly was very high amplitude but only a few stations wide, it was assumed to be caused by a cultural feature and removed from the projected lines used for modeling.

LINE E

Because Line E traverses outcropping limestone on its southern end, the gravity profile of Line E was modeled first in order to constrain depths on the other lines. There are no wells in the immediate area with which to constrain depths or lithologies. The nearest well (Phillips Petroleum Mountainview State A-1) is located about 8 km northeast of the survey area, but well logs were not examined. Figure 19 shows the modeled profile of Line E, and Table 2 describes the rock bodies used in all modeled profiles. The limestone on the south end of the line, the Pennsylvanian Horquilla Limestone, is modeled at between 150 and 300 m thick, which is an estimate based on a cross-section by Drewes (1971a) through that particular limestone butte. The north end of the profile shows a very thin layer of sediments underlain by Precambrian Continental Granodiorite at a depth of 7 m. This may be too shallow; Drewes (1971a) mapped outcrop of Continental Granodiorite about 1 km east of the north end of the profile, but there are no intrusive rocks exposed in the immediate area. The proximity of the granodiorite to the surface on that end was necessary to fit the gravity profile with the given densities, but it is possible that either the density used for limestone is too high, at ρ=2.5 g/cc, or the limestone thickness has been underestimated. Heiland (1968) gives several densities (determined by various workers) for limestones at between 2.67 and 2.84 g/cc, with one value for a limestone of 2.07. Kearey and Brooks (1991) give an approximate density range for limestone of 2.60 to 2.80 g/cc, so it seems that dropping the density of the limestone to a value less than 2.5 g/cc would not be reasonable.

On the other hand, boosting the thickness of the limestone to about 400 m

47

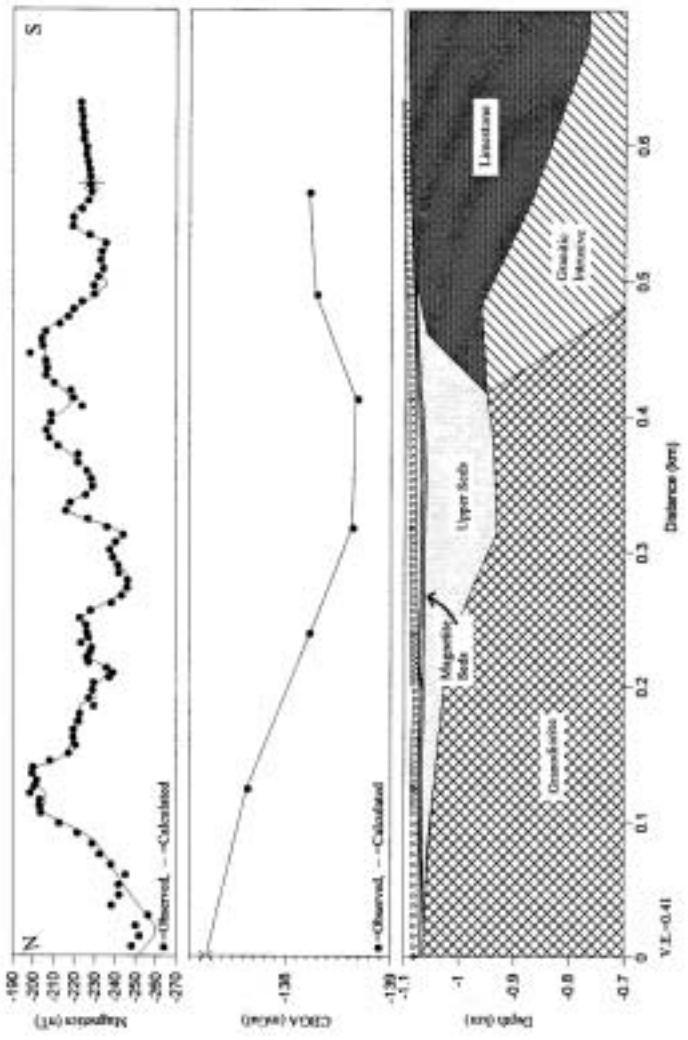

Figure 19. Modeled gravity and magnetic profile along Line E. Magnetite Seds unit (0.001 to 0.0025 cgs) was inserted near surface, within Upper Seds unit to fit the variable magnetic profile.

Table 2. Description of modeled rock units. Modeled bodies can be seen in Figs. 19 through 24; 27; 29.

Body Name	Density (g/cc)	Magnetic Susceptibility (cgs units)	Remanent Magnetization			Comments
			Intensity (cgs units)	Inclination (degrees)	Declination (degrees)	
Upper sediments	2.2	0.00002				
Dense sediments	2.4	0.00002				Line B only; produce slight grav highs in washes
Magnetite sediments	2.25	0.001 to 0.0025				Line E only; produce magnetic variations that cannot be modeled by changing bedrock suscept.
Lower sediments	2.2	0.0001 to 0.00025				Produce mag anomalies that cannot be modeled by changing bedrock suscept.
Dike(?) A	2.67	0.001	0.008	-60	-170	Line V only; dike or mineralized contact zone; two adits within 300m; can be modeled as having no remanence if strike angle reduced
Dike(?) B	2.67	0.0004	0.001	-60	-170	Lines V and Santa Rita Road; possible andesitic dike like that observed on butte above line V
Volcanic Flow	2.5	0.0006	0.002	-70	-160	Line D only; possibly an ash flow tuff or other volcanic unit
Granitic Intrusive	2.67	0.00055 to 0.00065				Corresponds to Tertiary granitic rocks of Drewes (1971a)
Limestone	2.5	0.00004				Corresponds to Pennsylvanian Horquilla Limestone of Drewes (1971a)
Continental Granodiorite	2.67	0.0002				Corresponds to Continental Granodiorite of Drewes (1971a)

48

deepens the granodiorite on the north end to about 50 m depth, which causes modeled bedrock on Line AC (which shares that northernmost gravity station of Line E) to be too deep, demonstrated by highly exaggerated subsurface topographic features which must be modeled onto the bedrock surface. The densities and depths modeled on Line E appeared to be a reasonable compromise.

The granitic intrusive, modeled after the Tertiary Granitic rocks of Drewes (1971a), which is shown as underlying the limestone on Line E, was added to fit the magnetic data. Susceptibilities of limestones are generally quite low (R.F. Butler, pers. comm., 1998). Dobrin (1976) gives a range for limestones of $2x10^{-6}$ to $2.8x10^{-4}$ cgs (as measured in the lab). The value of susceptibility used in this profile for the limestone was $4.0x10^{-5}$ cgs. The underlying intrusive was assigned a susceptibility of $6x10^{-4}$cgs, which is somewhat less than the average of $6.47x10^{-4}$cgs given in Dobrin (1976) for acid igneous rocks.

The geologic source of the variable magnetic response between the north and south ends of the profile is unknown. The short wavelengths suggest a shallower source than bedrock. In fact, modeling the bedrock as multiple prisms of varying susceptibilities was not successful because the short wavelengths could not be fit. Instead, a layer of high-susceptibility sediments ($1.0x10^{-3}$ to $2.5x10^{-3}$cgs) was inserted into the low-susceptibility Upper Seds unit, close to the surface, and the magnetic curve fits closely. This does not mean to imply the actual existence of one shallow layer of sediments of slighly varying magnetic susceptibilities. The magnetic susceptibilities, thickness, and the depth of this layer all can be varied and the anomalies still can be fit well.

The cause of the magnetic response may be a series of buried stream channels which accumulated different amounts of magnetite or magnetite-bearing rocks, depending upon upstream source rocks eroding at the time. While there are no intermediate or mafic volcanic flows mapped in the adjacent highlands, possible sources might be the Precambrian granodiorite or Tertiary intrusives that are exposed only 1 km upstream. Very short-wavelength anomalies such as the one located at about 0.3 km may be due to lightning-induced remanent magnetization (R.F. Butler, pers. comm., 1998).

Drewes (1976) analyzed the chemistry and mineral content of the plutonic rocks of the Santa Rita Mountains. Of 19 samples of Continental Granodiorite, 6 of which were slightly metamorphosed, the average volume of magnetite by point count was 2.1%, and the range in volumes was from 0.4% to 4.4%. An analysis of the Tertiary granitic rocks also showed some variation, from 0.3% for the Helvetia Stock (located about 5 km to the southeast) to 1.4% for the Sycamore Stock (in the Sycamore Canyon area, about 3.0 km to the northeast). Tertiary rhyolite porphyry and vitrophere dikes outcrop about 0.8 km upstream from Line E. However the magnetite content given by Drewes (1972) of a trace to 0.1% would seem to preclude the Box Canyon dike swarm as a source for the magnetic anomaly. It is possible that the source rock for the anomaly has eroded completely out of the highlands and exists only as sediments.

LINE AC

The modeled profiles of Line AC is presented in Fig. 20. Modeling suggests the Continental Granodiorite bedrock is close to the surface at the SE end of the line, where it intersects the north end of Line E. Bedrock deepens northwestward due to faulting and possibly erosion.

The gravity model indicates the presence of several faults along the profile. Near-surface dip of these faults is modeled at between 55° and 65°. A fault was modeled at about 1.8 km to coincide with a fault scarp observed at this location, and to coincide with the abrupt magnetic change and a curious anomaly in the gravity profile at this point. This short-wavelength gravity anomaly cannot be closely fit with the model chosen, and indicates a source closer to the surface than the modeled bedrock. The anomaly occurs exactly at the base of the fault scarp which rises to the east, at station sra-5.5. Projected northeastward, the anomaly intersects a fault mapped by Drewes (1971a); both are shown on Fig. 2. The model indicates a near-surface fault dip of about 63°. A second probable fault is modeled at 1.6 km along the profile. Projected northeastward, it also intersects the lower, curved tail of the same fault of Drewes (1971a). The model indicates a near-surface fault dip of about 58°. It appears that the fault Drewes mapped splays into two faults. Figure 2 shows a geologic map of the field area after Drewes (1971a) and included are likely fault locations based on the gravity data in this study.

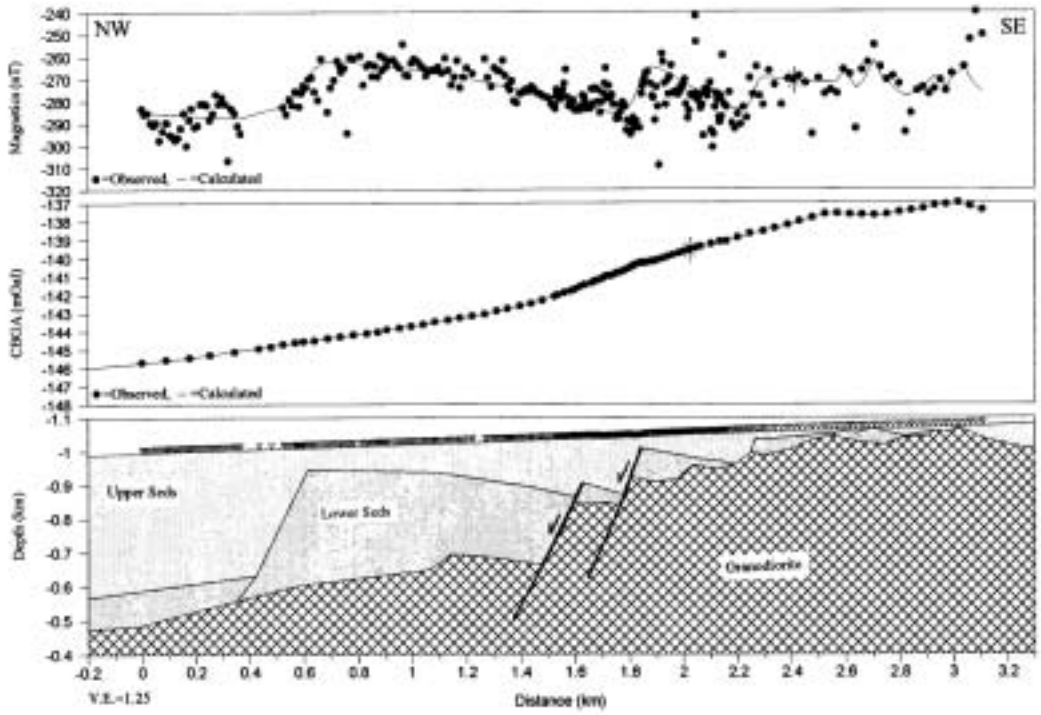

Figure 20. Modeled gravity and magnetic profile along Line AC. Lower Seds unit of higher susceptibility than Upper Seds was required to fit the magnetic profile. Fault scarp is located at 1.85 km.

52

What appear to be faults at about 1.15 km and 2.0 km on the modeled profile are apparently just vestiges of projecting to a straight line, because they are not evident on the original, unprojected gravity profile (see Fig. 5). On the other hand, a small shift in the CBGA located between 504 m and 550 m on the original profile is nearly imperceptible on the projected model profile (between 0.48 and 0.53 km) and was not modeled as a fault. However it seems possible that it is a fault. All data on the original profile (Fig. 5) from 0 to 831 m were taken on the same day and were tightly controlled by field base station readings. Figure 4 shows several apparent tares for the local field base station, and on that particular day, day number 35559 from year 1900, there were no obvious tares between base station readings. Therefore the presence of a fault at this location seems plausible.

The magnetic profile of Line AC is rather noisy, especially along the southeast end with a number of one- and two-station wide spikes. These might be explained by lightning strikes which can cause extreme local magnetic remanence on the order of 10 to 100 nT (R.F. Butler, pers. comm., 1998).

The creation of the Lower Seds unit was required to model the observed magnetic profiles. The magnetic anomalies could not be fit well merely by dividing the bedrock into prisms of various susceptibilities. The sharp rise in magnetic response at about 1.8 km requires a source much nearer the surface. However, modeling the magnetic profile strictly by increasing the susceptibility of the Upper Seds was not successful either. The abrupt increase at the scarp could be modeled in this manner, but none of the rest of the line fit well. The magnetic response seems to require a unit located between the Upper

Seds and the Granodiorite, divided into blocks of varying susceptibilities between $1.0x10^{-4}$ cgs and $2.5x10^{-4}$. This unit has no obvious equivalent on Drewes geologic map of the area. It may be one of the older Quaternary or Tertiary alluvial units that has been buried by younger alluvium. The surface of the scarp itself appears to be the Pleistocene Q2a soil unit described by Pearthree and Calvo (1987), judging by its strong red color. The soil unit is believed to be formed upon very coarse-grained, poorly sorted deposits which overlie finer-grained basin fill deposits and broad bedrock pediments . It seems likely to have been derived by the erosion of a susceptible unit in the highlands, perhaps one of the Tertiary intrusives.

The extreme topography of the Lower Seds unit at 0.6 km does not seem very realistic, and its position and even its existence should not be taken literally. It is simply one explanation for the magnetic anomaly located there. The wide, low-amplitude anomaly between 0.5 and 1.6 km is just as easily modeled by inserting an intrusive of higher susceptibility ($6x10^{-4}$cgs) than the granodiorite at that location and removing all Lower Seds units, as seen in Fig. 21. However the very abrupt edge of the magnetic increase at the fault scarp at 1.8 km cannot be modeled by inserting a wedge of this same intrusive unit, and still requires a source closer to the surface. It seems likely that the profile is caused by some complex combination of sediments of significant magnetic susceptibility at some depth, as well as the presence of intrusive plugs of magnetic susceptibility higher than the Continental Granodiorite.

55

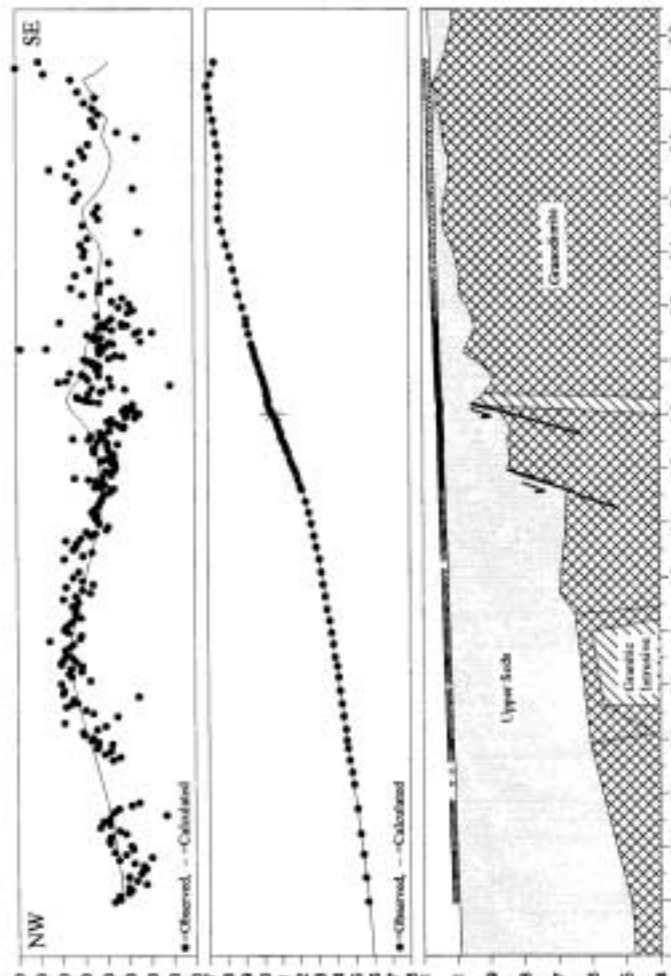

Figure 21. Modeled gravity and magnetic profile along Line AC using different units. Tertiary Granitic Intrusive was inserted to fit broad mag high in NW half of profile. Wedge of same rock at 1.85 km was not shallow or susceptible enough to fit the magnetic data.

LINE B

The first station of Line B (srb-0 at 0 km) is also found on Line AC at 1.58 km (station sra-17). The intersection coincides with a modeled fault identified on Line AC (the westernmost fault of Fig. 20). The same units were modeled in Line B as were modeled in Line AC, with the exception of an additional Dense Seds unit. The gravity profile in Fig. 22 shows small peaks which coincide with observed washes along the line. These peaks are apparently due at least in part by the topographic lows of the washes. The dashed line on the gravity profile is modeled gravity without the addition of denser units beneath the washes, and very slight peaks are evident at the washes, implying a topographic cause. To better fit these peaks, however, the Dense Seds unit was added. The density of the unit is 2.4 g/cc, higher than the 2.2 g/cc applied to the Upper and Lower Seds units. The peaks cannot be modeled reasonably by adjusting bedrock topography because they require highly exaggerated bedrock features. This implies a source closer to the surface than the modeled bedrock. One might expect the presence of heavy magnetite sands to be the cause of the gravity anomalies, but the magnetic profile disproves this. The magnetic response at the first wash, located at 0.13 km, shows a sharp spike downward. Adding a magnetite body here would result in a spike upward, not downward. The response at the second wash at 0.35 km resembles that of a dipole, and can be modeled by adding a magnetite-bearing body. However none of the responses at washes on the line, at 0.47 to 0.49 km, 0.55 to 0.60 km, and 0.62 to 0.67 km, demonstrates the presence of abundant magnetite in the washes, although narrow

stringers of magnetite sands are seen in most of the washes. Magnetite bodies would produce positive spikes on the magnetic profile which are not evident.

The magnetic and gravity anomaly profiles taken together would suggest the presence of dense yet non- or low-magnetic rocks, possibly much of it the limestones and dolomites eroding off the buttes in the east end of the area, or perhaps weathered Continental Granodiorite whose magnetite has been mostly oxidized. The noisiness of the magnetic profile does seem to indicate that the shallow sediments vary in susceptibility.

58

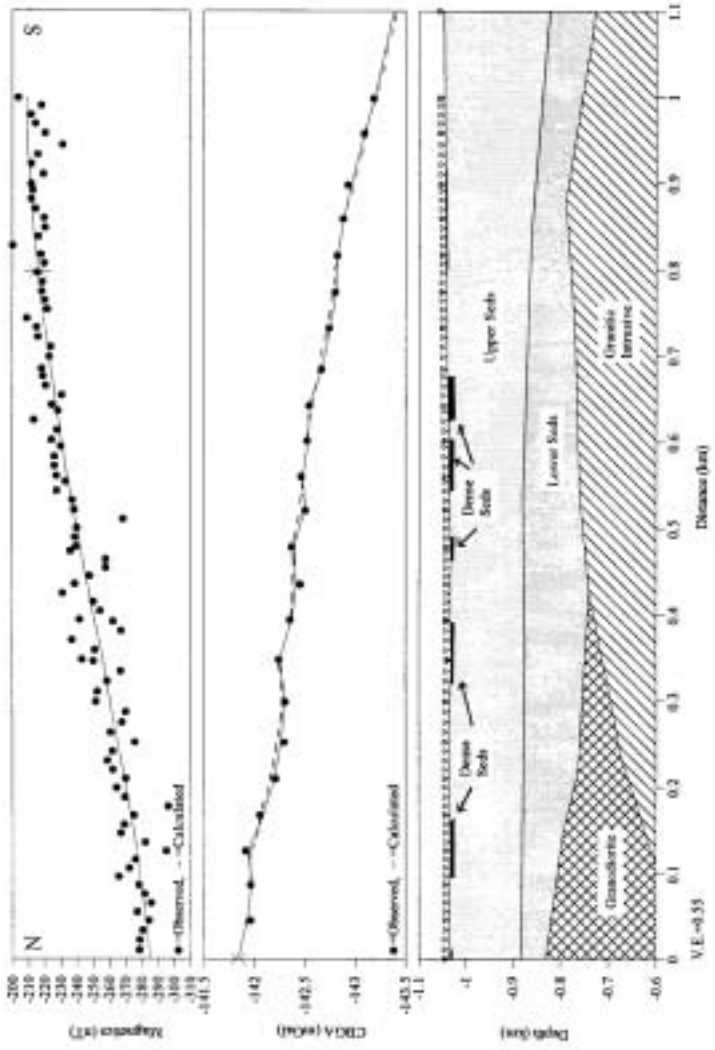

Figure 22. Modeled gravity and magnetic profile along Line B. Dense Seds units of density 2.4g/cc were inserted near surface to fit gravity highs located in washes. Dashed line is gravity profile modeled without the Dense Seds units.

LINE D

The southernmost station on Line B (srb-46 at about 1.0 km on Fig. 22) is also located on Line D at station srd-54, at 1.16 km (Fig. 23). An additional rock unit with a reverse-polarity remanent magnetization was added to the profile of Line D to fit the large negative magnetic anomaly located between 1.7 and 2.6 km.

The gravity profile appears to indicate the presence of two faults. The very slight increase in CBGA at station srd-28, at 0.58 km (Fig 23), corresponds to a fault mapped by Drewes (1971a) through Secs. 5, 7, and 8 of T18S, R15E (see Fig. 2). The model indicates a near-surface fault dip of about 66°. The sharper anomaly at 0.89 km, station srd-42, could not be adequately modeled and requires a steeply dipping shallower source. This sharp anomaly is similar in appearance to the gravity anomaly on Line AC at 1.8 km (Fig. 20), which coincides with an apparent fault scarp at the surface. As on Line AC, it implies the existence of a unit denser than the Upper and Lower Seds units (both of which were modeled at $\rho = 2.2$g/cc), which is faulted closer to the surface than the approximately 325 m depth of the modeled bedrock.

It is possible that the abrupt increase in gravity at 0.89 km is due to a tare in the gravity meter, because no local field base station was used on that day. The Gould-Simpson base was read at about 9 A.M. and again at 6 P.M. of that day, so it is not possible to determine if a small tare is responsible for the increase in the data. However the location of this apparent anomaly on Line D is approximately where one of Drewes mapped faults, if projected southwestward about 1.1 km, would intersect Line D (see Fig. 2). This is the same fault that, if extended, intersects a Line-AC anomaly at 1.5 km

60

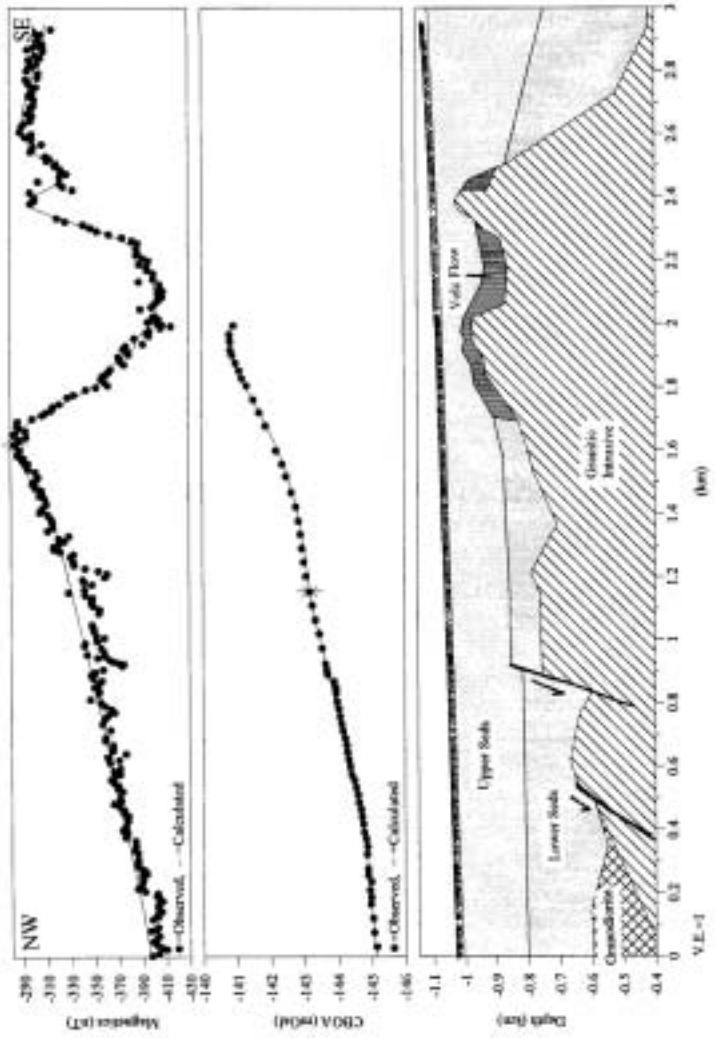

Figure 23. Modeled gravity and magnetic profile along Line D. The Volcanic Flow unit was assigned a reverse polarity to fit the magnetic low in the SE half of the profile. Gravity data suggest two normal faults.

(Fig. 20).

The magnetic anomaly profile of Line D shows a large minimum of 0.8 to 1.0 km width, with an amplitude of about —100nT. This was probably the most interesting feature in the entire area and the most difficult to model. After trial and error, the causal unit was assigned a susceptibility of 6.0×10^{-4}cgs and a remanent intensity of 2.0×10^{-3}cgs. Values for inclination and declination of -60°and -170°, respectively, modeled by Gettings and Gettings (1996) in the San Pedro Basin area were used as a starting point in modeling this anomaly. However, the anomaly could not be adequately fit, and eventually the final values for inclination and declination were set at -70° and -160°, respectively. Assigning a reverse polarity to the unit is not unrealistic if one considers that the Paleocene Epoch, during which many intrusives and dikes in the area were emplaced, was dominantly reversed polarity (R.F. Butler, pers. comm., 1998).

It might be speculated that some type of volcanic flow, perhaps an ash-flow tuff of Paleocene age, was deposited in the area of the anomaly. The location of this anomaly in reference to the buttes jutting up on the east end of the field area is particularly interesting. The anomaly occurs between about 0.5 and 0.7 km west of where the western face of these buttes disappears into the alluvium, suggesting the possibility that the rocks observed on the buttes may exist below the sediments at the location of the anomaly. The limestone and dolomite units of this butte, like the Mississippian Escabrosa Limestone and Devonian Martin Formation, would be expected to have very low magnetic susceptibilities, and their placement above a bedrock of higher magnetic susceptibility might be expected to produce a negative magnetic anomaly. This could not

be modeled successfully however. The profile seems to require a unit with a fairly strong reverse-polarity remanent magnetization, or an extreme increase in the susceptibilities of the Continental Granodiorite and Tertiary intrusives in the area.

National Uranium Resource Evaluation (NURE) aeromagnetic data examined by Gettings (1996) show several negative anomalies along a north-south flight line which passed about 1 km east of the Line D anomaly. The negative anomaly of Line D is not evident in these data. However, there is a smaller, -50 nT anomaly located 2 km southeast of the Line D feature, just beyond the south side of the limestone butte shown in Sec. 16 of Fig. 2. There is no obvious source for this anomaly. Two larger anomalies of about —180 nT are located about 5.5 and 8 km south of the Line D feature. The flight line crossed the Continental Granodiorite at both locations, so it is unclear what is causing the anomaly (Gettings, 1996). One possibility is that unmapped Tertiary stocks underlie the granodiorite at both locations and were intruded during an interval of reversed geomagnetic polarity.

The gradual increase in magnetic response toward the southeast on Line D is modeled as an intrusion of granite, corresponding to the Tertiary (Paleocene) granitic rocks of Drewes (1971a). This fits well with the model of Line E, which shows the same intrusive underlying the adjacent butte composed of Pennsylvanian Horquilla limestone mapped by Drewes (1971a). There is also a slight increase in magnetic response between 0.2 and about 1 km of the northwest side of Line D, and a slight drop in magnetic response between about 1 and 1.2 km, neither of which the final model fits well. The increase in response may be due to the presence of a smaller plug of granite with a higher

susceptibility than the modeled Tertiary intrusive (at $6.5x10^{-4}$cgs), or as speculated on Line AC, the presence of a sedimentary unit derived from susceptible units in the mountains further east. The drop in response might be the same reverse-polarity unit (the Volc Flow unit) modeled in the southeast half of the line. The Lower Seds unit, which on Line AC was adequate to model a magnetic increase near the west end of the line, is not quite adequate for Line D. The data appear to require a much more susceptible Lower Sed unit, or the same unit located much closer to the surface.

LINE V

Gravity data were not obtained for Line V, so depths to interfaces were constrained by intersections with other lines: Line AC at 0.03 km, Line B at 0.431 km, and the last station of Line E at 18 m northeast of the last station of Line V. Figure 24 shows the modeled section of Line V. The Granitic Intrusion was modeled as being present beneath the limestone on the east end of the line, in keeping with the model for Line E. A small plug of the same rock was inserted near the west end of the line to boost the modeled magnetic curve to fit the slight increase in magnetic response there.

The extremely sharp magnetic feature at about 1.85 km on Line V was first thought to be caused by a buried steel pipe or some other cultural feature. There are at least 2 mine adits located about 300 m south of this anomaly, in the faulted Escabrosa Limestone of the westernmost butte in Sec. 4 of T18S, R15E (see Fig. 2). To rule out the existence of some type of pipeline, a small grid consisting of 6 short lines, each about 108 m in length, was magnetically surveyed. The lines are about 8 m apart, with 3 of them located north of Line V and 3 located south. Figure 25 shows the relative location of the grid in reference to Line V. Note that geographical positions of the lines were not surveyed in, they were simply paced in the field.

Figure 26 shows the magnetic response along these lines. The anomaly is visible on the 2 lines closest to Line V, one line located 8 m north and one 8 m south of Line V. The amplitude and the width of the anomaly are smaller however, and the anomaly seems to be a discrete body, and not a pipe, as demonstrated by the reduction in response on adjacent lines. Using estimated northing and easting coordinates for these stations,

65

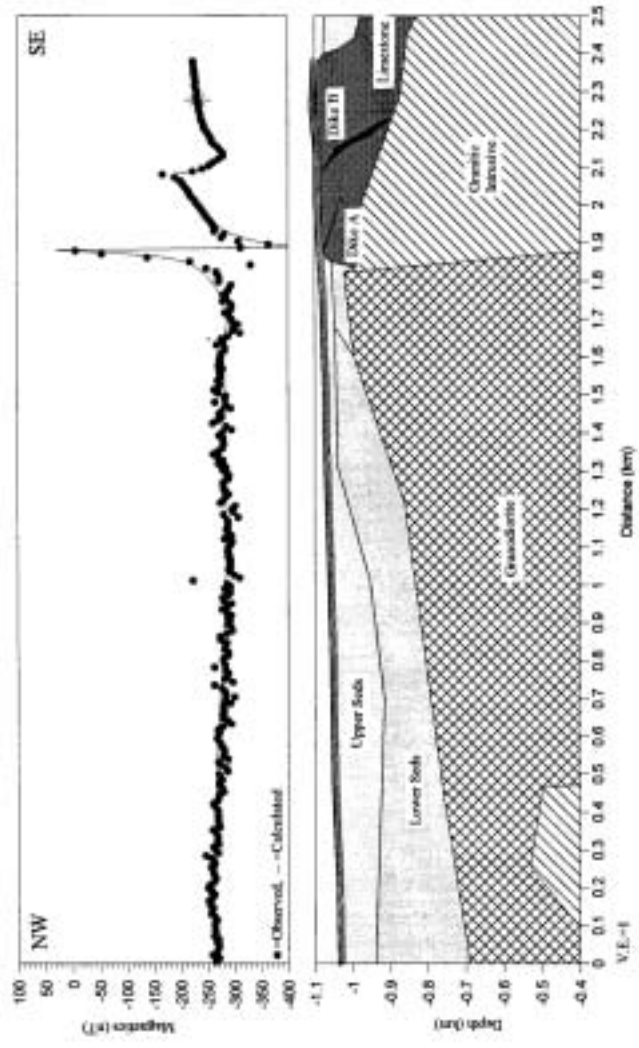

Figure 24. Modeled magnetic profile along Line V. Both anomalies near SE end of line were modeled as dikes of reverse polarity.

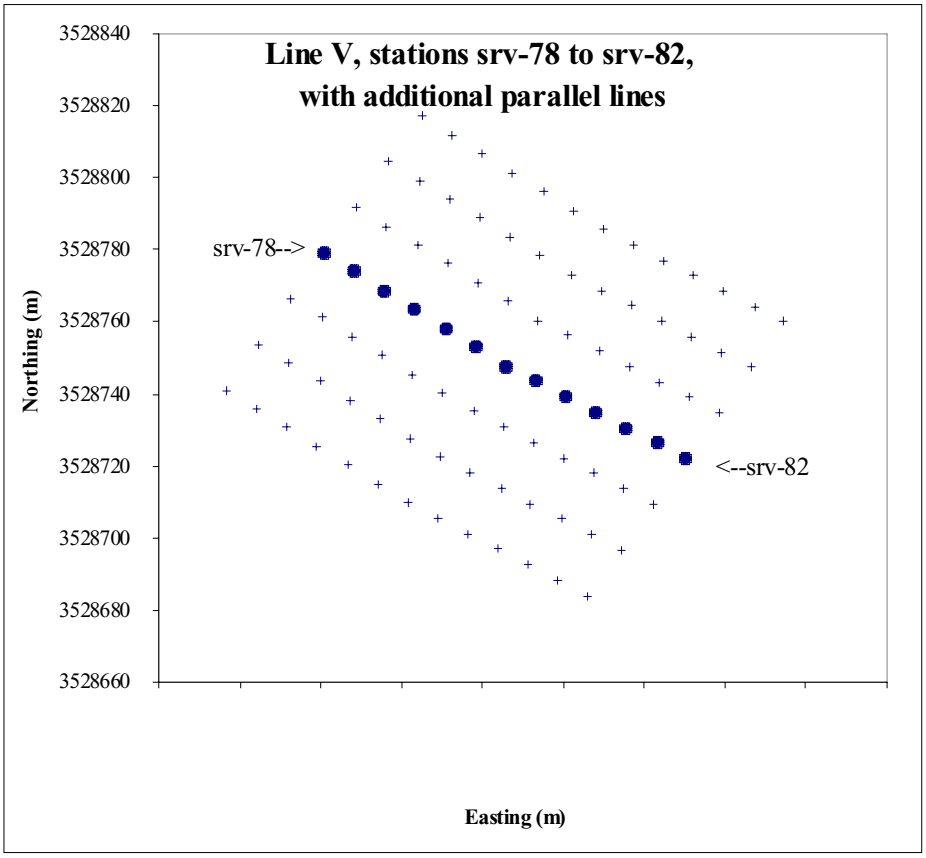

Figure 25. Location of offset magnetic survey lines to detail anomaly of Line V. Line V, stations srv-78 through srv-82, is shown in the center of the grid. Lines were offset by about 8 m.

67

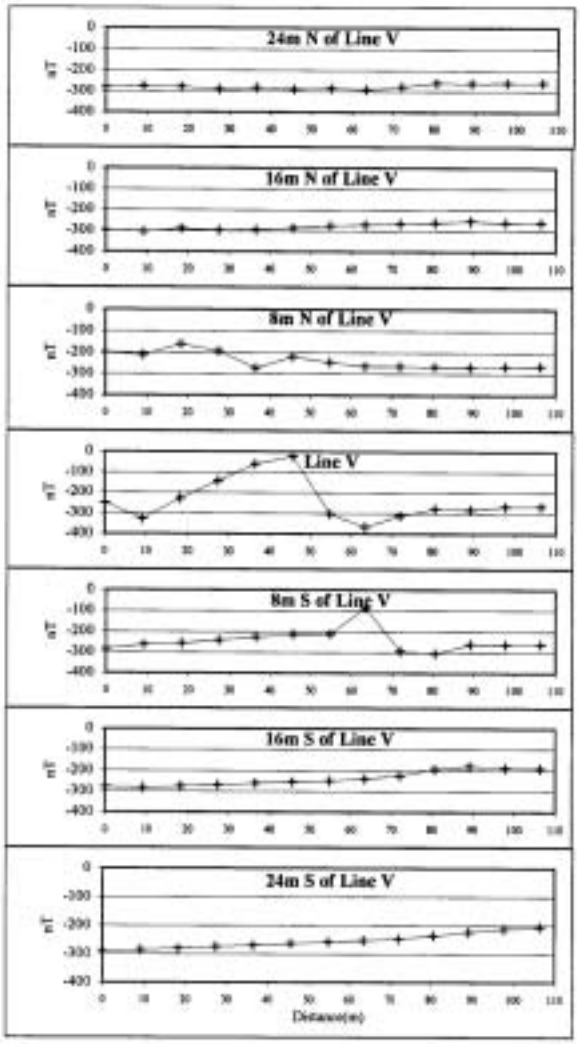

Figure 26. Magnetic profiles on offset survey lines to detail anomaly of Line V. Much smaller anomalies are evident on the two lines closest to Line V.

the strike of the body appears to be about N70°W. Had these survey lines been extended to the northwest and southeast, the horizontal extent of the feature might be better delineated.

The feature at this location initially was modeled as a dike with high magnetic susceptibility, but the low magnetic response immediately adjacent to the high could not be fit. Only after applying a remanent magnetism of reverse polarity could this drop be fit reasonably well. The feature is modeled as having a remanent magnetism intensity of $8x10^{-3}$ cgs, inclination of -60°, and declination of -170°. These values are similar to the volcanic flow feature of Line D, with a remanent intensity of $2x10^{-3}$ cgs, inclination of -70°, and declination of -160°. This is the same feature referred to as Dike A on Table 2. The feature occurs precisely at the west edge of Drewes mapped Horquilla Limestone (see Fig. 2). If there is an intrusive contact beneath that limestone, it is plausible that the anomaly is caused by some local skarn-type mineralization, especially in light of the nearby mining adits.

It must be kept in mind that the software being used is a 2-dimensional modeling package. All defined prisms, or rock contacts, are assumed to be infinite in extent perpendicular to the direction of the profile. The survey lines are also assumed to cross magnetic features of interest at a 90° angle, perpendicular to the strike direction of the feature or rock contact. If this does not hold true in the field, then the modeled magnetic profiles will not be equivalent to the field magnetic profiles even if susceptibilities and contact locations are correct. For example, if the modeled strike angle (i.e., the angle at which the profile crosses the strike of the geologic features, normally presumed to be

90°) of Line V was changed to 40° to reflect its angle with the estimated strike of the anomaly located at 1.85 km, the model that previously fit the anomaly no longer works. However, what does work is a body with a magnetization of $8x10^{-3}$cgs and no remanence, which may be more likely than the previously modeled body, which had reverse-polarity remanent magnetism. Figure 27 shows Line V modeled at this 40° strike angle. The feature labeled Dike B was also changed to a normal polarity, and intensity of magnetization was adjusted to $2x10^{-3}$cgs. The general shape of the anomaly is fit quite well, although adjustments would have to be made for susceptibilities and positions of other rock units to fit the entire line. This demonstrates the complexity of magnetic modeling. It also demonstrates that the feature causing the anomaly may be a localized area, such as an intrusive contact with limestone producing a skarn mineralized with highly susceptible minerals such as magnetite or pyrrhotite (M.E. Gettings, pers.comm., 1998).

A second interesting magnetic feature on Line V is located at about 2.1 km. This feature also could not be successfully modeled as a susceptible body with no remanence, assuming the strike of the line is perpendicular to the strike of the feature. The feature is referred to in this study as Dike B , and was assigned the same values for remanent magnetization as Dike A . These model parameters seem to provide a reasonable fit to the data. The positive spike of this anomaly occurs between stations srv-87 and srv-87.2, on the north slope of the butte composed of Horquilla limestone. At the top of this same butte is a narrow dike (< 1 m) of what appears to be andesitic rock. Although no dikes

were apparent along the north side of the butte, the presence of this andesitic dike would seem to lend credence to modeling the feature as a dike.

71

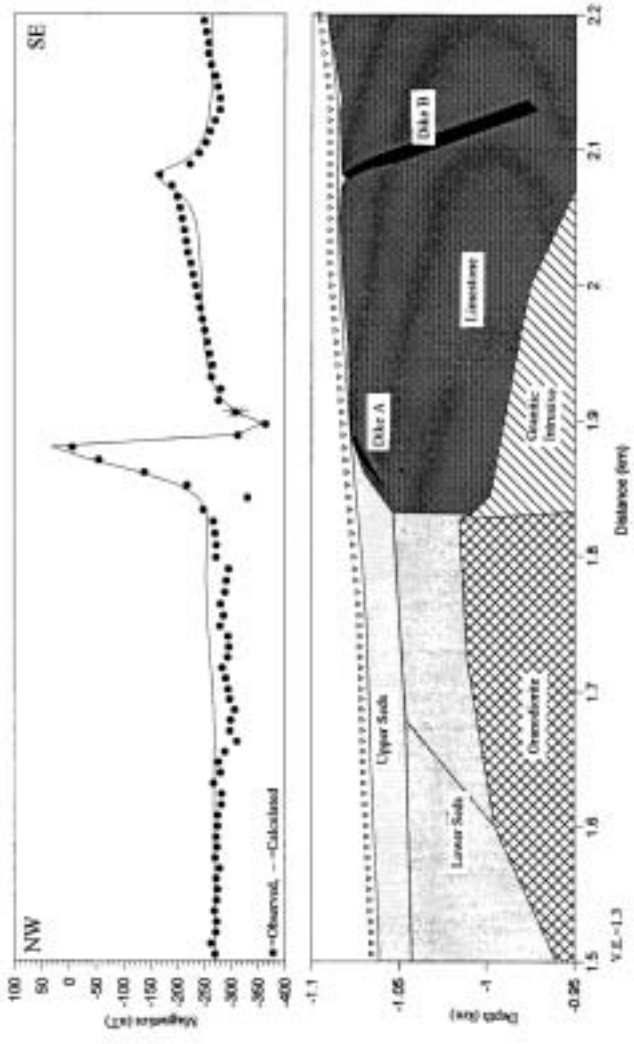

Figure 27. Modeled magnetic profile of Line V using different "strike" direction (see text for discussion). Geologic features are modeled as striking 40° from profile instead of 90°. Dike A and Dike B were assigned normal polarity. Note that shape of Dike A anomaly can be fit well with these parameters.

VLF DATA ALONG LINE V

VLF Method

The Geonics Limited EM16 unit was used to perform a Very Low Frequency (VLF) electromagnetic survey along Line V. A brief summary of the method follows. Powerful radio transmitters used for military communications and operated at frequencies from about 15 to 25 kHz are utilized in this method. The electromagnetic field produced by these transmitters induces electric currents in conductors such as ore bodies, and these induced currents in turn produce secondary magnetic fields near the conductor. The VLF instrument acts as a receiver and measures components of the field at the surface, which is the resultant of both the primary and the induced secondary electromagnetic fields. Conductive bodies of interest must strike approximately in the direction of the transmitter to produce measurable variations in the electromagnetic field (Klein and Lajoie, 1992).

The particular instrument used, the EM16, measures the in-phase and the quadrature (out-of-phase) components of the vertical magnetic field as a percentage of the horizontal primary field. The unit contains a module for tuning to two different transmitting stations, NAA at Cutler, Maine, which operates at 24.0 kHz, and NLK at Seattle, Washington, operating at 24.8 kHz (McNeill and Labson, 1991).

The VLF method was utilized in the field area in the hopes of pinpointing fault locations along the west end of Line V. Local workers have had success in locating faults with the VLF method (J. Fink, pers. comm., 1997), because the method responds to conductors such as water and clays which might be found in faulted bedrock. Because it is actually a high-frequency method, in terms of typical frequencies used in geophysical

exploration, it tends to be noisy and responsive to sources such as creeks and topographic highs (Klein and Lajoie, 1992). The skin depth, or effective depth of penetration, of this method is fairly shallow, because of the inverse dependence upon frequency (Sheriff, 1991):

$$\delta = 500(\rho/f)^{1/2} \qquad \text{(meters)}$$

where ρ is resistivity of the medium in ohm-m, and f is frequency of the transmitter. Assuming an overburden resistivity of 100 ohm-m, which is an estimate commonly used by the Mining and Geological Engineering Department of this university (Thomas, pers. comm., 1998), effective depth of penetration would be expected to be in the range of 30 m in the field area. On the limestone bedrock at the east end of the line, depth of penetration is probably deeper. Telford et al. (1976) give a resistivity range for limestones of 50 to 10^7 ohm-m. If the resistivity of the limestone is assumed to be between 100 and 10,000 ohm-m, effective depth of penetration would be expected to be between about 30 and 320 m on the east end of the line.

Interpretation of VLF data is fairly simple if closely situated, multiple conductors are not involved. Locations of conductors are determined by the cross-over point , marking the change from positive to negative polarity of the in-phase and quadrature components. Depth to the conductive body can be estimated from the map distance between the maximum positive and negative peaks of the in-phase component (Klein and Lajoie, 1992). According to the Geonics EM16 reference manual, to locate conductors which are adjacent, one must use the steepest gradients of the plotted field, rather than the cross-over points.

VLF Station Locations

The VLF data were collected at the same stations as the magnetic data, at 8 m spacings. Figure 28 shows the data plotted as in-phase and out-of-phase components versus distance from the west end of the line. The topmost graph is data from the Cutler, Maine transmitter, while the graph below displays data using the Seattle transmitter. The magnetic data as well as the topographic profile along the line are also displayed.

75

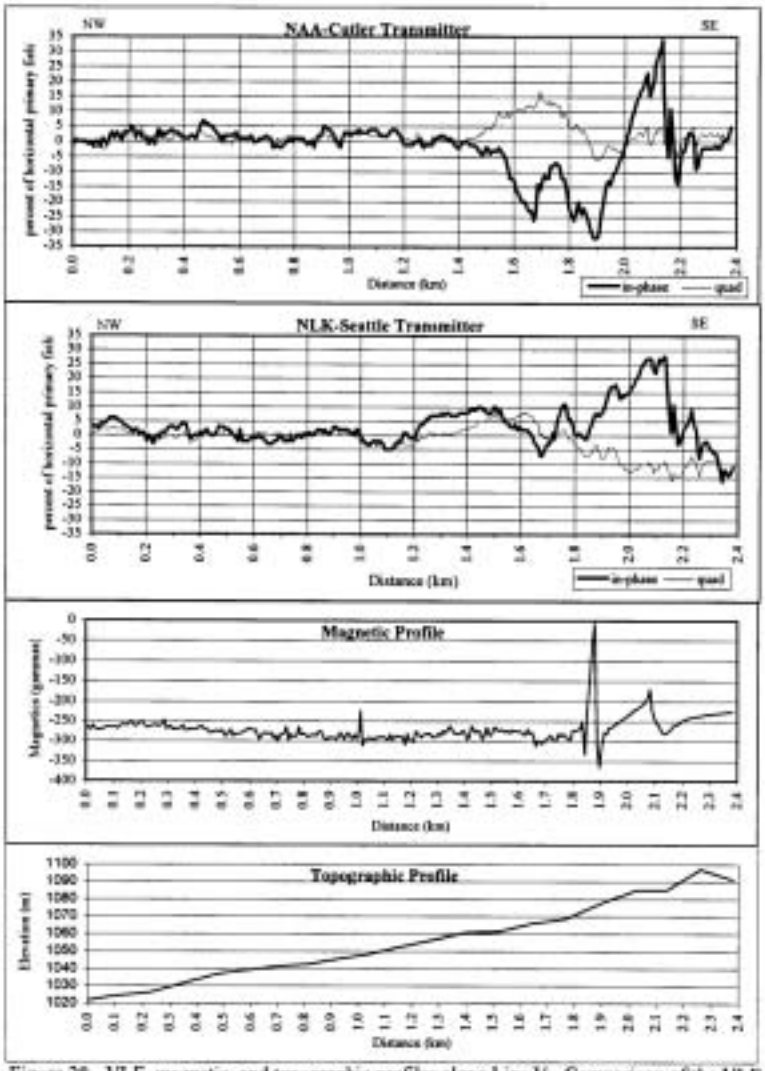

Figure 28. VLF, magnetic, and topographic profiles along Line V. Comparison of the VLF anomalies with the topographic profile shows that VLF response in this case is uncorrelated to topography.

VLF and Magnetic Interpretation

There appear to be several very small anomalies on the west end of Line V. One that shows up in the Seattle graph, at between 0.1 and 0.2 km, is probably due to a wash that was traversed between 0.17 and 0.23 km, and that trended in a northwest direction toward the Seattle transmitter. The same anomaly does not show up on the Cutler plot, indicating that whatever conductor may be present trends perpendicular to northeast, or northwest toward Seattle. Conductors must trend roughly in the direction of the transmitter (that is, point toward the transmitter) to cause an anomaly. This would seem to indicate that the cause of the small anomaly is indeed the wash, probably due to water located beneath the surface.

The causes of other minor features on the west end of the VLF profiles are unclear. It seems unlikely that they are related to faulting because depth to bedrock in the area, using the gravity model of Line AC, is on the order of a couple hundred meters. Depth of penetration in the sediments as stated above is perhaps on the order of 30 m.

More interesting anomalies appear on the eastern portion of Line V shown in Fig. 28. The topographic profile, when compared to the VLF profiles, indicates that these anomalies are unrelated to topography. There appear to be multiple conductors involved, and because both transmitters produce a response to them, the conductors are probably trending in a more northward direction than either northwest (in the direction of Seattle) or northeast (in the direction of Cutler). There appears to be a major anomaly located at about 2.0 km, using the cross-over point of the Cutler graph. At first glance this may be assumed to be the contact of the more resistive limestone in the east with the more

conductive sediments to the west. However, the anomaly occurs about 100 m east of the contact with the limestone. Perhaps the total response is due to the superimposition of conductive responses of small mineralized zones on a larger negative anomaly caused by the highly resistive limestone. Two small conductors appears to be superimposed upon the anomaly at 1.8 km and 1.85 km. The in-phase component of the Cutler data at 1.85 km corresponds to a sharp magnetic anomaly at the same location and is probably related to it. The steep gradient of the in-phase component of an anomaly located at 2.15 km corresponds to a magnetic anomaly at the same location that was modeled as a dike. The very sharp, lower amplitude spike on the east side of the anomaly, which can be seen on both Cutler and Seattle graphs, is probably caused by a deep gully located at 2.16 km.

SANTA RITA ROAD

The general shape of the magnetic profile for Santa Rita Road, shown in Fig. 29, resembles that of Line AC, although the scales are considerably different. The Tertiary intrusive on this line was divided into 3 blocks of susceptibilities $5.5x10^{-4}$, $6.0x10^{-4}$, and $6.5x10^{-4}$ cgs to fit the calculated profile to Drewes (1971a) mapped outcrop. Using a single intensity was not successful. There is a broad magnetic high of about 1.5 to 2 km width along the western half of the profile, probably due to an accumulation of susceptible sediments (the Lower Seds at 0.00025 cgs), the presence of a Tertiary stock, or both. The response is rather smooth up to about 2.8 km, where there is a small negative anomaly, and past this point the variability of the response increases. The negative anomaly at 2.8 km may reflect a fault. The rest of the line to the east is modeled as reflecting the proximity of the Tertiary intrusives to the surface. The anomaly at 3.8 km coincides with the location of a small hill composed of the intrusive just off the north side of the road. Huerfano Butte, also composed of the Tertiary intrusives, is located off the south side of the road at 4.1 to 4.5 km. A contact between the Tertiary granitic intrusive and Precambrian intrusive occurs at about 6.3 km (Drewes, 1971a), and this is displayed in the model.

A very strong, short-wavelength negative magnetic anomaly can be seen at about 6 km. It is followed by a weaker short-wavelength positive anomaly which may be related to it. To fit this observed negative anomaly, a dike with a remanent magnetization of reverse polarity was required. This feature is somewhat puzzling and may be an unidentified cultural feature of some kind. It appears to extend for about 150 m however,

and is most likely produced by a dike emplaced during a reversed geomagnetic polarity. The feature also was modeled with no remanence but with different strike directions to determine whether it might be simply a mineralized zone. This model attempt was not successful; depending on the modeled strike direction, dip, and depth extent of the unit, the anomalies produced could not be made strongly negative.

Inspection of the magnetic profile of this line seems to reveal a highly variable nature to the susceptibilities of the Tertiary intrusives. One would expect the Tertiary bedrock to be located very close to the surface between about 3 to 6.2 km, judging by the proximity of outcrop mapped by Drewes (1971a). The response is very noisy however, and varies by some 150 to 250 nT. This would seem to indicate that in areas underlain by very shallow Tertiary intrusives, the magnetic response may not be very helpful in locating faults. Their response is possibly obscured by that of the intrusive. Gravity anomaly and magnetic anomaly maps would probably prove considerably more useful than profiles in future studies in the area. Features such as faults would probably show up as trends on these maps, and their 3-dimensional extent would be apparent.

80

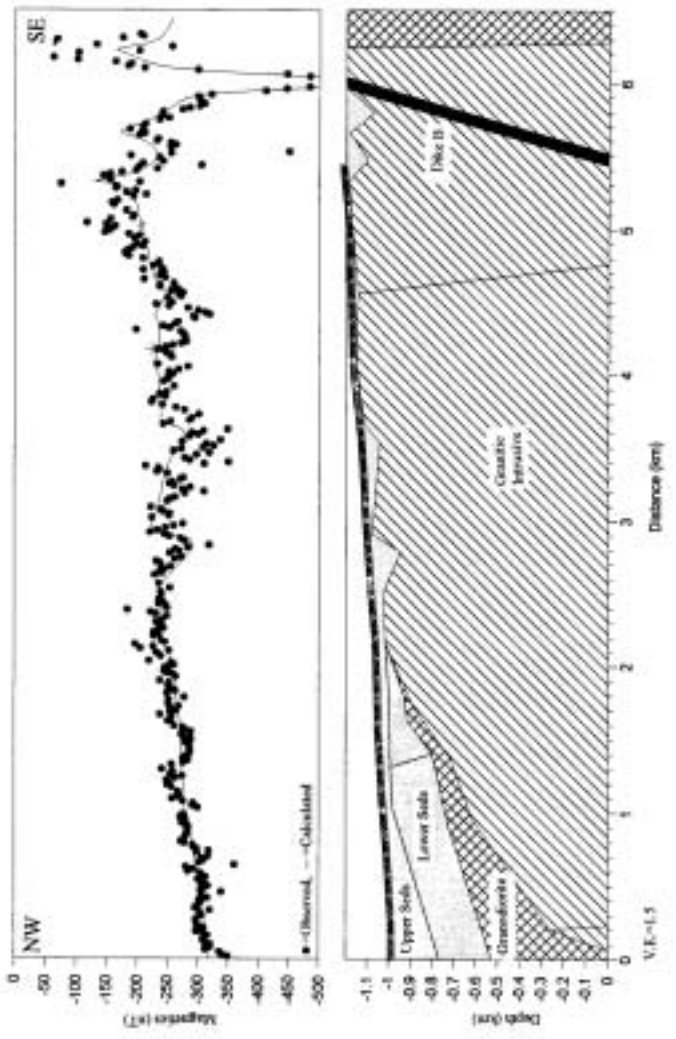

Figure 29. Modeled gravity and magnetic profile along Santa Rita Road. Dike B feature modeled as reverse polarity.

CONCLUSIONS

Gravity data in the northeast corner of the Santa Rita Experimental Range are shown to be particularly helpful in locating faults. The magnetic data do not appear to be nearly as useful due to the apparent range in susceptibilities displayed by the Tertiary granitic intrusives. However they do appear to reveal the presence of dikes with reverse-polarity remanent magnetism in the area.

The gravity data pinpoint fault locations along Lines AC and D. The faults correlate well with those mapped by Drewes (1971a), and near-surface dips on the faults appear to be high angle, between about 55° and 70°. It is not clear how well fault dips may be resolved. If low-angle normal faults exist at greater depths along these lines, as some workers theorize (see Johnson and Loy, 1992), they probably cannot be resolved or distinguished from basement topography.

Small gravity anomalies along these lines indicate that a unit more dense than the 2.2 g/cc used for the Upper Seds unit exists between these sediments and bedrock (modeled at 2.67 g/cc). The anomalies cannot be fit by adjusting bedrock alone. The magnetic data also suggest the presence of a unit between the Upper Seds and the bedrock below. On line A, an abrupt shift in magnetic response cannot be modeled simply by varying susceptibilities of the surficial sediments or the bedrock. Modeling the magnetic profile on Line A seems to require a more susceptible unit between the two. Broader magnetic anomalies on the west portion of the same two lines may be modeled in two ways: by inserting a susceptible unit between the Upper Seds and Continental

Granodiorite, or by inserting a plug of the Tertiary granitic intrusive. Both are plausible models.

VLF data do not appear to be helpful in identifying faults in the area, but they do indicate a conductive body located at the westernmost edge of the limestone butte straddling Secs. 4 and 9 in Fig. 2. Magnetic data along the same line also indicate a possible mineralized zone at the same location, perhaps caused by a Tertiary intrusive contact. Another magnetic anomaly further east on the flank of the butte is probably indicative of an intermediate-composition dike. An andesitic dike is observed on the easternmost summit of the limestone butte, above the line location.

A large negative magnetic anomaly of about 100 nT on Line D is difficult to analyze. It was modeled as a volcanic unit with a reverse-polarity magnetic remanence. A nearby aeromagnetic flight line displays several negative anomalies within 8 km south of the anomaly. They may be indicative of near-surface Tertiary plugs or volcanic flows with a reverse-polarity remanent magnetism. They may also indicate zones within the Continental Granodiorite and Tertiary intrusives where magnetite has been altered or replaced. This is less likely because the zones could not be modeled successfully when they were assigned zero susceptibility.

Magnetic data along Santa Rita Road seem to indicate high variability in magnetic susceptibility of the Tertiary granitic rocks. A very strong, very short-wavelength negative magnetic anomaly on the far southeast end of the line was modeled as a dike of reverse-polarity remanent magnetism. However, it may simply be due to an unidentified cultural source, but if so, it must be of significant horizontal extent of 150 to 300 m.

REFERENCES

Anzalone, S.A., 1995, The Helvetia area porphyry systems, Pima County, Arizona, *in*, Pierce, F.W., and Bolm, J.G., eds., 1995, Porphyry Copper Systems of the American Cordillera, Arozona Geological Society Digest, v. 20, p. 436-441.

Breiner, S., 1992, Magnetics, applications for portable magnetometers, *in*, Van Blaricom, R., ed., 1992, Practical Geophysics II for the Exploration Geologist: Northwest Mining Association, p. 313-381.

Carmichael, R.S., 1982, CRC Handbook of Physical Properties of Rocks: CRC Press, Inc., 345 p.

Cordell, L., Keller, G.R., and Hildenbrand, T.G., 1982, Bouguer gravity map of the Rio Grande rift: U.S. Geological Survey Geophysical Investigations Map GP-949, scale 1:1000000.

Dobrin, M.B., 1976, Introduction to Geophysical Prospecting: Mcgraw-Hill, Inc., 630 p.

Drewes, H., 1971a, Geologic map of the Sahuarita quadrangle, southeast of Tucson, Pima county, Arizona: U.S. Geological Survey Miscellaneous Geologic Investigations Map I-613, scale 1:48000.

Drewes, H., 1971b, Mesozoic stratigraphy of the Santa Rita Mountains, southeast of Tucson, Arizona: U.S. Geological Survey Professional. Paper 658-C, 81p.

Drewes, H., 1972, Cenozoic rocks of the Santa Rita Mountains, southeast of Tucson, Arizona: U.S. Geological Survey Professional Paper 746, 66p.

Drewes, H., 1976, Plutonic rocks of the Santa Rita Mountains, southeast of Tucson, Arizona: U.S. Geological Survey Professional Paper 915, 75 p.

Drewes, H., 1981, Tectonics of Southeastern Arizona: U.S. Geological Survey Professional Paper 1144, 96 p.

Gettings, P.E., Gettings, M.E., and Bultman, M.W., 1995, Data collection and reduction procedures for 1900 km of total intensity magnetic field data collected with a truck-mounted system in southeastern Arizona, southwestern Colorado, and northwestern Wyoming: U.S. Geological Survey Open-File Report 95-32, 13p.

Gettings, P.E., and Gettings, M.E., 1996, Modelling of a magnetic and gravity anomaly profile from the Dragoon Mountains to Sierra Vista, southeastern Arizona: U.S. Geological Survey Open-File Report 96-288, 15 p.

Gettings, M.E., 1996, Aeromagnetic, radiometric and gravity data for Coronado National Forest, *in*, du Bray, E.A., ed., 1996, Mineral Resource Potential and Geology of Coronado National Forest, Southeastern Arizona and Southwestern New Mexico: U.S. Geological Survey Bulletin 2083-A-K, p. 77-101.

Heiland, C.A., 1968, Geophysical Exploration: Hafner Publishing Co., 1013 p.

Johnson, R.A., and Loy, K.L., 1992, Seismic reflection evidence for seismogenic low-angle faulting in southeastern Arizona: Geology, v. 20, p. 597-600.

Kearey, P., and Brooks, M., 1991, An Introduction to Geophysical Exploration: Blackwell Scientific Publications, 254 p.

Klein, J., and Lajoie, J. J., 1992, Electromagnetics, electromagnetic prospecting for minerals, *in*, Van Blaricom, R., ed., 1992, Practical Geophysics II for the Exploration Geologist: Northwest Mining Association, p. 383-535.

Marquardt, D.W., 1963, An algorithm for least-squares estimation of non-linear parameters, J. SIAM, v. 11, p. 431-441.

McNeill, J. D., and Labson, V. F., 1991, Geological mapping using VLF radio fields, *in*, Nabighian, M. N., ed., 1991, Electromagnetic Mehtods in Applied Geophysics, Vol. 2: Society of Exploration Geophysicists, p. 521-640.

Pearthree, P.A., Menges, C.M., and Mayer, L., 1983, Distribution, recurrence, and possible tectonic implication of late Quaternary faulting in Arizona: State of Arizona Bureau of Geology and Mineral Technology Open-File Report 83-20, 52 p.

Pearthree, P.A., and Calvo, S.S., 1987, The Santa Rita fault zone: evidence for large magnitude earthquakes with very long recurrence intervals, Basin and Range Province of southeastern Arizona: Bulletin of the Seismological Society of America, v. 77, p. 97-116.

Plouff, D., 1966, Digital terrain corrections based on geographic coordinates. Paper presented at the 36th Annual Meeting of Society of Exploration Geophysicists, Houston, Texas. Abstract Geophysics, v. 31, no. 6, p.1208.

Rieth, A., Seismic reflection evidence for seismogenic low-angle normal faults: M.S. Thesis, in preparation, University of Arizona.

Robbins, S.L., and Oliver, H.W., 1970, On making inner-zone terrain corrections to gravity data: U.S. Geological Survey In-House Memorandum.

Rutledge, J.T., 1984, A shallow seismic refraction survey over a late quaternary fault scarp west of the Santa Rita Mountains, Arizona: M.S. Thesis, University of Arizona, 93 p.

Sheriff, R.E., 1991, Encyclopedic Dictionary of Exploration Geophysics: Society of Exploration Geophysics, 376 p.

Talwani, M., Worzel, J., Landisman, M., 1959, Rapid gravity computations for two-dimensional bodies with application to the Mendocino submarine fracture zone: Journal of Geophysical Research, v. 64, p. 49-59.

Tanbal, K.M., 1987, A gravity survey over late quaternary fault scarps west of the Santa Rita Mountains, Arizona: M.S. Thesis, University of Arizona, 55 p.

Telford, W.M., Geldart, L.P., Sheriff, R.E., and Keys, D.A., 1976, Applied Geophysics: Cambridge University Press, 860 p.

Webring, M., 1985, SAKI: a FORTRAN program for generalized linear inversion of gravity and magnetic profiles: U.S. Geological Survey Open-File Report 85-122, 29 p.

West, R.E., 1992, Gravity, the land gravity exploration method, *in*, Van Blaricom, R., ed., 1992, Practical Geophysics II for the Exploration Geologist: Northwest Mining Association, p. 177-233.

APPENDIX A: GRAVITY DATA

	Latitude Deg.	Dec.Min.	Longitude Deg.	Dec.Min.	Elev units	Elevation	Observed Gravity (mGal)	Free Air Anomaly (mGal)	Simple Bouguer Anomaly (?=2.67g/cc)	Complete Bouguer Anomaly (?=2.67g/cc)	Inner Zone Terrain Correction (?=2.67g/cc)	Total Terrain Correction	Uncertainty in CBGA at ?=2.67 g/cc (mGal)	
sra-01	31	54.247	-110	49.352	m	1033.43	979130.61	-26.20	-141.84	-142.11	0	0.87	0.18	Local base
sra-02	31	54.267	-110	49.098	m	1043.86	979130.50	-23.13	-139.94	-140.18	0	0.90	0.18	
sra-02.5	31	54.269	-110	49.105	m	1043.41	979130.52	-23.25	-140.00	-140.24	0.01	0.91	0.18	
sra-03	31	54.269	-110	49.113	m	1042.47	979130.68	-23.38	-140.03	-140.25	0.02	0.92	0.18	
sra-03.5	31	54.270	-110	49.119	m	1041.66	979130.81	-23.50	-140.06	-140.28	0.02	0.92	0.18	
sra-04	31	54.271	-110	49.124	m	1040.59	979131.00	-23.64	-140.08	-140.31	0.02	0.92	0.18	
sra-04.5	31	54.273	-110	49.128	m	1040.15	979131.04	-23.74	-140.13	-140.33	0.04	0.94	0.19	
sra-05	31	54.274	-110	49.132	m	1039.52	979131.20	-23.77	-140.09	-140.29	0.04	0.94	0.19	
sra-05.5	31	54.272	-110	49.141	m	1037.87	979131.46	-24.02	-140.16	-140.35	0.04	0.95	0.19	
sra-06	31	54.274	-110	49.150	m	1037.86	979131.40	-24.09	-140.22	-140.43	0.02	0.93	0.19	
sra-06.5	31	54.273	-110	49.156	m	1038.36	979131.22	-24.11	-140.30	-140.53	0.01	0.91	0.18	
sra-07	31	54.272	-110	49.164	m	1039.02	979131.01	-24.12	-140.38	-140.60	0.02	0.92	0.18	
sra-07.5	31	54.275	-110	49.172	m	1038.78	979130.97	-24.23	-140.47	-140.72	0	0.89	0.18	
sra-08	31	54.277	-110	49.181	m	1038.22	979131.01	-24.37	-140.55	-140.80	0	0.89	0.18	
sra-08.5	31	54.277	-110	49.187	m	1037.72	979131.06	-24.48	-140.60	-140.85	0	0.89	0.18	
sra-09	31	54.277	-110	49.193	m	1037.19	979131.13	-24.57	-140.63	-140.88	0	0.89	0.18	
sra-09.5	31	54.279	-110	49.201	m	1037.1	979131.06	-24.67	-140.72	-140.96	0	0.89	0.18	
sra-10	31	54.279	-110	49.206	m	1036.98	979131.03	-24.73	-140.77	-141.02	0	0.89	0.18	
sra-10.5	31	54.275	-110	49.215	m	1035.76	979131.24	-24.90	-140.80	-141.02	0.02	0.91	0.18	
sra-11	31	54.273	-110	49.223	m	1035.92	979131.15	-24.93	-140.85	-141.10	0	0.89	0.18	
sra-11.5	31	54.273	-110	49.231	m	1036.04	979131.04	-25.01	-140.94	-141.18	0	0.89	0.18	
sra-12	31	54.272	-110	49.241	m	1036.49	979130.85	-25.06	-141.04	-141.30	0	0.88	0.18	
sra-12.5	31	54.272	-110	49.249	m	1035.72	979130.97	-25.17	-141.07	-141.31	0.01	0.89	0.18	
sra-13	31	54.271	-110	49.255	m	1036.37	979130.76	-25.18	-141.15	-141.40	0	0.88	0.18	
sra-14	31	54.269	-110	49.272	m	1036.18	979130.69	-25.31	-141.26	-141.52	0	0.87	0.17	
sra-15	31	54.267	-110	49.284	m	1035.53	979130.73	-25.46	-141.34	-141.61	0	0.87	0.17	
sra-16	31	54.266	-110	49.297	m	1035.25	979130.63	-25.65	-141.49	-141.76	0	0.87	0.17	
sra-17	31	54.269	-110	49.306	m	1034.87	979130.63	-25.77	-141.57	-141.84	0	0.87	0.17	

sra-18	31	54.270	-110	49.322	m	1034.17	979130.67	-25.95	-141.68	-141.94	0	0.87	0.17
sra-19	31	54.271	-110	49.338	m	1033.41	979130.70	-26.15	-141.79	-142.06	0	0.86	0.17
sra-20	31	54.262	-110	49.347	m	1033.18	979130.65	-26.26	-141.87	-142.15	0	0.86	0.17
sra-22	31	54.267	-110	49.375	m	1032.34	979130.61	-26.57	-142.08	-142.36	0	0.86	0.17
sra-24	31	54.269	-110	49.403	m	1030.98	979130.71	-26.89	-142.26	-142.53	0	0.86	0.17
sra-26	31	54.272	-110	49.429	m	1029.72	979130.85	-27.15	-142.37	-142.65	0	0.85	0.17
sra-28	31	54.273	-110	49.458	m	1028.56	979130.93	-27.43	-142.52	-142.80	0	0.85	0.17
sra-30	31	54.272	-110	49.485	m	1027.49	979131.02	-27.67	-142.64	-142.92	0	0.85	0.17
sra-32	31	54.273	-110	49.515	m	1026.34	979131.05	-27.98	-142.83	-143.11	0	0.85	0.17
sra-34	31	54.276	-110	49.545	m	1025.08	979131.22	-28.21	-142.91	-143.20	0	0.84	0.17
sra-36	31	54.279	-110	49.573	m	1023.81	979131.38	-28.45	-143.01	-143.30	0	0.84	0.17
sra-38	31	54.281	-110	49.601	m	1022.77	979131.47	-28.68	-143.13	-143.42	0	0.84	0.17
sra-40	31	54.289	-110	49.630	m	1021.65	979131.61	-28.89	-143.21	-143.51	0	0.83	0.17
sra-42	31	54.295	-110	49.657	m	1020.44	979131.71	-29.18	-143.36	-143.66	0	0.83	0.17
sra-44	31	54.302	-110	49.684	m	1019.25	979131.86	-29.41	-143.46	-143.76	0	0.82	0.16
sra-46	31	54.317	-110	49.707	m	1018.22	979131.99	-29.62	-143.55	-143.86	0	0.82	0.16
sra-48	31	54.324	-110	49.737	m	1017.13	979132.10	-29.85	-143.66	-143.96	0	0.82	0.16
sra-50	31	54.343	-110	49.753	m	1016.39	979132.16	-30.04	-143.77	-144.08	0	0.81	0.16
sra-52	31	54.360	-110	49.773	m	1015.63	979132.28	-30.18	-143.83	-144.14	0	0.81	0.16
sra-54	31	54.374	-110	49.801	m	1013.97	979132.55	-30.44	-143.90	-144.22	0	0.80	0.16
sra-56	31	54.388	-110	49.827	m	1013	979132.67	-30.64	-144.00	-144.33	0	0.79	0.16
sra-58	31	54.398	-110	49.855	m	1011.54	979132.88	-30.90	-144.09	-144.41	0	0.79	0.16
sra-60	31	54.409	-110	49.883	m	1010.58	979132.98	-31.11	-144.19	-144.53	0	0.78	0.16
sra-62	31	54.424	-110	49.904	m	1009.3	979133.17	-31.33	-144.27	-144.60	0	0.78	0.16
sra-64	31	54.446	-110	49.916	m	1008.33	979133.35	-31.48	-144.31	-144.65	0	0.78	0.16
sra-66	31	54.456	-110	49.943	m	1007.08	979133.53	-31.70	-144.39	-144.73	0	0.77	0.15
sra-68	31	54.458	-110	49.972	m	1005.69	979133.66	-32.00	-144.53	-144.88	0	0.77	0.15
sra-70	31	54.458	-110	50.002	m	1004.59	979133.79	-32.21	-144.62	-144.97	0	0.77	0.15
sra-74	31	54.457	-110	50.062	m	1003.07	979133.91	-32.56	-144.80	-145.15	0	0.76	0.15
sra-78	31	54.459	-110	50.122	m	1000.62	979134.23	-33.00	-144.97	-145.33	0	0.75	0.15
sra-82	31	54.473	-110	50.168	m	998.83	979134.46	-33.33	-145.10	-145.46	0	0.75	0.15
sra-86	31	54.506	-110	50.214	m	996.1	979134.93	-33.75	-145.21	-145.58	0	0.74	0.15
sra-90	31	54.538	-110	50.262	m	993.93	979135.27	-34.13	-145.35	-145.72	0	0.73	0.15
srb-02	31	54.249	-110	49.323	m	1034.58	979130.53	-25.94	-141.70	-141.97	0	0.87	0.18
srb-04	31	54.229	-110	49.339	m	1034.36	979130.54	-25.96	-141.70	-141.97	0	0.87	0.18
srb-06	31	54.211	-110	49.353	m	1031.98	979131.01	-26.20	-141.68	-141.92	0.01	0.89	0.18
srb-08	31	54.191	-110	49.366	m	1033.91	979130.45	-26.14	-141.83	-142.06	0.03	0.91	0.18

srb-10	31	54.172	-110	49.383	m	1035.23	979130.05	-26.11	-141.95	-142.22	0	0.87	0.17
srb-12	31	54.152	-110	49.398	m	1035.27	979129.94	-26.18	-142.03	-142.30	0	0.87	0.17
srb-14	31	54.130	-110	49.413	m	1033.91	979130.13	-26.38	-142.08	-142.31	0.02	0.90	0.18
srb-16	31	54.107	-110	49.429	m	1030.42	979130.81	-26.75	-142.05	-142.25	0.03	0.93	0.19
srb-18	31	54.084	-110	49.442	m	1032.92	979130.19	-26.56	-142.15	-142.36	0.03	0.92	0.18
srb-20	31	54.065	-110	49.457	m	1032.53	979130.15	-26.70	-142.23	-142.46	0.02	0.91	0.18
srb-22	31	54.040	-110	49.457	m	1031.89	979130.31	-26.70	-142.16	-142.38	0.01	0.92	0.18
srb-24	31	54.019	-110	49.467	m	1034.17	979129.73	-26.55	-142.28	-142.51	0	0.90	0.18
srb-26	31	53.996	-110	49.467	m	1035.26	979129.51	-26.40	-142.25	-142.47	0	0.91	0.18
srb-28	31	53.974	-110	49.471	m	1036.06	979129.27	-26.37	-142.30	-142.53	0	0.91	0.18
srb-30	31	53.951	-110	49.474	m	1037.39	979128.96	-26.24	-142.32	-142.55	0	0.91	0.18
srb-32	31	53.928	-110	49.478	m	1039.21	979128.44	-26.16	-142.44	-142.67	0	0.91	0.18
srb-34	31	53.902	-110	49.483	m	1040.67	979128.05	-26.07	-142.51	-142.75	0	0.91	0.18
srb-36	31	53.879	-110	49.486	m	1041.73	979127.74	-26.02	-142.59	-142.81	0	0.92	0.18
srb-38	31	53.856	-110	49.491	m	1040.81	979127.86	-26.15	-142.61	-142.83	0	0.92	0.18
srb-40	31	53.833	-110	49.493	m	1041.53	979127.62	-26.14	-142.69	-142.89	0.01	0.94	0.19
srb-42	31	53.811	-110	49.496	m	1042.37	979127.38	-26.09	-142.73	-142.94	0	0.93	0.19
srb-44	31	53.781	-110	49.512	m	1043.36	979126.99	-26.13	-142.88	-143.10	0	0.93	0.19
src-01	31	54.267	-110	49.085	m	1044.49	979130.44	-22.99	-139.87	-140.10	0	0.91	0.18
src-02	31	54.260	-110	49.075	m	1044.96	979130.45	-22.83	-139.76	-139.99	0	0.91	0.18
src-03	31	54.253	-110	49.063	m	1045.63	979130.41	-22.65	-139.65	-139.89	0	0.91	0.18
src-04	31	54.245	-110	49.052	m	1046.24	979130.36	-22.50	-139.58	-139.80	0	0.92	0.18
src-05	31	54.239	-110	49.042	m	1046.88	979130.33	-22.32	-139.47	-139.69	0	0.92	0.18
src-06	31	54.233	-110	49.030	m	1047.64	979130.27	-22.14	-139.37	-139.60	0	0.92	0.18
src-07	31	54.225	-110	49.018	m	1048.49	979130.16	-21.98	-139.30	-139.52	0	0.93	0.19
src-08	31	54.217	-110	49.008	m	1048.93	979130.14	-21.85	-139.22	-139.44	0	0.93	0.19
src-10	31	54.200	-110	48.988	m	1049.59	979130.14	-21.62	-139.07	-139.28	0	0.94	0.19
src-12	31	54.179	-110	48.975	m	1049.68	979130.19	-21.52	-138.97	-139.16	0	0.96	0.19
src-14	31	54.163	-110	48.965	m	1051.03	979129.92	-21.35	-138.96	-139.14	0	0.97	0.19
src-16	31	54.164	-110	48.937	m	1052.72	979129.78	-20.98	-138.77	-138.95	0	0.97	0.19
src-18	31	54.160	-110	48.909	m	1054.09	979129.71	-20.61	-138.56	-138.73	0	0.98	0.2
src-20	31	54.146	-110	48.881	m	1055.03	979129.65	-20.37	-138.43	-138.59	0	0.99	0.2
src-22	31	54.131	-110	48.857	m	1056.64	979129.47	-20.03	-138.26	-138.43	0	0.99	0.2
src-24	31	54.113	-110	48.831	m	1057.89	979129.36	-19.73	-138.10	-138.27	0	0.99	0.2
src-26	31	54.100	-110	48.807	m	1059.06	979129.30	-19.41	-137.92	-138.07	0	1.00	0.2
src-28	31	54.086	-110	48.780	m	1060.21	979129.25	-19.08	-137.72	-137.86	0	1.02	0.2
src-30	31	54.074	-110	48.754	m	1061.15	979129.22	-18.81	-137.55	-137.68	0	1.03	0.21

src-32	31	54.065	-110	48.727	m	1062.14	979129.04	-18.67	-137.52	-137.64	0	1.04	0.21
src-34	31	54.056	-110	48.699	m	1062.97	979128.80	-18.65	-137.59	-137.70	0	1.05	0.21
src-36	31	54.050	-110	48.672	m	1063.79	979128.57	-18.61	-137.65	-137.73	0	1.07	0.21
src-38	31	54.042	-110	48.644	m	1064.81	979128.33	-18.53	-137.68	-137.75	0	1.09	0.22
src-40	31	54.037	-110	48.615	m	1065.69	979128.20	-18.38	-137.63	-137.69	0	1.10	0.22
src-42	31	54.031	-110	48.586	m	1066.35	979128.17	-18.20	-137.52	-137.58	0	1.10	0.22
src-44	31	54.021	-110	48.560	m	1066.98	979128.14	-18.02	-137.41	-137.47	0	1.10	0.22
src-46	31	54.006	-110	48.536	m	1067.81	979128.05	-17.84	-137.32	-137.38	0	1.11	0.22
src-48	31	53.992	-110	48.511	m	1068.62	979128.01	-17.60	-137.18	-137.21	0	1.13	0.23
src-50	31	53.976	-110	48.490	m	1069.91	979127.78	-17.42	-137.14	-137.17	0	1.13	0.23
src-52	31	53.962	-110	48.466	m	1071.36	979127.57	-17.16	-137.04	-137.06	0	1.15	0.23
src-54	31	53.957	-110	48.438	m	1072.7	979127.07	-17.24	-137.27	-137.26	0	1.17	0.23
src-56	31	53.946	-110	48.412	m	1074.28	979126.54	-17.27	-137.48	-137.46	0	1.19	0.24
srd-02	31	54.144	-110	50.108	m	1006.92	979132.63	-32.22	-144.90	-145.21	0	0.80	0.16
srd-04	31	54.126	-110	50.089	m	1008.32	979132.37	-32.03	-144.86	-145.17	0	0.81	0.16
srd-06	31	54.109	-110	50.067	m	1009.39	979132.20	-31.85	-144.79	-145.09	0	0.82	0.16
srd-08	31	54.098	-110	50.041	m	1011.44	979131.82	-31.58	-144.76	-145.06	0	0.82	0.16
srd-10	31	54.087	-110	50.015	m	1012.81	979131.59	-31.37	-144.70	-144.99	0	0.83	0.17
srd-11	31	54.080	-110	50.003	m	1013.71	979131.38	-31.29	-144.72	-145.01	0	0.83	0.17
srd-12	31	54.071	-110	49.993	m	1014.59	979131.24	-31.15	-144.68	-144.97	0	0.83	0.17
srd-13	31	54.062	-110	49.982	m	1015.49	979131.02	-31.08	-144.71	-145.00	0	0.83	0.17
srd-14	31	54.054	-110	49.971	m	1016.21	979130.96	-30.91	-144.62	-144.92	0	0.83	0.17
srd-15	31	54.047	-110	49.962	m	1016.78	979130.82	-30.86	-144.63	-144.92	0	0.84	0.17
srd-17	31	54.031	-110	49.940	m	1018.28	979130.54	-30.66	-144.60	-144.89	0	0.84	0.17
srd-18	31	54.021	-110	49.929	m	1019.2	979130.34	-30.56	-144.61	-144.90	0	0.84	0.17
srd-19	31	54.013	-110	49.917	m	1019.9	979130.22	-30.45	-144.58	-144.86	0	0.84	0.17
srd-20	31	54.007	-110	49.905	m	1020.71	979130.11	-30.31	-144.52	-144.80	0	0.85	0.17
srd-21	31	53.997	-110	49.894	m	1021.51	979129.95	-30.20	-144.51	-144.78	0	0.85	0.17
srd-22	31	53.987	-110	49.884	m	1022.32	979129.83	-30.07	-144.46	-144.74	0	0.85	0.17
srd-23	31	53.980	-110	49.874	m	1022.96	979129.72	-29.96	-144.43	-144.71	0	0.85	0.17
srd-24	31	53.971	-110	49.862	m	1023.68	979129.61	-29.84	-144.39	-144.65	0	0.86	0.17
srd-25	31	53.963	-110	49.851	m	1024.57	979129.46	-29.70	-144.35	-144.62	0	0.86	0.17
srd-26	31	53.955	-110	49.841	m	1025.03	979129.43	-29.59	-144.29	-144.56	0	0.86	0.17
srd-27	31	53.945	-110	49.830	m	1025.84	979129.30	-29.45	-144.24	-144.51	0	0.86	0.17
srd-28	31	53.939	-110	49.820	m	1026.3	979129.28	-29.32	-144.16	-144.43	0	0.86	0.17
srd-29	31	53.930	-110	49.809	m	1027.05	979129.17	-29.19	-144.12	-144.39	0	0.86	0.17
srd-30	31	53.922	-110	49.799	m	1027.69	979129.05	-29.09	-144.09	-144.35	0	0.87	0.17

srd-31	31	53.914	-110	49.788	m	1028.27	979128.97	-28.99	-144.05	-144.31	0	0.87	0.17
srd-32	31	53.907	-110	49.776	m	1029.09	979128.83	-28.86	-144.01	-144.28	0	0.87	0.17
srd-33	31	53.899	-110	49.766	m	1029.75	979128.73	-28.75	-143.97	-144.24	0	0.87	0.17
srd-34	31	53.892	-110	49.754	m	1030.49	979128.63	-28.62	-143.93	-144.18	0	0.88	0.18
srd-35	31	53.883	-110	49.744	m	1031.21	979128.51	-28.50	-143.89	-144.14	0	0.88	0.18
srd-36	31	53.875	-110	49.733	m	1031.95	979128.40	-28.37	-143.84	-144.10	0	0.88	0.18
srd-37	31	53.867	-110	49.721	m	1032.63	979128.30	-28.25	-143.80	-144.06	0	0.88	0.18
srd-38	31	53.858	-110	49.711	m	1033.46	979128.16	-28.12	-143.77	-144.01	0	0.89	0.18
srd-39	31	53.848	-110	49.699	m	1034.2	979128.03	-28.01	-143.73	-143.98	0	0.89	0.18
srd-40	31	53.842	-110	49.691	m	1034.84	979127.90	-27.93	-143.73	-143.98	0	0.89	0.18
srd-41	31	53.836	-110	49.679	m	1035.41	979127.84	-27.81	-143.67	-143.92	0	0.89	0.18
srd-42	31	53.837	-110	49.660	m	1034.45	979128.21	-27.74	-143.50	-143.73	0	0.90	0.18
srd-43	31	53.839	-110	49.645	m	1035.62	979128.01	-27.58	-143.46	-143.70	0	0.90	0.18
srd-44	31	53.839	-110	49.628	m	1037.27	979127.71	-27.37	-143.43	-143.67	0	0.90	0.18
srd-46	31	53.824	-110	49.601	m	1039	979127.47	-27.05	-143.32	-143.56	0	0.90	0.18
srd-48	31	53.807	-110	49.579	m	1040.96	979127.12	-26.77	-143.26	-143.49	0	0.91	0.18
srd-50	31	53.794	-110	49.556	m	1041.89	979127.03	-26.56	-143.15	-143.37	0	0.92	0.18
srd-52	31	53.778	-110	49.533	m	1043.22	979126.84	-26.32	-143.06	-143.27	0	0.93	0.19
srd-54	31	53.759	-110	49.516	m	1044.3	979126.67	-26.13	-142.99	-143.19	0	0.94	0.19
srd-56	31	53.747	-110	49.487	m	1046.11	979126.39	-25.84	-142.90	-143.09	0	0.95	0.19
srd-58	31	53.727	-110	49.469	m	1047.23	979126.20	-25.65	-142.84	-143.02	0	0.96	0.19
srd-60	31	53.707	-110	49.452	m	1048.88	979125.89	-25.43	-142.80	-142.97	0	0.97	0.19
srd-62	31	53.689	-110	49.435	m	1050.18	979125.64	-25.25	-142.76	-142.93	0	0.98	0.2
srd-64	31	53.673	-110	49.414	m	1051.87	979125.35	-25.00	-142.70	-142.87	0	0.98	0.2
srd-66	31	53.657	-110	49.394	m	1053.28	979125.12	-24.77	-142.63	-142.79	0	0.99	0.2
srd-68	31	53.643	-110	49.369	m	1054.54	979124.98	-24.51	-142.51	-142.66	0	1.00	0.2
srd-70	31	53.630	-110	49.341	m	1055.99	979124.83	-24.19	-142.35	-142.50	0	1.01	0.2
srd-72	31	53.619	-110	49.319	m	1057.21	979124.69	-23.95	-142.25	-142.39	0	1.01	0.2
srd-74	31	53.608	-110	49.294	m	1058.47	979124.58	-23.65	-142.09	-142.21	0	1.03	0.21
srd-76	31	53.597	-110	49.268	m	1059.91	979124.43	-23.33	-141.94	-142.05	0	1.04	0.21
srd-78	31	53.590	-110	49.245	m	1061.22	979124.31	-23.05	-141.80	-141.90	0	1.05	0.21
srd-80	31	53.581	-110	49.219	m	1062.67	979124.20	-22.70	-141.61	-141.71	0	1.05	0.21
srd-82	31	53.570	-110	49.194	m	1064.14	979124.06	-22.37	-141.45	-141.54	0	1.06	0.21
srd-84	31	53.556	-110	49.172	m	1065.45	979123.97	-22.03	-141.25	-141.34	0	1.07	0.21
srd-85	31	53.547	-110	49.161	m	1066	979123.97	-21.85	-141.13	-141.21	0	1.08	0.22
srd-86	31	53.538	-110	49.149	m	1066.74	979123.90	-21.68	-141.05	-141.12	0	1.09	0.22
srd-87	31	53.530	-110	49.138	m	1067.63	979123.82	-21.48	-140.95	-141.02	0	1.09	0.22

srd-88	31	53.521	-110	49.127	m	1068.49	979123.73	-21.29	-140.85	-140.91	0	1.10	0.22
srd-89	31	53.513	-110	49.121	m	1068.85	979123.68	-21.22	-140.82	-140.87	0	1.11	0.22
srd-90	31	53.503	-110	49.110	m	1069.96	979123.46	-21.08	-140.80	-140.86	0	1.11	0.22
srd-91	31	53.492	-110	49.102	m	1070.71	979123.29	-21.00	-140.82	-140.85	0	1.13	0.23
srd-92	31	53.476	-110	49.096	m	1071.23	979123.04	-21.07	-140.94	-140.96	0	1.15	0.23
sre-2.6	31	53.895	-110	48.409	m	1074.33	979126.23	-17.50	-137.71	-137.66	0	1.22	0.24
sre-15	31	53.830	-110	48.403	m	1075.12	979125.39	-18.01	-138.31	-138.24	0	1.24	0.25
sre-22	31	53.789	-110	48.389	m	1077.43	979124.47	-18.15	-138.71	-138.65	0	1.23	0.25
sre-30	31	53.746	-110	48.354	m	1079.71	979123.91	-17.95	-138.77	-138.70	0	1.24	0.25
sre-37	31	53.710	-110	48.326	m	1082.35	979123.72	-17.28	-138.39	-138.31	0.02	1.25	0.25
sre-43	31	53.670	-110	48.316	m	1089.03	979122.47	-16.42	-138.28	-138.24	0.04	1.21	0.24
sre-50	31	53.583	-110	48.426	m	1127.32	979114.15	-12.80	-138.95	-138.60	0.13	1.55	0.31
srf-01	31	54.382	-110	49.946	m	1008.5	979133.11	-31.58	-144.43	-144.76	0	0.78	0.16
srf-02	31	54.306	-110	50.002	m	1006.74	979133.25	-31.88	-144.53	-144.85	0	0.79	0.16
srf-03	31	54.224	-110	50.056	m	1005.24	979133.30	-32.18	-144.66	-144.98	0	0.80	0.16
srf-04	31	54.163	-110	50.127	m	1005.58	979132.90	-32.40	-144.92	-145.24	0	0.80	0.16
srf-06	31	54.032	-110	50.241	f	3298	979132.42	-32.80	-145.29	-145.59	0	0.81	1.02
srf-07	31	53.962	-110	50.283	m	1006.63	979131.66	-33.04	-145.68	-145.97	0	0.82	0.17
srf-08	31	53.882	-110	50.295	f	3310	979130.97	-32.92	-145.81	-146.10	0	0.83	1.02
srf-09	31	53.802	-110	50.310	f	3316	979130.31	-32.91	-146.01	-146.29	0	0.84	1.02
srf-10	31	53.724	-110	50.376	m	1010.54	979129.81	-33.37	-146.44	-146.70	0	0.86	0.17
srf-12	31	53.422	-110	50.571	f	3336	979126.86	-33.97	-147.75	-148.00	0	0.87	1.02
srf-13	31	53.299	-110	50.639	m	1018.67	979126.40	-33.69	-147.68	-147.93	0	0.87	0.17
srf-14	31	53.129	-110	50.736	f	3353	979125.03	-33.81	-148.17	-148.40	0	0.89	1.02
srf-16	31	52.839	-110	50.957	m	1026.25	979123.49	-33.64	-148.48	-148.71	0	0.90	0.18
srf-17	31	52.683	-110	50.982	m	1031.09	979122.40	-33.03	-148.40	-148.62	0	0.92	0.18
srg-01	31	52.579	-110	50.936	m	1039.39	979120.85	-31.88	-148.18	-148.40	0	0.92	0.18
srg-02	31	52.587	-110	50.949	m	1038.3	979121.03	-32.04	-148.22	-148.44	0	0.92	0.18
srg-03	31	52.594	-110	50.961	m	1037.11	979121.24	-32.21	-148.26	-148.48	0	0.92	0.18
srg-04	31	52.600	-110	50.973	m	1035.81	979121.45	-32.40	-148.31	-148.53	0	0.92	0.18
srg-05	31	52.603	-110	50.986	m	1034.48	979121.69	-32.58	-148.34	-148.56	0	0.92	0.18
srg-06	31	52.611	-110	50.999	m	1033.88	979121.80	-32.67	-148.36	-148.57	0	0.92	0.18
srg-07	31	52.619	-110	51.010	m	1033.31	979121.86	-32.79	-148.42	-148.64	0	0.92	0.18
srg-08	31	52.627	-110	51.022	m	1032.8	979121.90	-32.93	-148.49	-148.72	0	0.91	0.18
srg-09	31	52.634	-110	51.034	m	1031.9	979122.04	-33.06	-148.53	-148.76	0	0.91	0.18
srg-10	31	52.641	-110	51.046	m	1030.79	979122.26	-33.21	-148.55	-148.77	0	0.91	0.18
srg-11	31	52.648	-110	51.058	m	1029.71	979122.41	-33.39	-148.61	-148.84	0	0.91	0.18

srg-12	31	52.656	-110	51.070	m	1028.38	979122.63	-33.59	-148.67	-148.89	0	0.91	0.18
srg-13	31	52.664	-110	51.083	m	1027.66	979122.74	-33.72	-148.71	-148.93	0	0.91	0.18
srg-14	31	52.671	-110	51.095	m	1027.55	979122.71	-33.79	-148.77	-148.99	0	0.91	0.18
srg-15	31	52.678	-110	51.107	m	1026.6	979122.83	-33.97	-148.85	-149.07	0	0.91	0.18
srg-16	31	52.686	-110	51.122	m	1025.62	979122.98	-34.14	-148.90	-149.12	0	0.91	0.18
srg-17	31	52.693	-110	51.134	m	1025.12	979123.08	-34.20	-148.91	-149.13	0	0.91	0.18
srg-18	31	52.699	-110	51.146	m	1024.35	979123.18	-34.35	-148.97	-149.19	0	0.91	0.18
srg-19	31	52.705	-110	51.158	m	1023.42	979123.34	-34.48	-149.00	-149.22	0	0.91	0.18
srg-20	31	52.712	-110	51.171	m	1022.47	979123.49	-34.64	-149.05	-149.27	0	0.91	0.18
srg-21	31	52.717	-110	51.185	m	1021.59	979123.64	-34.76	-149.08	-149.30	0	0.90	0.18
srg-22	31	52.725	-110	51.197	m	1020.7	979123.78	-34.90	-149.12	-149.35	0	0.90	0.18
srg-23	31	52.732	-110	51.211	m	1019.76	979123.95	-35.04	-149.15	-149.39	0	0.89	0.18
srg-24	31	52.739	-110	51.224	m	1018.76	979124.12	-35.18	-149.18	-149.41	0	0.89	0.18
srg-25	31	52.746	-110	51.239	m	1017.72	979124.32	-35.32	-149.20	-149.44	0	0.88	0.18
srg-26	31	52.753	-110	51.253	m	1016.73	979124.52	-35.43	-149.20	-149.45	0	0.88	0.18
srg-27	31	52.759	-110	51.269	m	1015.87	979124.61	-35.61	-149.29	-149.53	0	0.88	0.18
srg-28	31	52.765	-110	51.284	m	1014.82	979124.79	-35.77	-149.32	-149.58	0	0.87	0.17
srg-29	31	52.771	-110	51.298	m	1014.02	979124.94	-35.87	-149.34	-149.59	0	0.87	0.17
srg-30	31	52.777	-110	51.311	m	1013.26	979125.04	-36.01	-149.39	-149.64	0	0.87	0.17
srg-31	31	52.785	-110	51.324	m	1012.37	979125.19	-36.15	-149.43	-149.68	0	0.87	0.17
srg-32	31	52.789	-110	51.337	m	1011.61	979125.34	-36.24	-149.44	-149.70	0	0.86	0.17

APPENDIX B: PORTABLE MAGNETOMETER DATA

Station	NAD 27 Easting(m)	NAD 27 Northing(m)	Reading average (nT)	Corrected for diurnal to base sra-01 (=48680.7) (nT)	IGRF (nT)	Corrected for IGRF (nT)	Comments
sra-00.1	517195.4	3529671.7	48734.8	48720.7	48955.7	-235.0	
sra-00.2	517190.3	3529672.1	48660.3	48646.2	48955.7	-309.5	
sra-00.3	517185.2	3529672.4	48686.9	48672.7	48955.7	-282.9	
sra-01	516780.9	3529633.4	48680.7		48955.0	-274.3	Primary Base
sra-02	517180.1	3529672.8	48695.7	48681.4	48955.7	-274.3	
sra-02.1	517174.9	3529673.7	48680.9	48666.5	48955.7	-289.2	
sra-02.5	517169.7	3529674.7	48691.1	48676.6	48955.7	-279.1	
sra-02.51	517163.6	3529675.3	48692.0	48677.5	48955.7	-278.2	
sra-03	517157.5	3529675.8	48697.6	48683.0	48955.7	-272.7	
sra-03.5	517148.3	3529678.2	48702.7	48688.1	48955.7	-267.6	
sra-04	517139.9	3529678.6	48702.1	48687.5	48955.7	-268.2	
sra-04.1	517136.5	3529680.6	48699.8	48685.1	48955.7	-270.6	
sra-04.5	517133.1	3529682.5	48698.8	48684.0	48955.7	-271.7	
sra-04.51	517130.1	3529683.5	48696.6	48681.8	48955.7	-273.9	
sra-05	517127.2	3529684.4	48693.1	48678.3	48955.7	-277.5	
sra-05.1	517119.9	3529682.8	48678.0	48663.1	48955.7	-292.6	
sra-05.5	517112.5	3529681.2	48678.4	48663.4	48955.7	-292.3	
sra-05.51	517106.0	3529682.7	48681.2	48666.1	48955.7	-289.6	
sra-06	517099.4	3529684.1	48679.1	48663.9	48955.7	-291.8	
sra-06.1	517094.3	3529683.5	48682.7	48667.5	48955.7	-288.2	
sra-06.5	517089.2	3529682.9	48676.9	48661.7	48955.7	-294.1	
sra-06.51	517083.3	3529682.0	48675.5	48660.2	48955.7	-295.5	
sra-07	517077.4	3529681.2	48681.2	48665.8	48955.7	-289.9	
sra-07.1	517070.5	3529683.8	48681.7	48666.3	48955.7	-289.4	
sra-07.5	517063.5	3529686.3	48688.4	48672.8	48955.7	-282.9	
sra-07.51	517067.4	3529684.7	48677.8	48662.1	48955.7	-293.6	
sra-07.52	517055.3	3529688.5	48690.2	48674.5	48955.7	-281.2	
sra-08	517049.8	3529689.9	48688.8	48673.0	48955.7	-282.7	
sra-08.1	517045.0	3529690.3	48685.6	48669.8	48955.7	-285.9	
sra-08.5	517040.2	3529690.7	48683.1	48667.2	48955.7	-288.5	
sra-08.51	517035.4	3529690.8	48684.1	48668.1	48955.7	-287.5	
sra-09	517030.7	3529691.0	48683.2	48667.2	48955.7	-288.5	
sra-09.1	517024.8	3529692.2	48689.5	48673.4	48955.7	-282.2	
sra-09.5	517019.0	3529693.3	48689.7	48673.7	48955.6	-282.0	
sra-09.51	517014.4	3529693.5	48694.2	48678.1	48955.6	-277.6	
sra-10	517009.9	3529693.6	48692.9	48676.7	48955.6	-278.9	
sra-10.1	517005.2	3529691.3	48693.3	48677.1	48955.6	-278.6	
sra-10.2	517000.6	3529689.0	48698.2	48681.9	48955.6	-273.8	
sra-10.5	516995.9	3529686.7	48692.6	48676.2	48955.6	-279.4	
sra-10.51	516992.0	3529685.6	48693.9	48677.4	48955.6	-278.2	
sra-10.52	516988.2	3529684.5	48706.5	48689.9	48955.6	-265.7	
sra-11	516984.4	3529683.4	48699.4	48682.8	48955.6	-272.8	
sra-11.1	516977.9	3529683.3	48695.1	48678.5	48955.6	-277.1	
sra-11.5	516971.4	3529683.3	48691.0	48674.3	48955.6	-281.2	
sra-11.51	516965.8	3529682.6	48686.7	48670.0	48955.5	-285.6	
sra-11.52	516960.3	3529681.9	48691.4	48674.5	48955.5	-281.0	
sra-12	516954.7	3529681.2	48697.2	48680.2	48955.5	-275.3	

sra-12.1	516948.7	3529680.9	48697.8	48680.8	48955.5	-274.7	
sra-12.5	516942.6	3529680.5	48691.1	48674.0	48955.5	-281.5	
sra-12.51	516937.8	3529679.8	48690.4	48673.3	48955.5	-282.2	
sra-13	516932.9	3529679.1	48697.5	48680.3	48955.5	-275.2	
sra-13.1	516926.4	3529678.3	48688.6	48671.4	48955.5	-284.0	
sra-13.2	516919.8	3529677.5	48690.0	48672.6	48955.4	-282.9	
sra-13.3	516913.3	3529676.7	48689.0	48671.5	48955.4	-283.9	
sra-14	516906.7	3529675.9	48692.7	48675.1	48955.4	-280.3	
sra-14.1	516902.0	3529674.8	48694.7	48677.1	48955.4	-278.3	
sra-14.2	516897.3	3529673.8	48695.0	48677.4	48955.4	-278.0	
sra-14.3	516892.5	3529672.8	48690.2	48672.5	48955.4	-282.9	
sra-15	516887.8	3529671.7	48688.5	48670.7	48955.4	-284.7	
sra-15.1	516880.7	3529670.7	48689.3	48671.4	48955.4	-284.0	
sra-15.2	516873.6	3529669.8	48688.5	48670.5	48955.4	-284.9	
sra-16	516866.5	3529668.8	48689.1	48671.0	48955.3	-284.4	
sra-16.1	516861.8	3529671.1	48693.5	48675.3	48955.3	-280.1	
sra-16.2	516857.1	3529673.4	48691.7	48673.4	48955.3	-281.9	
sra-17	516852.3	3529675.8	48690.6	48672.3	48955.3	-283.0	=srb-0
sra-17.1	516846.3	3529675.8	48690.8	48672.4	48955.3	-282.8	
sra-17.2	516840.3	3529675.9	48695.0	48676.5	48955.3	-278.8	
sra-17.3	516834.4	3529676.0	48707.4	48688.9	48955.3	-266.3	
sra-18	516828.4	3529676.1	48701.0	48682.5	48955.3	-272.8	
sra-18.1	516807.6	3529677.5	48695.9	48677.3	48955.2	-277.9	
sra-18.2	516812.8	3529677.2	48694.4	48675.7	48955.2	-279.6	
sra-18.3	516818.0	3529676.8	48696.9	48678.1	48955.2	-277.1	
sra-18.4	516823.2	3529676.5	48698.3	48679.4	48955.3	-275.8	
sra-19	516802.4	3529677.9	48697.8	48678.9	48955.2	-276.3	
sra-19.1	516798.7	3529673.9	48699.0	48679.9	48955.2	-275.3	
sra-19.2	516795.0	3529669.9	48696.1	48677.0	48955.2	-278.2	
sra-19.3	516791.3	3529665.9	48690.2	48671.1	48955.2	-284.1	
sra-20	516787.6	3529662.0	48673.4	48670.8	48955.2	-284.4	
sra-20.5	516776.5	3529664.3	48675.7	48673.0	48955.2	-282.1	
sra-21	516765.5	3529666.6	48678.4	48675.7	48955.2	-279.5	
sra-21.5	516754.6	3529668.8	48679.2	48676.5	48955.1	-278.7	
sra-22	516743.8	3529670.9	48679.7	48676.9	48955.1	-278.2	
sra-22.5	516733.1	3529671.7	48680.6	48677.8	48955.1	-277.3	
sra-23	516722.4	3529672.5	48680.8	48678.0	48955.1	-277.1	
sra-23.5	516711.5	3529673.7	48683.0	48680.1	48955.1	-275.0	
sra-24	516700.6	3529674.8	48684.2	48681.2	48955.1	-273.9	
sra-24.5	516689.9	3529675.3	48681.8	48678.8	48955.1	-276.3	
sra-25	516679.2	3529675.7	48682.8	48679.7	48955.1	-275.3	
sra-25.5	516668.8	3529677.6	48681.3	48678.2	48955.1	-276.9	
sra-26	516658.4	3529679.5	48681.0	48677.9	48955.1	-277.2	
sra-26.5	516649.5	3529687.8	48676.9	48673.7	48955.0	-281.4	
sra-27	516640.7	3529696.1	48678.9	48674.5	48955.0	-280.6	
sra-27.1	516631.5	3529691.4	48688.2	48683.6	48955.0	-271.4	
sra-27.2	516622.2	3529686.7	48684.0	48679.4	48955.0	-275.6	
sra-28	516612.9	3529682.0	48686.2	48681.6	48955.0	-273.5	
sra-28.5	516602.9	3529681.1	48690.7	48686.0	48955.0	-269.0	
sra-29	516592.8	3529680.1	48697.5	48692.7	48955.0	-262.3	
sra-29.5	516581.7	3529680.6	48692.7	48687.9	48955.0	-267.1	
sra-30	516570.6	3529681.0	48693.2	48688.3	48955.0	-266.6	
sra-30.5	516559.9	3529681.1	48694.4	48689.5	48955.0	-265.5	
sra-31	516549.3	3529681.2	48686.0	48681.1	48955.0	-273.9	
sra-31.5	516536.3	3529681.8	48690.0	48685.0	48955.0	-269.9	
sra-32	516523.3	3529682.3	48698.5	48693.5	48954.9	-261.4	

sra-32.5	516511.9	3529684.0	48640.1	48635.0	48954.9	-319.9	
sra-33	516500.5	3529685.8	48685.3	48680.2	48954.9	-274.8	<25m from fence
sra-33.5	516478.3	3529686.7	48692.1	48686.9	48954.9	-268.0	"
sra-35	516456.0	3529687.5	48694.6	48689.3	48954.9	-265.6	"
sra-35.5	516443.9	3529690.5	48690.6	48685.2	48954.9	-269.7	
sra-36	516431.8	3529693.5	48685.9	48680.4	48954.9	-274.4	
sra-36.5	516420.4	3529690.7	48698.2	48692.6	48954.8	-262.2	
sra-37	516409.0	3529688.0	48690.8	48684.9	48954.8	-269.6	
sra-37.5	516398.1	3529691.8	48687.7	48681.7	48954.9	-273.1	
sra-38	516387.2	3529695.7	48694.4	48688.4	48954.9	-266.5	
sra-38.5	516375.4	3529698.9	48699.8	48693.8	48954.9	-261.1	
sra-39	516363.5	3529702.1	48693.2	48687.2	48954.9	-267.7	
sra-39.5	516352.6	3529706.6	48695.7	48689.7	48954.9	-265.2	
sra-40	516341.7	3529711.0	48694.2	48688.2	48955.0	-266.7	
sra-40.5	516331.3	3529713.9	48694.7	48688.7	48955.0	-266.3	
sra-41	516320.9	3529716.7	48694.2	48688.2	48955.0	-266.8	
sra-41.5	516310.5	3529719.5	48691.9	48685.9	48955.0	-269.1	
sra-42	516300.1	3529722.3	48695.4	48689.4	48955.0	-265.6	
sra-42.5	516289.4	3529725.5	48697.0	48690.9	48955.0	-264.1	
sra-43	516278.7	3529728.8	48698.8	48692.8	48955.1	-262.3	
sra-43.5	516268.0	3529732.1	48699.8	48693.7	48955.1	-261.4	
sra-44	516257.3	3529735.3	48697.9	48691.8	48955.1	-263.3	
sra-44.5	516248.3	3529742.2	48692.2	48686.1	48955.1	-269.0	
sra-45	516239.3	3529749.0	48692.6	48686.5	48955.1	-268.7	
sra-45.5	516230.4	3529755.9	48706.3	48700.2	48955.1	-254.9	
sra-46	516221.4	3529762.7	48695.8	48689.7	48955.2	-265.5	
sra-46.5	516209.5	3529765.8	48697.4	48691.3	48955.2	-263.9	
sra-47	516197.7	3529768.9	48699.6	48693.4	48955.2	-261.8	
sra-47.5	516185.8	3529772.1	48699.3	48693.1	48955.2	-262.2	
sra-48	516174.0	3529775.2	48696.7	48690.5	48955.2	-264.8	
sra-48.5	516167.7	3529783.9	48700.4	48694.2	48955.3	-261.1	
sra-49	516161.5	3529792.6	48695.0	48688.8	48955.3	-266.5	
sra-49.5	516155.2	3529801.3	48701.7	48695.5	48955.3	-259.8	
sra-50	516148.9	3529810.1	48692.0	48685.8	48955.3	-269.5	
sra-50.5	516140.9	3529818.0	48697.0	48690.7	48955.3	-264.6	
sra-51	516132.9	3529826.0	48692.5	48686.2	48955.3	-269.2	
sra-51.5	516124.8	3529833.9	48698.0	48691.7	48955.4	-263.6	7m from steel post
sra-52	516116.8	3529841.9	48696.9	48690.6	48955.4	-264.8	"
sra-52.5	516105.8	3529848.3	48688.6	48682.3	48955.4	-273.1	
sra-54	516072.9	3529867.8	48665.5	48694.3	48955.5	-261.2	
sra-54.1	516063.1	3529873.9	48665.9	48694.7	48955.5	-260.8	
sra-54.2	516053.4	3529880.0	48632.0	48660.7	48955.5	-294.8	
sra-54.3	516043.7	3529886.1	48661.1	48689.9	48955.5	-265.6	
sra-54.4	516033.9	3529892.3	48659.6	48688.3	48955.6	-267.2	
sra-56	516031.3	3529893.9	48662.2	48690.9	48955.6	-264.7	
sra-56.1	516020.3	3529898.5	48664.6	48693.3	48955.6	-262.3	
sra-56.2	516009.3	3529903.1	48661.5	48690.2	48955.6	-265.4	
sra-56.3	515998.3	3529907.8	48652.7	48681.3	48955.6	-274.3	
sra-58	515987.3	3529912.4	48648.2	48676.8	48955.6	-278.8	
sra-58.1	515976.3	3529917.2	48688.5	48717.2	48955.6	-238.4	
sra-58.2	515965.3	3529922.0	48668.6	48697.3	48955.6	-258.4	
sra-58.3	515954.3	3529926.7	48647.3	48675.9	48955.7	-279.8	
sra-60	515943.3	3529931.5	48665.2	48679.6	48955.7	-276.0	
sra-60.1	515934.9	3529938.4	48671.7	48686.1	48955.7	-269.6	

sra-60.2	515926.4	3529945.4	48671.0	48685.4	48955.7	-270.3	
sra-60.3	515917.9	3529952.3	48667.2	48681.6	48955.7	-274.1	
sra-62	515909.4	3529959.2	48668.0	48682.4	48955.7	-273.4	parallel to fence,
sra-62.1	515904.9	3529969.7	48664.7	48679.0	48955.8	-276.7	~10m to S
sra-62.2	515900.4	3529980.1	48658.7	48673.1	48955.8	-282.7	"
sra-62.3	515895.9	3529990.6	48665.0	48679.3	48955.8	-276.5	"
sra-64	515891.3	3530001.1	48665.5	48679.9	48956.0	-276.1	"
sra-64.1	515880.6	3530005.6	48659.6	48673.9	48956.0	-282.1	"
sra-64.2	515870.0	3530010.1	48662.2	48676.5	48956.0	-279.5	"
sra-64.3	515859.3	3530014.6	48655.4	48669.7	48956.0	-286.3	"
sra-66	515848.6	3530019.2	48658.8	48673.0	48956.0	-283.0	"
sra-66.1	515837.1	3530019.8	48663.5	48677.1	48956.0	-279.0	"
sra-66.2	515825.7	3530020.4	48662.1	48675.6	48956.0	-280.4	"
sra-66.3	515814.3	3530021.1	48662.5	48675.9	48956.1	-280.1	"
sra-68	515802.9	3530021.7	48665.0	48678.4	48956.1	-277.7	"
sra-68.1	515790.9	3530021.8	48671.5	48684.7	48956.0	-271.4	"
sra-68.2	515779.0	3530021.8	48668.1	48681.2	48956.0	-274.9	"
sra-68.3	515767.0	3530021.9	48667.6	48680.5	48956.0	-275.5	"
sra-70	515755.1	3530022.0	48670.7	48683.5	48956.0	-272.4	"
sra-70.1	515743.3	3530021.7	48671.9	48684.6	48956.0	-271.4	"
sra-70.2	515731.5	3530021.5	48649.8	48662.3	48955.9	-293.6	
sra-70.3	515719.7	3530021.2	48640.2	48652.4	48955.9	-303.6	
sra-70.4	515707.9	3530020.9	48641.2	48653.1	48955.9	-302.8	
sra-70.5	515696.2	3530020.7	48655.0	48666.4	48955.9	-289.5	
sra-70.6	515684.4	3530020.4	48649.9	48661.0	48955.9	-294.9	
sra-70.7	515672.6	3530020.1	48653.4	48664.5	48955.9	-291.4	
sra-74	515660.8	3530019.8	48659.1	48670.1	48955.9	-285.7	
sra-74.1	515649.0	3530020.3	48661.4	48672.2	48955.8	-283.6	
sra-74.2	515637.2	3530020.8	48637.9	48648.7	48955.8	-307.1	
sra-74.3	515625.4	3530021.3	48663.6	48674.3	48955.8	-281.6	
sra-74.4	515613.6	3530021.8	48666.8	48677.1	48955.8	-278.7	
sra-74.5	515601.8	3530022.3	48663.9	48674.3	48955.8	-281.5	
sra-74.6	515590.0	3530022.8	48668.2	48678.4	48955.8	-277.3	
sra-74.7	515578.2	3530023.3	48659.7	48669.9	48955.8	-285.8	
sra-78	515566.4	3530023.8	48656.8	48666.9	48955.7	-288.8	
sra-78.1	515555.7	3530027.7	48664.2	48673.8	48955.8	-282.0	
sra-78.2	515545.1	3530031.6	48664.9	48674.4	48955.8	-281.4	
sra-78.3	515534.4	3530035.5	48664.7	48674.2	48955.8	-281.6	
sra-78.4	515523.8	3530039.3	48655.2	48664.6	48955.8	-291.2	
sra-78.5	515513.1	3530043.2	48654.3	48663.7	48955.8	-292.1	
sra-78.6	515502.5	3530047.1	48663.0	48672.3	48955.8	-283.5	
sra-82	515494.0	3530050.2	48657.8	48667.0	48955.8	-288.8	
sra-82.1	515485.5	3530057.3	48646.6	48655.4	48955.8	-300.4	
sra-82.2	515477.1	3530064.3	48661.4	48670.1	48955.9	-285.7	
sra-82.3	515468.6	3530071.4	48654.8	48663.5	48955.9	-292.4	
sra-82.4	515460.2	3530078.4	48650.5	48659.1	48955.9	-296.8	
sra-82.5	515451.7	3530085.5	48649.7	48658.3	48956.0	-297.7	
sra-82.6	515443.3	3530092.5	48651.3	48659.8	48956.0	-296.2	
sra-82.7	515434.9	3530099.6	48652.4	48660.5	48956.0	-295.5	
sra-82.8	515426.4	3530106.6	48658.3	48666.1	48956.1	-289.9	
sra-86	515421.9	3530110.4	48658.4	48666.1	48956.1	-289.9	
sra-86.1	515412.3	3530117.8	48663.6	48662.4	48956.1	-293.7	
sra-86.2	515402.7	3530125.3	48659.5	48658.2	48956.1	-298.0	
sra-86.3	515393.2	3530132.7	48667.8	48666.2	48956.2	-289.9	
sra-86.4	515383.6	3530140.2	48666.8	48665.0	48956.2	-291.2	

sra-86.5	515374.0	3530147.6	48668.3	48666.3	48956.2	-289.9	
sra-86.6	515364.4	3530155.0	48672.9	48670.6	48956.3	-285.7	
sra-86.7	515354.8	3530162.5	48672.7	48670.2	48956.3	-286.1	
sra-90	515345.2	3530169.9	48675.5	48672.8	48956.3	-283.5	
srb-0	516852.3	3529675.8	48663.0	48670.5	48955.3	-284.8	=sra-17
srb-0.1	516845.7	3529666.1	48669.3	48676.5	48955.3	-278.8	
srb-0.2	516839.0	3529656.5	48668.9	48676.0	48955.2	-279.2	
srb-0.3	516832.4	3529646.8	48667.4	48674.4	48955.1	-280.7	
srb-02	516825.7	3529637.2	48663.5	48670.3	48955.0	-284.8	
srb-02.1	516819.7	3529628.4	48671.3	48677.7	48955.0	-277.3	
srb-02.2	516813.7	3529619.6	48662.6	48668.8	48954.9	-286.1	
srb-02.3	516807.6	3529610.8	48666.6	48672.7	48954.9	-282.1	
srb-04	516801.6	3529602.0	48670.5	48676.4	48954.8	-278.4	
srb-04.1	516796.1	3529593.3	48683.0	48688.6	48954.7	-266.1	
srb-04.2	516790.5	3529584.6	48676.6	48682.0	48954.7	-272.6	
srb-04.3	516785.0	3529575.9	48673.1	48678.4	48954.6	-276.2	
srb-06	516779.5	3529567.3	48653.0	48658.9	48954.6	-295.6	
srb-06.1	516774.3	3529558.3	48666.3	48672.1	48954.5	-282.4	
srb-06.2	516769.0	3529549.4	48681.4	48687.2	48954.4	-267.2	
srb-06.3	516763.7	3529540.5	48679.2	48684.9	48954.4	-269.4	
srb-08	516758.5	3529531.6	48673.2	48678.9	48954.3	-275.4	
srb-08.1	516752.0	3529522.6	48651.7	48657.3	48954.2	-296.9	
srb-08.2	516745.5	3529513.5	48678.9	48684.5	48954.2	-269.7	
srb-08.3	516739.0	3529504.5	48683.7	48689.3	48954.1	-264.8	
srb-10	516732.4	3529495.5	48678.1	48683.7	48954.1	-270.4	
srb-10.1	516726.4	3529486.4	48685.9	48691.4	48954.0	-262.5	
srb-10.2	516720.3	3529477.4	48689.4	48694.9	48953.9	-259.1	
srb-10.3	516714.2	3529468.3	48686.4	48691.7	48953.9	-262.2	
srb-12	516708.2	3529459.3	48672.5	48677.8	48953.8	-276.0	
srb-12.1	516702.2	3529449.0	48687.5	48692.7	48953.7	-261.0	
srb-12.2	516696.2	3529438.6	48680.5	48685.7	48953.7	-268.0	
srb-12.3	516690.2	3529428.3	48678.1	48683.3	48953.6	-270.3	
srb-14	516684.2	3529418.0	48696.5	48701.6	48953.6	-251.9	
srb-14.1	516678.3	3529407.7	48695.5	48700.6	48953.5	-252.9	
srb-14.2	516672.4	3529397.4	48689.6	48694.6	48953.4	-258.8	
srb-14.3	516666.5	3529387.1	48681.1	48686.1	48953.4	-267.3	
srb-14.4	516660.6	3529376.8	48697.9	48702.9	48953.3	-250.4	
srb-16	516659.6	3529375.1	48705.1	48710.1	48953.3	-243.2	
srb-16.1	516654.7	3529365.0	48697.1	48702.0	48953.2	-251.2	
srb-16.2	516649.9	3529354.8	48711.2	48716.1	48953.2	-237.1	
srb-16.3	516645.0	3529344.7	48680.6	48685.5	48953.1	-267.6	
srb-16.4	516640.2	3529334.5	48685.6	48690.4	48953.0	-262.6	
srb-18	516639.4	3529332.8	48706.5	48711.2	48953.0	-241.8	
srb-18.1	516633.4	3529323.9	48693.6	48698.3	48953.0	-254.7	
srb-18.2	516627.5	3529315.1	48697.9	48702.6	48952.9	-250.3	
srb-18.3	516621.5	3529306.2	48716.7	48721.4	48952.8	-231.4	
srb-20	516615.5	3529297.3	48720.3	48714.0	48952.8	-238.8	
srb-20.1	516615.4	3529287.3	48710.9	48704.5	48952.7	-248.2	
srb-20.2	516615.3	3529277.3	48701.3	48694.8	48952.7	-257.8	
srb-20.3	516615.1	3529267.3	48701.3	48694.7	48952.6	-257.9	
srb-20.4	516615.0	3529257.3	48723.0	48716.4	48952.5	-236.2	
srb-22	516614.9	3529251.9	48719.7	48713.0	48952.5	-239.5	
srb-22.1	516611.3	3529241.9	48720.3	48713.5	48952.4	-239.0	
srb-22.2	516607.7	3529231.9	48719.1	48712.1	48952.4	-240.2	
srb-22.3	516604.1	3529221.9	48690.8	48683.7	48952.3	-268.6	

srb-24	516600.5	3529211.9	48721.0	48713.8	48952.2	-238.4
srb-24.1	516600.3	3529200.4	48722.0	48714.8	48952.2	-237.4
srb-24.2	516600.0	3529189.0	48731.7	48724.4	48952.1	-227.7
srb-24.3	516599.8	3529177.5	48726.3	48718.9	48952.0	-233.1
srb-26	516599.6	3529170.6	48732.0	48724.5	48952.0	-227.4
srb-26.1	516598.1	3529159.2	48733.0	48725.4	48951.9	-226.4
srb-26.2	516596.5	3529147.9	48733.0	48725.4	48951.8	-226.4
srb-26.3	516594.9	3529136.5	48729.1	48721.3	48951.7	-230.4
srb-28	516593.9	3529129.0	48734.9	48727.1	48951.7	-224.6
srb-28.1	516592.4	3529117.6	48731.5	48723.7	48951.6	-228.0
srb-28.2	516590.9	3529106.2	48746.0	48738.0	48951.5	-213.5
srb-28.3	516589.3	3529094.9	48730.8	48722.7	48951.5	-228.8
srb-30	516588.4	3529088.1	48734.9	48726.8	48951.4	-224.6
srb-30.1	516586.8	3529076.7	48728.6	48720.4	48951.3	-231.0
srb-30.2	516585.2	3529065.4	48738.7	48730.3	48951.3	-221.0
srb-30.3	516583.5	3529054.1	48740.4	48731.9	48951.2	-219.3
srb-32	516582.2	3529045.1	48741.2	48732.6	48951.1	-218.5
srb-32.1	516580.3	3529031.1	48738.8	48727.8	48951.0	-223.2
srb-32.2	516578.8	3529019.5	48737.7	48726.8	48951.0	-224.2
srb-32.3	516577.2	3529007.9	48745.5	48734.6	48950.9	-216.2
srb-34	516575.6	3528996.3	48746.2	48735.3	48950.8	-215.4
srb-34.1	516574.3	3528985.7	48750.3	48741.4	48950.7	-209.3
srb-34.2	516572.9	3528975.1	48737.5	48728.5	48950.7	-222.1
srb-34.3	516571.6	3528964.4	48739.3	48730.3	48950.6	-220.3
srb-36	516570.3	3528954.5	48740.8	48731.7	48950.5	-218.8
srb-36.1	516568.4	3528943.5	48740.5	48731.4	48950.5	-219.1
srb-36.2	516566.5	3528932.4	48743.6	48734.4	48950.4	-216.0
srb-36.3	516564.7	3528921.4	48739.3	48730.1	48950.3	-220.3
srb-38	516563.0	3528911.8	48741.4	48732.1	48950.3	-218.2
srb-38.1	516561.9	3528900.9	48758.8	48749.4	48950.2	-200.8
srb-38.2	516560.9	3528890.0	48743.1	48733.6	48950.2	-216.5
srb-38.3	516559.8	3528879.2	48738.9	48729.4	48950.1	-220.7
srb-40	516558.7	3528868.3	48739.4	48729.8	48950.0	-220.2
srb-40.1	516557.6	3528857.3	48744.8	48735.2	48950.0	-214.7
srb-40.2	516556.4	3528846.2	48747.2	48737.5	48949.9	-212.4
srb-40.3	516555.2	3528835.2	48746.5	48736.8	48949.9	-213.1
srb-42	516554.4	3528827.8	48747.4	48737.6	48949.9	-212.3
srb-42.1	516549.7	3528817.5	48740.2	48730.3	48949.8	-219.5
srb-42.2	516545.0	3528807.1	48747.4	48737.5	48949.8	-212.2
srb-42.3	516540.3	3528796.7	48743.5	48733.5	48949.7	-216.2
srb-42.4	516535.6	3528786.3	48728.2	48718.2	48949.7	-231.5
srb-44	516530.0	3528773.9	48738.9	48728.9	48949.6	-220.8
srb-44.1	516528.2	3528763.0	48745.0	48734.9	48949.6	-214.7
srb-44.2	516526.4	3528752.1	48747.7	48737.5	48949.5	-212.0
srb-44.3	516524.5	3528741.1	48741.2	48730.9	48949.5	-218.5
srb-46	516523.1	3528732.4	48755.8	48745.5	48949.4	-204.0
src-01	517200.4	3529671.3	48712.7	48698.0	48955.7	-257.7
src-01.1	517204.6	3529668.0	48707.5	48692.8	48955.7	-262.9
src-01.2	517208.8	3529664.7	48698.0	48683.1	48955.7	-272.5
src-01.3	517213.0	3529661.4	48688.4	48673.5	48955.6	-282.2
src-02	517217.3	3529658.1	48699.1	48684.1	48955.6	-271.5
src-02.1	517222.0	3529655.1	48693.3	48678.2	48955.6	-277.4
src-02.2	517226.7	3529652.1	48701.1	48686.0	48955.6	-269.6
src-02.3	517231.4	3529649.0	48706.1	48691.0	48955.6	-264.6
src-03	517236.1	3529646.0	48693.5	48678.3	48955.6	-277.3

src-03.1	517240.3	3529642.3	48694.4	48679.1	48955.6	-276.4
src-03.2	517244.6	3529638.6	48694.4	48679.2	48955.5	-276.4
src-03.3	517248.9	3529634.9	48693.9	48678.6	48955.5	-276.9
src-04	517253.1	3529631.2	48693.2	48677.9	48955.5	-277.6
src-04.1	517257.1	3529628.4	48694.0	48678.6	48955.5	-276.9
src-04.2	517261.1	3529625.5	48696.5	48681.0	48955.5	-274.4
src-04.3	517265.1	3529622.7	48696.0	48680.6	48955.5	-274.9
src-05	517269.1	3529619.9	48697.8	48682.3	48955.5	-273.2
src-05.1	517273.9	3529617.1	48700.2	48684.6	48955.5	-270.8
src-05.2	517278.7	3529614.3	48689.0	48673.4	48955.4	-282.0
src-05.3	517283.5	3529611.6	48682.8	48667.2	48955.4	-288.3
src-06	517288.3	3529608.8	48686.1	48670.4	48955.4	-285.0
src-06.1	517293.1	3529605.4	48693.5	48677.7	48955.4	-277.6
src-06.2	517297.9	3529601.9	48692.8	48677.0	48955.4	-278.4
src-06.3	517302.7	3529598.5	48692.7	48676.9	48955.4	-278.4
src-07	517307.5	3529595.0	48728.9	48712.9	48955.3	-242.4
src-07.1	517311.4	3529591.1	48694.6	48678.1	48955.3	-277.2
src-07.2	517308.8	3529593.7	48718.0	48701.2	48955.3	-254.1
src-07.3	517315.3	3529587.3	48691.9	48674.9	48955.3	-280.4
src-07.4	517319.3	3529583.4	48694.2	48677.1	48955.3	-278.2
src-08	517323.2	3529579.5	48688.7	48671.5	48955.3	-283.7
src-08.1	517327.0	3529575.6	48690.3	48673.0	48955.3	-282.3
src-08.2	517330.9	3529571.7	48676.7	48659.3	48955.3	-296.0
src-08.3	517334.7	3529567.8	48697.5	48680.0	48955.2	-275.3
src-08.4	517338.5	3529563.8	48696.5	48678.9	48955.2	-276.3
src-08.5	517342.3	3529559.9	48694.6	48676.8	48955.2	-278.4
src-08.6	517346.2	3529556.0	48697.3	48679.5	48955.2	-275.7
src-08.7	517350.0	3529552.1	48700.7	48682.8	48955.2	-272.4
src-10	517353.8	3529548.2	48679.4	48661.3	48955.2	-293.9
src-10.1	517356.8	3529542.6	48672.1	48653.8	48955.1	-301.4
src-10.2	517359.9	3529536.9	48678.1	48659.7	48955.1	-295.4
src-10.3	517362.9	3529531.3	48690.2	48671.7	48955.1	-283.4
src-10.4	517366.0	3529525.7	48696.5	48677.9	48955.1	-277.1
src-10.5	517369.0	3529520.0	48693.7	48675.1	48955.0	-280.0
src-10.6	517372.0	3529514.4	48695.9	48677.1	48955.0	-277.9
src-10.7	517373.0	3529512.5	48686.2	48667.2	48955.0	-287.8
src-10.8	517374.1	3529510.6	48683.8	48664.8	48955.0	-290.2
src-12	517375.1	3529508.7	48684.9	48665.7	48955.0	-289.3
src-12.1	517375.1	3529500.3	48695.3	48676.1	48954.9	-278.8
src-12.2	517375.1	3529491.9	48686.6	48667.2	48954.9	-287.6
src-12.3	517375.1	3529480.7	48714.2	48694.7	48954.8	-260.1
src-12.4	517382.7	3529480.7	48693.1	48673.0	48954.8	-281.9
src-14	517390.4	3529480.7	48691.9	48671.7	48954.8	-283.1
src-14.1	517401.6	3529481.0	48698.4	48678.1	48954.8	-276.7
src-14.2	517412.8	3529481.2	48684.6	48664.3	48954.8	-290.5
src-14.3	517424.0	3529481.4	48682.1	48661.8	48954.8	-293.0
src-16	517435.2	3529481.7	48688.6	48668.3	48954.8	-286.5
src-16.1	517446.1	3529480.0	48684.1	48663.8	48954.8	-291.0
src-16.2	517457.0	3529478.2	48691.7	48671.4	48954.8	-283.4
src-16.3	517467.9	3529476.5	48687.0	48666.6	48954.8	-288.1
src-18	517478.8	3529474.8	48705.0	48684.6	48954.8	-270.2
src-18.1	517490.0	3529468.5	48697.6	48677.2	48954.8	-277.6
src-18.2	517501.1	3529462.3	48710.0	48689.6	48954.8	-265.2
src-18.3	517512.3	3529456.0	48697.0	48676.6	48954.8	-278.2
src-20	517523.4	3529449.8	48692.9	48672.4	48954.8	-282.4
src-21	517542.1	3529435.7	48684.8	48687.6	48954.6	-267.0

src-22	517560.8	3529421.7	48678.6	48681.2	48954.6	-273.4	
src-23	517581.6	3529405.3	48669.9	48672.4	48954.5	-282.1	
src-24	517602.5	3529388.9	48681.7	48683.9	48954.5	-270.6	
src-25	517621.2	3529376.6	48681.2	48683.3	48954.4	-271.1	
src-26	517639.9	3529364.2	48683.0	48684.9	48954.4	-269.4	
src-27	517660.7	3529351.5	48680.1	48681.9	48954.4	-272.5	
src-28	517681.6	3529338.7	48657.4	48658.9	48954.3	-295.4	
src-29	517702.4	3529327.1	48682.6	48683.9	48954.3	-270.4	
src-30	517723.1	3529315.5	48675.8	48676.8	48954.3	-277.5	
src-31	517744.3	3529307.2	48677.8	48678.7	48954.3	-275.5	
src-32	517765.5	3529298.9	48676.3	48677.1	48954.2	-277.2	
src-33	517787.4	3529291.0	48687.1	48687.6	48954.2	-266.6	
src-34	517809.4	3529283.0	48685.2	48685.5	48954.2	-268.7	
src-35	517831.2	3529278.0	48660.9	48661.1	48954.2	-293.1	
src-36	517853.0	3529272.9	48687.3	48687.3	48954.2	-266.8	
src-37	517874.9	3529265.1	48691.0	48690.8	48954.1	-263.3	
src-38	517896.8	3529257.3	48699.0	48698.7	48954.1	-255.5	
src-39	517919.5	3529252.3	48689.3	48688.7	48954.1	-265.4	
src-40	517942.1	3529247.4	48683.8	48683.1	48954.1	-271.0	
src-41	517965.0	3529242.4	48685.5	48684.7	48954.1	-269.4	
src-42	517987.8	3529237.4	48682.1	48681.1	48954.1	-273.0	
src-43	518008.8	3529228.1	48660.6	48659.4	48954.1	-294.6	
src-44	518029.7	3529218.8	48669.2	48667.9	48954.0	-286.1	
src-45	518048.5	3529205.1	48679.5	48678.1	48954.0	-276.0	
src-46	518067.3	3529191.4	48681.0	48679.4	48954.0	-274.6	
src-47	518086.7	3529178.5	48678.3	48676.5	48954.0	-277.5	
src-48	518106.1	3529165.7	48680.8	48678.9	48953.9	-275.1	
src-49	518123.0	3529150.5	48684.7	48682.5	48953.9	-271.3	
src-50	518139.9	3529135.4	48680.3	48678.0	48953.8	-275.9	5m from fence
src-51	518159.1	3529122.8	48688.0	48685.5	48953.8	-268.3	"
src-52	518178.3	3529110.1	48731.1	48728.4	48953.8	-225.4	"
src-53	518199.6	3529105.7	48691.5	48688.6	48953.7	-265.1	
src-54	518221.0	3529101.3	48703.8	48700.7	48953.7	-253.0	=sre-0
src-55	518242.1	3529091.5	48716.5	48713.2	48953.6	-240.5	
src-56	518263.1	3529081.7	48706.9	48702.9	48953.6	-250.7	
sre-0	518221.0	3529101.3	48703.8	48700.7	48953.7	-253.0	=src-54
sre-0.01	518224.8	3529094.7	48669.2	48705.2	48953.6	-248.4	
sre-0.02	518228.6	3529088.0	48665.4	48701.4	48953.6	-252.2	
sre-0.03	518232.4	3529081.4	48667.0	48703.1	48953.6	-250.5	
sre-0.04	518236.2	3529074.7	48660.7	48696.8	48953.6	-256.8	
sre-0.05	518240.0	3529068.0	48678.7	48715.0	48953.6	-238.6	
sre-0.06	518243.7	3529061.4	48674.8	48711.1	48953.6	-242.5	
sre-0.07	518247.5	3529054.7	48675.0	48711.4	48953.6	-242.2	
sre-0.08	518251.3	3529048.1	48671.2	48708.0	48953.6	-245.6	
sre-0.09	518255.1	3529041.4	48678.3	48715.2	48953.6	-238.4	
sre-0.10	518258.9	3529034.7	48683.6	48720.6	48953.6	-233.0	
sre-0.11	518262.6	3529028.1	48687.1	48724.2	48953.6	-229.4	
sre-0.12	518266.4	3529021.4	48694.5	48731.7	48953.6	-221.9	
sre-0.13	518270.2	3529014.8	48703.4	48740.6	48953.6	-213.0	
sre-1	518274.0	3529008.1	48751.1	48748.7	48952.9	-204.2	
sre-1.5	518273.8	3529002.9	48756.0	48749.4	48952.9	-203.4	
sre-2	518273.7	3528997.6	48751.6	48749.1	48952.9	-203.8	
sre-2.5	518273.5	3528992.4	48760.5	48753.8	48952.9	-199.1	
sre-3	518273.4	3528987.2	48754.5	48751.9	48952.9	-201.0	
sre-3.5	518273.2	3528982.0	48757.6	48750.8	48952.9	-202.1	

sre-4	518273.1	3528976.8	48755.8	48753.0	48952.9	-200.0
sre-4.5	518272.9	3528971.5	48759.5	48752.6	48952.9	-200.3
sre-5	518272.7	3528966.3	48747.3	48744.3	48952.9	-208.6
sre-5.5	518274.0	3528960.6	48742.1	48735.2	48952.9	-217.7
sre-6	518275.3	3528954.9	48734.9	48731.8	48952.9	-221.1
sre-6.5	518276.5	3528949.2	48739.9	48732.9	48952.9	-220.0
sre-7	518277.8	3528943.5	48736.1	48732.8	48952.8	-220.0
sre-7.5	518279.1	3528937.8	48737.2	48730.1	48952.8	-222.7
sre-8	518280.3	3528932.1	48733.1	48729.7	48952.8	-223.1
sre-8.5	518281.6	3528926.4	48729.8	48722.6	48952.7	-230.1
sre-9	518282.9	3528920.7	48728.6	48725.1	48952.7	-227.6
sre-9.5	518284.2	3528915.1	48730.6	48723.4	48952.7	-229.3
sre-10	518285.4	3528909.4	48726.2	48722.5	48952.7	-230.1
sre-10.5	518284.7	3528905.0	48722.4	48715.1	48952.6	-237.6
sre-11	518283.9	3528900.7	48716.9	48713.2	48952.6	-239.4
sre-11.5	518283.1	3528896.4	48723.6	48716.2	48952.6	-236.3
sre-12	518282.4	3528892.1	48729.0	48725.1	48952.5	-227.4
sre-12.5	518281.6	3528887.8	48733.3	48725.8	48952.5	-226.7
sre-13	518280.9	3528883.5	48728.5	48724.4	48952.5	-228.0
sre-13.5	518280.1	3528879.2	48731.1	48723.6	48952.4	-228.8
sre-14	518279.3	3528874.9	48732.8	48728.7	48952.4	-223.7
sre-14.5	518278.6	3528870.6	48732.6	48725.1	48952.4	-227.3
sre-15	518277.8	3528866.2	48730.1	48725.7	48952.3	-226.6
sre-15.5	518279.3	3528860.8	48733.6	48726.0	48952.3	-226.2
sre-16	518280.9	3528855.4	48733.6	48729.1	48952.2	-223.1
sre-16.5	518282.4	3528849.9	48731.4	48723.8	48952.1	-228.4
sre-17	518283.9	3528844.5	48718.0	48713.3	48952.1	-238.8
sre-17.5	518285.4	3528839.1	48716.0	48708.3	48952.0	-243.7
sre-18	518286.9	3528833.6	48710.7	48705.7	48952.0	-246.2
sre-18.5	518288.5	3528828.2	48713.0	48705.2	48951.9	-246.6
sre-19	518290.0	3528822.7	48714.7	48709.5	48951.8	-242.3
sre-19.5	518291.5	3528817.3	48719.6	48709.9	48951.8	-241.9
sre-20	518293.0	3528811.9	48722.1	48712.4	48951.7	-239.3
sre-20.5	518294.5	3528806.4	48723.9	48713.9	48951.6	-237.7
sre-21	518296.0	3528801.0	48720.9	48710.9	48951.6	-240.6
sre-21.5	518297.6	3528795.6	48717.0	48707.0	48951.5	-244.5
sre-22	518299.1	3528790.1	48725.1	48715.0	48951.4	-236.5
sre-22.5	518302.6	3528785.2	48734.7	48724.5	48951.4	-227.0
sre-23	518306.1	3528780.2	48745.3	48735.0	48951.4	-216.4
sre-23.5	518309.6	3528775.2	48743.3	48733.0	48951.4	-218.5
sre-24	518313.0	3528770.2	48735.8	48725.4	48951.5	-226.1
sre-24.5	518316.5	3528765.3	48732.6	48722.1	48951.5	-229.3
sre-25	518320.0	3528760.3	48733.3	48722.8	48951.5	-228.7
sre-25.5	518323.5	3528755.3	48735.4	48724.8	48951.5	-226.6
sre-26	518327.0	3528750.4	48740.0	48729.3	48951.5	-222.1
sre-26.5	518330.5	3528745.4	48740.0	48729.3	48951.5	-222.2
sre-27	518334.0	3528740.4	48749.9	48739.1	48951.5	-212.4
sre-27.5	518337.5	3528735.5	48754.2	48743.3	48951.5	-208.2
sre-28	518341.0	3528730.5	48755.8	48744.7	48951.5	-206.8
sre-28.5	518344.5	3528725.5	48753.6	48742.5	48951.5	-209.0
sre-29	518348.0	3528720.6	48753.6	48742.5	48951.5	-209.0
sre-29.5	518351.5	3528715.6	48738.5	48727.3	48951.5	-224.2
sre-30	518355.0	3528710.6	48742.4	48731.2	48951.5	-220.3
sre-30.5	518358.1	3528706.0	48744.2	48732.9	48951.5	-218.6
sre-31	518361.3	3528701.3	48752.1	48740.8	48951.5	-210.7
sre-31.5	518364.5	3528696.7	48756.3	48744.9	48951.4	-206.6

sre-32	518367.6	3528692.0	48756.0	48744.2	48951.4	-207.2
sre-32.5	518370.8	3528687.4	48756.6	48744.7	48951.4	-206.7
sre-33	518374.0	3528682.7	48764.3	48752.4	48951.4	-198.9
sre-33.5	518377.1	3528678.1	48758.0	48746.2	48951.3	-205.1
sre-34	518380.3	3528673.4	48758.7	48746.8	48951.3	-204.5
sre-34.5	518383.5	3528668.8	48756.8	48745.0	48951.3	-206.3
sre-35	518386.7	3528664.1	48749.9	48738.1	48951.3	-213.2
sre-35.5	518389.8	3528659.5	48745.6	48733.8	48951.2	-217.5
sre-36	518393.0	3528654.8	48742.7	48730.9	48951.2	-220.3
sre-36.5	518396.2	3528650.2	48738.8	48727.1	48951.2	-224.1
sre-37	518399.3	3528645.5	48732.7	48720.9	48951.2	-230.3
sre-37.5	518400.6	3528639.3	48733.0	48721.2	48951.1	-229.9
sre-38	518401.9	3528633.0	48730.9	48719.1	48951.1	-231.9
sre-38.5	518403.1	3528626.8	48728.3	48716.6	48951.0	-234.4
sre-39	518404.4	3528620.5	48729.5	48717.8	48951.0	-233.2
sre-39.5	518405.6	3528614.3	48728.8	48717.1	48950.9	-233.8
sre-40	518406.9	3528608.0	48726.7	48715.0	48950.9	-235.9
sre-40.5	518408.1	3528601.8	48734.5	48722.8	48950.8	-228.1
sre-41	518409.4	3528595.5	48742.8	48731.1	48950.8	-219.7
sre-41.5	518410.7	3528589.3	48742.4	48730.7	48950.7	-220.0
sre-42	518411.9	3528583.0	48738.2	48726.5	48950.7	-224.2
sre-42.5	518413.2	3528576.8	48734.9	48723.2	48950.7	-227.4
sre-43	518414.4	3528570.5	48733.5	48721.8	48950.6	-228.8
sre-43.5	518415.4	3528564.9	48733.9	48722.3	48950.6	-228.3
sre-44	518416.3	3528559.4	48733.9	48722.2	48950.5	-228.3
sre-44.5	518417.3	3528553.8	48734.5	48722.8	48950.5	-227.7
sre-45	518418.3	3528548.2	48734.9	48723.3	48950.5	-227.2
sre-45.5	518419.2	3528542.7	48735.7	48724.1	48950.4	-226.3
sre-46	518420.2	3528537.1	48735.6	48724.0	48950.4	-226.4
sre-46.5	518421.1	3528531.5	48737.2	48725.6	48950.4	-224.8
sre-47	518422.1	3528525.9	48736.8	48725.2	48950.3	-225.1
sre-47.5	518423.0	3528520.4	48737.6	48726.0	48950.3	-224.3
sre-48	518424.0	3528514.8	48737.4	48725.8	48950.2	-224.4
sre-48.5	518425.0	3528509.2	48738.0	48726.4	48950.2	-223.8
sre-49	518425.9	3528503.7	48738.2	48726.7	48950.2	-223.5

srv-01	516362.2	3529712.8	48682.3	48691.9	48954.9	-263.0
srv-01.1	516369.1	3529708.6	48680.0	48689.6	48954.9	-265.3
srv-01.2	516376.0	3529704.4	48673.7	48683.2	48954.9	-271.7
srv-02	516382.9	3529700.2	48685.8	48695.3	48954.9	-259.6
srv-02.1	516389.9	3529696.0	48677.5	48686.9	48954.9	-268.0
srv-02.2	516396.8	3529691.8	48675.2	48684.5	48954.8	-270.3
srv-03	516403.7	3529687.6	48673.1	48682.4	48954.8	-272.4
srv-03.1	516410.6	3529683.4	48677.6	48686.9	48954.8	-267.9
srv-03.2	516417.6	3529679.2	48674.7	48683.9	48954.8	-270.9
srv-04	516424.5	3529675.0	48682.4	48691.5	48954.8	-263.3
srv-04.1	516431.4	3529670.8	48680.6	48689.7	48954.8	-265.1
srv-04.2	516438.3	3529666.6	48681.4	48690.5	48954.8	-264.3
srv-05	516445.3	3529662.4	48681.3	48690.4	48954.8	-264.4
srv-05.1	516452.6	3529658.0	48681.9	48690.9	48954.7	-263.8
srv-05.2	516460.0	3529653.6	48677.9	48686.9	48954.7	-267.8
srv-06	516467.4	3529649.2	48681.3	48690.2	48954.7	-264.5
srv-06.1	516474.8	3529644.9	48689.0	48697.9	48954.7	-256.8
srv-06.2	516482.2	3529640.5	48687.9	48696.7	48954.7	-258.0
srv-07	516489.5	3529636.1	48684.5	48693.2	48954.7	-261.4

srv-07.1	516496.9	3529631.7	48691.6	48700.3	48954.6	-254.4
srv-07.2	516504.3	3529627.4	48693.0	48701.7	48954.6	-252.9
srv-08	516511.7	3529623.0	48686.8	48695.4	48954.6	-259.3
srv-08.1	516519.1	3529618.6	48682.1	48690.6	48954.6	-264.0
srv-08.2	516526.5	3529614.2	48689.0	48697.5	48954.6	-257.1
srv-09	516533.8	3529609.8	48695.3	48703.7	48954.6	-250.9
srv-09.1	516541.2	3529605.5	48691.0	48699.4	48954.6	-255.2
srv-09.2	516548.6	3529601.1	48683.0	48691.4	48954.5	-263.2
srv-10	516556.0	3529596.7	48680.4	48688.7	48954.5	-265.9
srv-10.1	516562.5	3529592.9	48683.6	48691.8	48954.5	-262.7
srv-10.2	516569.1	3529589.2	48684.9	48693.2	48954.5	-261.3
srv-11	516575.6	3529585.4	48685.7	48693.9	48954.5	-260.5
srv-11.1	516582.1	3529581.6	48689.5	48697.8	48954.5	-256.7
srv-11.2	516588.7	3529577.9	48682.8	48691.0	48954.4	-263.4
srv-12	516595.2	3529574.1	48683.1	48691.4	48954.4	-263.0
srv-12.1	516601.7	3529570.3	48689.3	48697.6	48954.4	-256.8
srv-12.2	516608.3	3529566.5	48698.9	48707.2	48954.4	-247.2
srv-13	516614.8	3529562.8	48675.9	48684.2	48954.4	-270.2
srv-13.1	516621.4	3529559.0	48681.2	48689.5	48954.4	-264.8
srv-13.2	516627.9	3529555.2	48685.1	48693.4	48954.3	-261.0
srv-14	516634.4	3529551.4	48674.6	48682.9	48954.3	-271.4
srv-14.1	516641.0	3529547.7	48677.4	48685.7	48954.3	-268.6
srv-14.2	516647.5	3529543.9	48676.1	48684.4	48954.3	-269.9
srv-15	516654.0	3529540.1	48676.0	48684.3	48954.3	-269.9
srv-15.1	516660.5	3529536.0	48680.4	48688.7	48954.3	-265.5
srv-15.2	516667.0	3529531.9	48685.5	48693.9	48954.2	-260.4
srv-16	516673.4	3529527.9	48672.0	48680.3	48954.2	-273.9
srv-16.1	516679.9	3529523.8	48673.7	48682.1	48954.2	-272.1
srv-16.2	516686.3	3529519.7	48675.4	48683.8	48954.2	-270.4
srv-17	516692.8	3529515.6	48674.6	48682.9	48954.2	-271.2
srv-17.1	516699.2	3529511.5	48676.4	48684.8	48954.1	-269.4
srv-17.2	516705.7	3529507.4	48675.2	48683.6	48954.1	-270.6
srv-18	516712.2	3529503.3	48676.5	48684.9	48954.1	-269.2
srv-18.1	516718.6	3529499.2	48681.6	48689.9	48954.1	-264.2
srv-18.2	516725.1	3529495.1	48684.8	48693.2	48954.1	-260.9
srv-19	516731.5	3529491.0	48675.9	48684.2	48954.1	-269.8
srv-19.1	516738.0	3529486.9	48674.7	48683.1	48954.0	-270.9
srv-19.2	516744.4	3529482.9	48673.8	48682.2	48954.0	-271.8
srv-20	516750.9	3529478.8	48665.2	48673.0	48954.0	-281.0
srv-20.1	516757.4	3529474.7	48667.8	48675.4	48954.0	-278.5
srv-20.2	516763.8	3529470.6	48672.0	48679.6	48954.0	-274.4
srv-21	516770.3	3529466.5	48674.2	48681.7	48953.9	-272.2
srv-21.1	516777.1	3529462.5	48669.0	48676.4	48953.9	-277.5
srv-21.2	516783.9	3529458.5	48672.4	48679.7	48953.9	-274.2
srv-22	516790.7	3529454.6	48674.9	48682.2	48953.9	-271.7
srv-22.1	516797.5	3529450.7	48659.2	48666.4	48953.9	-287.5
srv-22.2	516804.4	3529446.7	48660.1	48667.3	48953.9	-286.6
srv-23	516811.3	3529442.7	48670.7	48677.7	48953.8	-276.1
srv-23.1	516818.1	3529438.8	48675.7	48682.7	48953.8	-271.2
srv-23.2	516824.9	3529434.8	48658.1	48665.0	48953.8	-288.8
srv-24	516831.8	3529430.9	48666.3	48673.2	48953.8	-280.6
srv-24.1	516838.6	3529426.8	48665.1	48671.9	48953.8	-281.9
srv-24.2	516845.4	3529422.6	48665.0	48671.7	48953.8	-282.1
srv-25	516852.2	3529418.5	48667.7	48674.3	48953.8	-279.4
srv-25.1	516859.1	3529414.4	48671.6	48678.1	48953.7	-275.7
srv-25.2	516866.0	3529410.3	48674.1	48680.5	48953.7	-273.2

srv-26	516872.8	3529406.3	48679.0	48685.3	48953.7	-268.4
srv-26.1	516879.6	3529402.2	48677.4	48683.6	48953.7	-270.1
srv-26.2	516886.4	3529398.1	48674.5	48680.6	48953.7	-273.0
srv-27	516893.3	3529394.0	48677.0	48683.1	48953.7	-270.5
srv-27.1	516900.0	3529389.9	48668.3	48674.3	48953.7	-279.3
srv-27.2	516906.8	3529385.8	48652.1	48658.1	48953.6	-295.5
srv-28	516913.5	3529381.6	48658.9	48664.8	48953.6	-288.9
srv-28.1	516920.2	3529377.5	48667.0	48672.8	48953.6	-280.8
srv-28.2	516926.8	3529373.3	48669.2	48674.9	48953.6	-278.7
srv-29	516933.5	3529369.2	48666.2	48671.8	48953.6	-281.8
srv-29.1	516940.3	3529365.1	48666.9	48672.5	48953.6	-281.1
srv-29.2	516947.0	3529360.9	48668.0	48673.5	48953.5	-280.1
srv-30	516953.7	3529356.8	48654.3	48659.7	48953.5	-293.8
srv-30.1	516960.7	3529353.1	48663.3	48668.6	48953.5	-284.9
srv-30.2	516967.6	3529349.3	48647.3	48652.5	48953.5	-301.0
srv-31	516974.5	3529345.5	48663.1	48668.2	48953.5	-285.3
srv-31.1	516981.4	3529341.7	48665.4	48670.4	48953.5	-283.1
srv-31.2	516988.3	3529338.0	48670.6	48675.6	48953.5	-277.9
srv-32	516995.3	3529334.2	48684.9	48689.8	48953.5	-263.6
srv-32.1	517002.2	3529330.3	48650.3	48655.2	48953.5	-298.3
srv-32.2	517009.2	3529326.6	48665.9	48670.7	48953.5	-282.8
srv-33	517016.1	3529322.8	48661.2	48665.9	48953.4	-287.5
srv-33.1	517022.6	3529319.1	48659.7	48664.3	48953.4	-289.2
srv-33.2	517029.1	3529315.3	48663.6	48668.1	48953.4	-285.3
srv-34	517035.7	3529311.5	48685.4	48689.9	48953.4	-263.6
srv-34.1	517042.2	3529307.9	48665.5	48669.8	48953.4	-283.6
srv-34.2	517048.7	3529304.1	48667.4	48671.8	48953.4	-281.6
srv-35	517055.3	3529300.4	48667.5	48671.8	48953.4	-281.6
srv-35.1	517062.2	3529296.0	48659.5	48663.7	48953.4	-289.7
srv-35.2	517069.2	3529291.5	48659.7	48663.8	48953.4	-289.5
srv-36	517076.2	3529287.1	48666.3	48670.4	48953.3	-282.9
srv-36.1	517083.2	3529282.7	48665.2	48669.0	48953.3	-284.3
srv-36.2	517090.1	3529278.3	48662.5	48666.1	48953.3	-287.2
srv-37	517097.1	3529273.8	48674.0	48677.6	48953.3	-275.7
srv-37.1	517104.1	3529269.4	48675.0	48678.5	48953.3	-274.8
srv-37.2	517111.1	3529265.0	48664.0	48667.2	48953.2	-286.1
srv-38	517118.0	3529260.6	48652.8	48655.9	48953.2	-297.3
srv-38.1	517125.0	3529256.2	48654.7	48657.7	48953.2	-295.5
srv-38.2	517132.0	3529251.7	48660.7	48663.6	48953.2	-289.6
srv-39	517138.9	3529247.3	48657.8	48660.6	48953.2	-292.6
srv-39.1	517145.9	3529242.9	48659.4	48662.0	48953.2	-291.1
srv-39.2	517152.9	3529238.5	48655.5	48658.1	48953.1	-295.1
srv-40	517159.9	3529234.0	48662.4	48664.9	48953.1	-288.2
srv-40.1	517166.3	3529230.2	48671.9	48674.3	48953.1	-278.8
srv-40.2	517172.8	3529226.4	48662.0	48664.4	48953.1	-288.7
srv-41	517179.3	3529222.6	48657.3	48657.1	48953.1	-296.0
srv-41.1	517185.8	3529218.8	48671.2	48670.9	48953.1	-282.1
srv-41.2	517192.3	3529215.0	48673.5	48673.2	48953.0	-279.9
srv-42	517198.8	3529211.2	48663.6	48663.2	48953.0	-289.8
srv-42.1	517205.3	3529207.4	48659.9	48659.4	48953.0	-293.6
srv-42.2	517211.8	3529203.6	48670.8	48670.4	48953.0	-282.6
srv-43	517218.2	3529199.8	48659.4	48659.0	48953.0	-294.0
srv-43.1	517224.7	3529196.0	48665.4	48664.9	48953.0	-288.1
srv-43.2	517231.2	3529192.1	48728.8	48728.3	48953.0	-224.7
srv-44	517237.7	3529188.3	48642.3	48641.7	48952.9	-311.2
srv-44.1	517244.2	3529184.5	48652.3	48651.7	48952.9	-301.2

srv-44.2	517250.7	3529180.7	48658.5	48657.8	48952.9	-295.1
srv-45	517257.2	3529176.9	48663.1	48662.5	48952.9	-290.4
srv-45.1	517264.0	3529172.8	48659.3	48658.6	48952.9	-294.3
srv-45.2	517270.9	3529168.7	48660.0	48659.3	48952.9	-293.5
srv-46	517277.8	3529164.6	48658.8	48658.0	48952.8	-294.8
srv-46.1	517284.7	3529160.6	48663.9	48663.1	48952.8	-289.8
srv-46.2	517291.5	3529156.5	48661.9	48661.0	48952.8	-291.8
srv-47	517298.4	3529152.4	48664.9	48664.0	48952.8	-288.7
srv-47.1	517305.3	3529148.3	48664.4	48663.5	48952.8	-289.3
srv-47.2	517312.1	3529144.2	48660.3	48659.3	48952.7	-293.4
srv-48	517319.0	3529140.1	48656.3	48655.4	48952.7	-297.4
srv-48.1	517325.9	3529136.0	48671.1	48670.1	48952.7	-282.6
srv-48.2	517332.8	3529131.9	48657.6	48656.6	48952.7	-296.1
srv-49	517339.6	3529127.8	48662.6	48661.5	48952.7	-291.1
srv-49.1	517346.5	3529123.7	48667.3	48666.2	48952.7	-286.4
srv-49.2	517353.4	3529119.7	48664.5	48663.4	48952.6	-289.3
srv-50	517360.2	3529115.6	48663.9	48662.8	48952.6	-289.9
srv-50.1	517366.9	3529111.5	48664.7	48663.5	48952.6	-289.1
srv-50.2	517373.6	3529107.4	48645.0	48643.8	48952.6	-308.8
srv-51	517380.2	3529103.3	48672.7	48671.4	48952.6	-281.1
srv-51.1	517386.9	3529099.3	48655.2	48653.9	48952.6	-298.7
srv-51.2	517393.5	3529095.2	48656.3	48654.9	48952.5	-297.6
srv-52	517400.2	3529091.1	48650.8	48649.4	48952.5	-303.1
srv-52.1	517406.9	3529087.0	48679.0	48677.5	48952.5	-275.0
srv-52.2	517413.5	3529083.0	48672.6	48671.1	48952.5	-281.3
srv-53	517420.2	3529078.9	48667.5	48666.0	48952.5	-286.5
srv-53.1	517426.8	3529074.8	48663.6	48662.1	48952.5	-290.4
srv-53.2	517433.5	3529070.7	48670.7	48669.1	48952.4	-283.3
srv-54	517440.1	3529066.7	48671.8	48670.2	48952.4	-282.3
srv-54.1	517446.8	3529062.6	48673.6	48671.9	48952.4	-280.5
srv-54.2	517453.5	3529058.5	48672.6	48670.9	48952.4	-281.5
srv-55	517460.1	3529054.4	48663.4	48661.7	48952.4	-290.7
srv-55.1	517467.2	3529050.4	48663.0	48661.3	48952.4	-291.1
srv-55.2	517474.3	3529046.4	48666.4	48664.6	48952.3	-287.7
srv-56	517481.4	3529042.4	48674.3	48672.4	48952.3	-279.9
srv-56.1	517488.5	3529038.3	48668.5	48666.6	48952.3	-285.7
srv-56.2	517495.5	3529034.3	48681.9	48680.0	48952.3	-272.3
srv-57	517502.6	3529030.3	48674.2	48672.3	48952.3	-280.0
srv-57.1	517509.7	3529026.2	48683.9	48681.9	48952.3	-270.3
srv-57.2	517516.8	3529022.2	48692.3	48690.3	48952.2	-261.9
srv-58	517523.9	3529018.2	48683.2	48681.2	48952.2	-271.1
srv-58.1	517531.0	3529014.1	48675.5	48673.5	48952.2	-278.7
srv-58.2	517538.1	3529010.1	48673.0	48671.0	48952.2	-281.2
srv-59	517545.1	3529006.1	48673.4	48671.3	48952.2	-280.9
srv-59.1	517552.2	3529002.1	48674.1	48671.9	48952.1	-280.2
srv-59.2	517559.3	3528998.0	48681.1	48678.9	48952.1	-273.2
srv-60	517566.4	3528994.0	48674.6	48672.4	48952.1	-279.7
srv-60.1	517573.2	3528989.9	48658.3	48656.0	48952.1	-296.1
srv-60.2	517580.1	3528985.8	48668.0	48665.7	48952.1	-286.4
srv-61	517586.9	3528981.8	48692.8	48690.4	48952.1	-261.6
srv-61.1	517593.7	3528977.7	48683.9	48681.5	48952.1	-270.5
srv-61.2	517600.6	3528973.6	48676.2	48673.8	48952.1	-278.2
srv-62	517607.4	3528969.6	48681.5	48679.1	48952.0	-273.0
srv-62.1	517614.2	3528965.5	48676.2	48673.7	48952.0	-278.3
srv-62.2	517621.1	3528961.4	48659.9	48657.3	48952.0	-294.7
srv-63	517627.9	3528957.3	48669.2	48666.6	48952.0	-285.4

srv-63.1	517634.8	3528953.3	48689.6	48686.9	48952.0	-265.0
srv-63.2	517641.6	3528949.2	48670.6	48667.9	48952.0	-284.1
srv-64	517648.4	3528945.1	48669.5	48666.8	48952.0	-285.1
srv-64.1	517655.3	3528941.0	48683.4	48680.6	48952.0	-271.3
srv-64.2	517662.1	3528937.0	48690.7	48687.9	48951.9	-264.0
srv-65	517668.9	3528932.9	48676.5	48679.3	48951.9	-272.6
srv-65.1	517675.7	3528928.8	48675.0	48677.7	48951.9	-274.2
srv-65.2	517682.5	3528924.7	48679.2	48681.9	48951.9	-270.0
srv-66	517689.3	3528920.7	48675.0	48677.7	48951.9	-274.2
srv-66.1	517696.1	3528916.6	48672.7	48675.2	48951.9	-276.6
srv-66.2	517702.8	3528912.5	48675.9	48678.2	48951.9	-273.6
srv-67	517709.6	3528908.4	48670.1	48672.4	48951.8	-279.5
srv-67.1	517716.4	3528904.4	48677.9	48680.1	48951.8	-271.7
srv-67.2	517723.2	3528900.3	48674.3	48676.5	48951.8	-275.3
srv-68	517730.0	3528896.2	48675.6	48677.8	48951.8	-274.0
srv-68.1	517736.8	3528892.1	48673.1	48675.2	48951.8	-276.6
srv-68.2	517743.5	3528888.1	48673.7	48675.7	48951.8	-276.0
srv-69	517750.3	3528884.0	48666.8	48668.6	48951.7	-283.2
srv-69.1	517757.1	3528879.9	48666.0	48667.7	48951.7	-284.0
srv-69.2	517763.9	3528875.8	48680.9	48682.6	48951.7	-269.1
srv-70	517770.7	3528871.8	48669.0	48670.6	48951.7	-281.1
srv-70.1	517777.5	3528868.2	48672.6	48674.1	48951.7	-277.6
srv-70.2	517784.3	3528864.6	48661.0	48662.5	48951.7	-289.2
srv-71	517791.1	3528861.0	48637.9	48639.3	48951.7	-312.4
srv-71.1	517798.0	3528857.4	48651.8	48653.1	48951.6	-298.6
srv-71.2	517804.8	3528853.9	48650.0	48651.1	48951.6	-300.5
srv-72	517811.6	3528850.3	48642.5	48643.5	48951.6	-308.1
srv-72.1	517818.4	3528846.7	48651.7	48652.7	48951.6	-298.9
srv-72.2	517825.3	3528843.1	48655.3	48656.2	48951.6	-295.4
srv-73	517832.1	3528839.6	48659.2	48660.1	48951.6	-291.4
srv-73.1	517838.9	3528836.0	48666.4	48667.2	48951.6	-284.3
srv-73.2	517845.7	3528832.4	48656.4	48657.2	48951.6	-294.3
srv-74	517852.5	3528828.8	48653.5	48654.3	48951.5	-297.3
srv-74.1	517859.4	3528825.2	48655.3	48656.1	48951.5	-295.4
srv-74.2	517866.2	3528821.7	48670.4	48671.1	48951.5	-280.4
srv-75	517873.0	3528818.1	48664.1	48664.7	48951.5	-286.8
srv-75.1	517880.5	3528813.8	48669.9	48670.5	48951.5	-280.9
srv-75.2	517888.0	3528809.4	48661.4	48661.9	48951.4	-289.5
srv-76	517895.6	3528805.1	48658.8	48659.3	48951.4	-292.1
srv-76.1	517903.1	3528800.8	48654.3	48654.8	48951.4	-296.6
srv-76.2	517910.6	3528796.4	48678.1	48678.4	48951.4	-272.9
srv-77	517918.2	3528792.1	48677.5	48677.8	48951.3	-273.5
srv-77.1	517925.7	3528787.8	48680.0	48680.2	48951.3	-271.1
srv-77.2	517933.3	3528783.4	48683.5	48683.6	48951.3	-267.6
srv-78	517940.8	3528779.1	48703.3	48701.4	48951.3	-249.8
srv-78.1	517948.3	3528773.9	48621.1	48619.2	48951.2	-332.1
srv-78.2	517955.8	3528768.7	48733.7	48731.8	48951.2	-219.4
srv-79	517963.3	3528763.4	48812.3	48810.4	48951.2	-140.8
srv-79.1	517970.8	3528758.2	48897.2	48895.2	48951.1	-56.0
srv-79.2	517978.3	3528753.0	48945.2	48943.2	48951.1	-8.0
srv-80	517985.8	3528747.8	48639.5	48637.4	48951.1	-313.7
srv-80.1	517993.2	3528743.5	48588.1	48585.9	48951.1	-365.2
srv-80.2	518000.7	3528739.2	48643.6	48641.4	48951.0	-309.6
srv-81	518008.1	3528734.9	48675.7	48673.5	48951.0	-277.5
srv-81.1	518015.6	3528730.6	48671.2	48669.0	48951.0	-282.0
srv-81.2	518023.0	3528726.3	48688.5	48686.2	48951.0	-264.8

srv-82	518030.5	3528722.0	48687.0	48684.7	48950.9	-266.3
srv-82.1	518037.9	3528717.7	48692.2	48689.8	48950.9	-261.1
srv-82.2	518045.4	3528713.4	48696.1	48693.6	48950.9	-257.3
srv-83	518052.8	3528709.1	48701.0	48698.6	48950.9	-252.3
srv-83.1	518060.2	3528705.2	48705.4	48702.9	48950.9	-248.0
srv-83.2	518067.5	3528701.2	48709.7	48707.2	48950.8	-243.7
srv-84	518074.9	3528697.3	48713.6	48711.1	48950.8	-239.7
srv-84.1	518082.3	3528693.4	48718.1	48715.6	48950.8	-235.2
srv-84.2	518089.6	3528689.4	48722.6	48720.0	48950.8	-230.8
srv-85	518097.0	3528685.5	48727.0	48724.4	48950.7	-226.3
srv-85.1	518103.9	3528681.2	48733.0	48730.3	48950.7	-220.4
srv-85.2	518110.8	3528677.0	48735.3	48732.6	48950.7	-218.1
srv-86	518117.8	3528672.7	48738.6	48735.9	48950.7	-214.8
srv-86.1	518124.7	3528668.4	48742.6	48739.9	48950.7	-210.8
srv-86.2	518131.6	3528664.2	48747.3	48744.5	48950.7	-206.2
srv-87	518138.5	3528659.9	48752.3	48749.5	48950.7	-201.2
srv-87.1	518145.5	3528655.7	48762.5	48759.7	48950.7	-191.0
srv-87.2	518152.4	3528651.4	48785.0	48782.2	48950.7	-168.5
srv-88	518159.3	3528647.2	48728.9	48726.1	48950.7	-224.6
srv-88.1	518166.2	3528642.9	48711.3	48708.4	48950.6	-242.2
srv-88.2	518173.2	3528638.6	48698.8	48695.9	48950.6	-254.7
srv-89	518180.1	3528634.4	48691.7	48688.8	48950.6	-261.9
srv-89.1	518187.0	3528630.1	48682.3	48679.2	48950.6	-271.4
srv-89.2	518193.9	3528625.9	48673.4	48670.3	48950.6	-280.3
srv-90	518200.9	3528621.6	48673.2	48670.1	48950.6	-280.5
srv-90.1	518207.8	3528617.2	48677.2	48674.0	48950.6	-276.6
srv-90.2	518214.8	3528612.8	48681.5	48678.3	48950.5	-272.3
srv-91	518221.8	3528608.4	48689.7	48686.4	48950.5	-264.1
srv-91.1	518228.8	3528604.0	48695.2	48691.8	48950.5	-258.7
srv-91.2	518235.8	3528599.6	48694.9	48691.6	48950.4	-258.9
srv-92	518242.7	3528595.2	48699.4	48696.0	48950.4	-254.4
srv-92.1	518249.7	3528590.8	48703.2	48699.8	48950.4	-250.6
srv-92.2	518256.7	3528586.4	48707.5	48704.1	48950.3	-246.3
srv-93	518263.7	3528582.0	48709.2	48705.8	48950.3	-244.5
srv-93.1	518270.6	3528577.6	48711.3	48707.8	48950.3	-242.5
srv-93.2	518277.6	3528573.2	48714.3	48710.8	48950.2	-239.5
srv-94	518284.6	3528568.8	48714.0	48710.5	48950.2	-239.7
srv-94.1	518291.6	3528564.4	48715.5	48711.9	48950.2	-238.2
srv-94.2	518298.6	3528560.0	48717.3	48713.8	48950.2	-236.4
srv-95	518305.5	3528555.6	48717.5	48713.9	48950.1	-236.2
srv-95.1	518312.5	3528551.7	48718.8	48715.2	48950.1	-234.9
srv-95.2	518319.4	3528547.9	48719.8	48716.2	48950.1	-233.9
srv-96	518326.4	3528544.0	48721.9	48718.3	48950.1	-231.8
srv-96.1	518333.4	3528540.1	48721.2	48717.5	48950.1	-232.6
srv-96.2	518340.3	3528536.3	48720.9	48717.2	48950.1	-233.0
srv-97	518347.3	3528532.4	48723.4	48719.7	48950.1	-230.4
srv-97.1	518354.2	3528528.5	48724.9	48721.1	48950.1	-229.0
srv-97.2	518361.2	3528524.7	48723.7	48719.9	48950.1	-230.2
srv-98	518368.2	3528520.8	48724.4	48720.6	48950.1	-229.5
srv-98.1	518375.1	3528516.9	48725.3	48721.5	48950.1	-228.7
srv-98.2	518382.1	3528513.1	48726.9	48723.1	48950.1	-227.0
srv-99	518389.0	3528509.2	48726.1	48722.3	48950.1	-227.8
srv-99.1	518396.0	3528505.3	48727.5	48723.7	48950.1	-226.5
srv-99.2	518403.0	3528501.5	48727.5	48723.6	48950.1	-226.5
srv-100	518409.9	3528497.6	48728.8	48724.9	48950.1	-225.3